INFORMATION TO USERS

This manuscript has been reproduced from the microfilm master. UMI films the text directly from the original or copy submitted. Thus, some thesis and dissertation copies are in typewriter face, while others may be from any type of computer printer.

The quality of this reproduction is dependent upon the quality of the copy submitted. Broken or indistinct print, colored or poor quality illustrations and photographs, print bleedthrough, substandard margins, and improper alignment can adversely affect reproduction.

In the unlikely event that the author did not send UMI a complete manuscript and there are missing pages, these will be noted. Also, if unauthorized copyright material had to be removed, a note will indicate the deletion.

Oversize materials (e.g., maps, drawings, charts) are reproduced by sectioning the original, beginning at the upper left-hand corner and continuing from left to right in equal sections with small overlaps.

ProQuest Information and Learning
300 North Zeeb Road, Ann Arbor, MI 48106-1346 USA
800-521-0600

Université d'Ottawa · University of Ottawa

UNIVERSITY OF OTTAWA

Studies on the Role(s) of Post-translational Modification(s) of Human Apolipoprotein B during Very Low Density Lipoprotein Assembly and Secretion

BY

Jelena Vukmirica

A Thesis Submitted to the School of Graduate Studies and Research
In Partial Fulfillment of the Requirements for the Degree of
DOCTOR OF PHILOSOPHY in Biochemistry

Department of Biochemistry, Microbiology, and Immunology
Faculty of Medicine

Ottawa, Ontario

Abstract

The role of two post-translational modifications, N-linked glycosylation and palmitoylation, of human apolipoprotein B (apoB) in the biosynthesis of hepatic apoB-containing very low density lipoproteins (VLDL) was investigated. Working with tunicamycin-treated rat hepatoma McA-RH7777 cells stably expressing human apoB variants, we found that inhibition of N-linked glycosylation decreased the secretion of apoB variants, without affecting translation. Detailed biochemical analysis was performed following site-specific mutagenesis at consensus N-linked glycosylation sites (using asparagine-to-glutamine substitution) within recombinant human apoB variants (*i.e.* apoB17, -B37, -B48, and -B50). Four notable features associated with the requirement of N-linked oligosaccharides during apoB biosynthesis were observed: (a) N-linked oligosaccharides were required for efficient secretion of the apoB polypeptide. (b) N-linked oligosaccharides were required for the assembly and secretion of the apoB-containing VLDL. (c) Removal of N-linked oligosaccharides was associated with accumulation of total intracellular apoB without specific apoB retention in the ER, and (d) Expression of mutant apoB lacking N-glycans was associated with changes in mass or activity of microsomal triglyceride transfer protein (MTP). Similar biochemical analysis was performed following site-specific mutagenesis at potential palmitoylation sites (using cysteine-to-serine substitution) within human apoB48. The cysteine-to-serine substitution had no effect on the secretion of apoB48-containing lipoproteins or apoB intracellular distribution. Thus, while N-linked glycosylation at the amino terminus of apoB represents an important requisite for proper biogenesis of apoB-containing VLDL, palmitoylation is not required for apoB-containing VLDL assembly and secretion.

Acknowledgements

I am most indebted to my research supervisor of the past six years, Dr. Zemin Yao. He allowed me to initiate my graduate studies, and greatly motivated research interest that ensures my professional achievements. He provided guidance and gave tireless support. Dr. Yao has been a true teacher and a mentor.

I am also indebted to three members of our laboratory, Khai Tran, Jing Shan, and Jane Yuan, who have provided outstanding technical support, and who have greatly accelerated the development of my research project.

I want to thank the following individuals for their help, support, ideas, and friendship throughout the past six years: Roger McLeod, Kerry Ko, Yuwei Wang, Rita Kohen, Robert Raffai, Dan McManus, Tanya Ramsamy, Stephanie Walters, Robert Brown, Philip Links, and Shermin Ramikhani. Thank you to Drs. Ross Milne, Yves Marcel, Ruth McPherson, Daniel Sparks, Heidi McBride, and Joshua Schultz for providing a nurturing working environment, and Ann Buie, Anna Toma, and Jennifer Edwards de Becerril for their excellent administrative assistance.

I am grateful to Drs. Ross Milne, Yves Marcel, Carol Shoulders, Marylin Farquhar, and Jean Vance for providing antibodies used in these studies, and Dr. Edward Fisher for providing the GFP-B46 cDNA construct. I thank Drs. Heidi McBride and John Ngsee for guidance and assistance in fluorescent microscopy studies, and Dr. Xiquan Liang for assistance with the palmitoylation assay.

I acknowledge technical assistance provided by the members of the animal research facility at the University of Ottawa Heart Institute.

I would like to extend gratitude to Dr. Zemin Yao for critical reading of this thesis, as well as to my dissertation committee members, Drs. Gregory Shelness, Daniel Sparks, Odette Laneuville and Alex Sorisky, for their contributions and advice leading to the completion of this dissertation.

I thank the Ontario Graduate Scholarship, Canadian Institutes of Health Research, and the School of Graduate Studies and Research at the University of Ottawa for providing financial support.

The completion of my graduate work would not be possible without the endless support from friends, namely Gerard Vassiliou, Anouk Leblanc, Jana Bogatin, Olja Pantic, Stana Smiljanic, Gordana Arizanovic, Tatjana Perosevic, and my family.

Dedications

For my friends and family, and especially, for my grandfather.

Table of Contents

List of Tables

List of Figures

Abbreviations

ALLN	N-acetyl-leucyl-leucyl-norleucinal
ABTS	azino-bis-ethylbenzthiazoline-sulphonic acid diammonium
ACAT	acyl-CoA: cholesterol acyltransferase
Apo	apolipoprotein
ATCC	American Type Culture Collection
BiP	immunoglobulin binding protein
BSA	bovine serum albumin
C-terminus	carboxyl-terminus
CE	cholesteryl ester
CHO	Chinese Hamster Ovary
DG	diacylglycerol
DGAT	acyl-coenzyme A: diacylglycerol acyltransferase
DMEM	Dulbecco's modified Eagle's medium
DRM	detergent-resistant microdomain
ECL	enhanced chemiluminescence
EDTA	ethylenediaminetetraacetic acid
ELISA	enzyme-linked immunosorbent assay
ER	endoplasmic reticulum
ERAD	ER-associated degradation
ERGIC	ER-Golgi intermediate compartment
FBS	fetal bovine serum
FCS	fetal calf serum

G418	geneticin
GlcNAc	N-acetylglucosamine
GFP	green fluorescent protein
GST	glutathione-S-transferase
HAT	hypoxanthine, aminopterine, thymidine
HB48	human apolipoprotein B48
HB100	human apolipoprotein B100
HDL	high density lipoproteins
HS	horse serum
LDL	low density lipoproteins
LRP	LDL receptor-related protein
LV	lipovitellin
MTP	microsomal triglyceride transfer protein
N-terminus	amino-terminus
OA	oleic acid
PAGE	polyacrylamide gel electrophoresis
PBS	phosphate buffered saline
PC	phosphatidylcholine
PDI	protein disulfide isomerase
PE	phosphatidylethanolamine
PEG	polyethylene glycol
PL	phospholipid
PMME	phosphatidylmonomethylethanolamine

RAP	receptor-associated protein
RB48	rat apolipoprotein B48
RB100	rat apolipoprotein B100
SDS	sodium dodecyl sulphate
SUV	small unilamellar vesicle
TG	triacylglycerol
TLC	thin-layer chromatography
UPR	unfolded protein response
VLDL	very low density lipoprotein
VTG	vitellogenin

Amino acids are referred to using the single letter code or the three-letter code.

A	Ala	Alanine
C	Cys	Cysteine
D	Asp	Aspartic Acid
E	Glu	Glutamic Acid
F	Phe	Phenylalanine
G	Gly	Glycine
H	His	Histidine
I	Ile	Isoleucine
K	Lys	Lysine
L	Leu	Leucine
M	Met	Methionine

N	Asn	Asparagine
P	Pro	Proline
Q	Gln	Glutamine
R	Arg	Arginine
S	Ser	Serine
T	Thr	Threonine
V	Val	Valine
W	Trp	Tryptophan
Y	Tyr	Tyrosine

Chapter 1 Introduction

1.1. Introduction

The function of lipoproteins, macromolecular complexes composed of varying amount of neutral lipid in their core that is surrounded by proteins (apolipoproteins) on surface, is to transport plasma cholesterol and triglyceride (TG) through the bloodstream. In humans, TG-rich VLDL ($d < 1.006$ g/ml) are produced in the liver, and once secreted into the bloodstream, transport TG from the liver to the peripheral tissue (1). Subsequent hydrolysis of TG from VLDL particles in plasma through the action of lipoprotein lipase generates denser intermediate density lipoproteins (IDL, $d = 1.006$-1.019 g/ml) that are further catabolized into cholesterol-enriched low-density lipoproteins (LDL, $d = 1.019$-1.063 g/ml) (1). The plasma LDL particles are recognized on the surface of cells and internalized through LDL receptor-mediated endocytosis (2). Overproduction of VLDL and decreased LDL catabolism can both lead to elevated concentration of plasma LDL, which is considered a major risk factor for development of atherosclerosis (1). Since plasma VLDL particles are the metabolic precursors of LDL, synthesis and secretion of the TG-rich VLDL represent a key determinant of the plasma concentration of atherogenic lipoproteins, with therapeutic approaches centered on attenuating the overproduction of TG-enriched VLDL particles by the liver.

Apolipoprotein B (apoB), the major protein component of VLDL, IDL, and LDL, plays a central role in lipoprotein metabolism (1). In human liver, the assembly of TG-rich VLDL involves recruitment of lipid by apoB following regulated biosynthesis of both apoB and lipid as well as the action of additional facilitating factors. The embryonic

lethality following apoB gene knockout studies in mice suggests an indispensable role for apoB during development and lipoprotein metabolism (3). Similarly, mutations in the apoB gene, as observed in subjects with hypobetalipoprotenemia, a disorder characterized by secretion of truncated forms of apoB, or observed in transgenic mice expressing altered apoB gene, lead to compromised hepatic VLDL assembly and secretion (4).

Efforts toward understanding the mechanism of hepatic VLDL assembly over the past two decades have focused with particular emphasis on examining the mechanism of TG recruitment by apoB, and also on determining the precise function(s) of microsomal triglyceride protein (MTP), a protein closely associated with VLDL production. Mutations in the gene encoding MTP have been identified as the proximal cause of abetalipoproteinemia, a recessive disorder characterized by deficiency in secretion of apoB-containing lipoproteins (5). To date, significant progress has been made in understanding the mechanisms of regulation of apoB biogenesis.

In this Chapter, I will summarize the current knowledge in the following areas. (a) Structure of apoB and apoB lipid-binding properties. (b) Unique features associated with regulation of apoB biogenesis. (c) Mechanism of VLDL assembly, including the subcellular location of VLDL maturation, the origin of recruited TG, and requirement of MTP and other factors in this process. (d) The role of multiple post-translational modifications of apoB, namely phosphorylation, formation of disulfide bonds, N-linked glycosylation, and palmitoylation, during VLDL assembly and secretion.

1.2. Apolipoprotein B

Two forms of apoB are found in the circulation, the full-length apoB100 and the N-terminal 48% of the full-length, designated as apoB48 (1). ApoB100 is the non-exchangeable constituent of VLDL particles (30-110 nm in diameter) secreted from the human liver. During catabolism of VLDL in plasma, apoB100 remains a constituent of the small and dense IDL and LDL particles (1). ApoB48, on the other hand, is generated following tissue-specific post-transcriptional mRNA editing of the apoB transcript. ApoB48 is secreted from the human intestine in the form of large TG-rich chylomicron particles (over 250 nm in diameter) (1). The mRNA editing process involves deamination of cytidine (C) at nucleotide 6666 to uridine (U), resulting in conversion of a glutamine codon at position 2153 of apoB100 into an in-frame stop codon (6,7). In humans, the mRNA editing process is confined to the intestine, while in some species, such as rats, mice, dogs, and horses, the mRNA editing occurs not only in the intestine but also in the liver (8). Both apoB100 and apoB48 can form VLDL, and a VLDL particle contains a single copy of apoB (9).

The cDNA sequence of apoB was determined by several groups independently (10-13). The complete amino acid sequence of the full-length human apoB100, deduced from its cDNA (12, 14-17), shows a large glycoprotein containing 4536 amino acid residues (Fig. 1.1*A*) (18). There are 20 potential N-linked glycosylation sites within human apoB100, of which 16 are glycosylated (Fig. 1.1*B*) (18). From a total of 25 cysteine residues found within apoB100, sixteen are involved in disulfide bond formation (19). Seven of these disulfide linkages are clustered within the N-terminal 500 amino acid

residues, suggesting the presence of a globular structure in this region (Fig. 1 1*C*) (19). Other modifications of the apoB structure that may have an impact on its function are fatty acylation (20-23) and phosphorylation (24) (see below).

The interaction of apoB100 with the LDL receptor has been identified as an important determining factor of cholesterol homeostasis. Binding of apoB100 to the LDL receptor occurs only after catabolism of VLDL to LDL, suggesting that both lipid composition and conformation of apoB may affect binding to the LDL receptor (2). Based on studies using apoB-specific monoclonal antibodies with known epitopes, the region surrounding the residue 3249 of apoB was identified as the LDL receptor-binding region (25). Sequence alignment following selective chemical modification suggested two C-terminal regions within human apoB100, spanning residues 3147-3157 (designated site A) and 3359-3367 (designated site B) as candidates for LDL receptor binding (14). The site B sequence shows similarity to the LDL receptor-binding domain of apoE (26), another ligand for the LDL receptor, and site B, but not site A, sequence is highly conserved among different vertebrate species (25). Studies using site-directed mutagenesis of apoB indicated that Site B residues (amino acids 3359-3369) do participate in binding to the LDL receptor (27). Furthermore, it has been proposed that the arginine residue at 3500 interacts with the carboxyl terminus after the conversion of triglyceride-rich VLDL to smaller cholesterol-rich LDL, permitting normal interaction between LDL and its receptor (27).

1.2.1. Apolipoprotein B structure

The extreme hydrophobicity and large size of apoB have hindered characterization of the tertiary structure of apoB. A "ribbon and bow" model has been proposed for the configuration of apoB100 on the surface of human LDL (28). According to this model, the first 89% of apoB forms a "ribbon" around LDL while the remainder 11% of apoB forms a "bow" that stretches back and crosses over the "ribbon" at the region that encompasses the LDL receptor binding site (28). The circumference of the sphere generated by β strands of the "ribbon" was suggested to be the determining factor of the neutral lipid core size. More recent studies using vitreous ice electron microscopy to determine the morphology of sodium-deoxycholate-solubilized apoB100 confirmed a ribbon-like structure for apoB (29). In these studies, only in a small proportion of molecules "bow" could be identified, leading to speculation that the "bow" observed in previous experiments is likely a result of an artifact of the technique, and that artifactually formed "bows" are less likely in vitrified molecules (29).

Computer modeling and algorithm predictions based on the primary amino acid sequence of apoB suggest that human apoB100 is comprised of 43% α-helix, 21% β-sheets, 20% random coil, and 16% β-turns (30). Furthermore, computer analysis has predicted a pentapartite structure model for the apoB100 polypeptide containing five structurally distinct domains, namely NH_2-βα1-β1-α2-β2-α3-COOH (Fig. 1.1*D*), in which the two domains of amphiphatic β-strands alternate with the three domains of amphipathic α-helices (31, 32). The pentapartite structure of apoB is conserved among nine vertebrate species (33).

Primary sequence homology between the N-termini of apoB and vitellogenin has identified apoB as a member of the vitellogenin gene superfamily (34, 35). Vitellogenin (VTG), synthesized in the liver of egg-laying animals, is an ancient lipid storage and transport protein that serves as a ligand for the delivery of nutrients to the egg yolk (34). Following secretion into the bloodstream and receptor-mediated endocytosis, VTG undergoes specific cleavage into several polypeptides, one of which, referred to as lipovitellin (LV), is the lipid-binding product (36). The crystal structure of lamprey LV (36) has been used for modeling of the N- terminal region of apoB (37).

Through phylogenetic analysis via sequence alignment (37), and database search for proteins containing more than 7 amphipathic β-sheets (32), homology between the N-terminal apoB primary amino acid sequence (residues 1-587) with that of LV was confirmed. Lamprey LV (200 kDa, 1807 amino acids), contains three domains (Fig. 1.2.): a globular N-terminal β-barrel (amino acids 17-296), an extended α-helical structure (amino acids 297-614) and a substantial C-terminal funnel-shaped lipid-binding cavity formed by two β-pleated sheets (amino acids 615-1807) (36). Lamprey LV is a homodimer that can associate with 27 molecules of phospholipid and 11 molecules of TG (36). Based on the coordinates of LV, the βα1 domain of apoB has been modeled (37). In this model, the N-terminal region of apoB (encompassing amino acids 21-263) consists of 13 β-strands that form a globular β-barrel stabilized by disulfide linkages (Fig. 1.3*B*). The amino acids 440-592 downstream of the globular β-barrel form 17 α-helices that are arranged in a double layered helical bundle (Fig. 1.3*D*). Mutagenesis studies have shown

that helices 13-17 of the α-helical domain of apoB are stabilized by salt-bridges (37). With this structural information, a model for the organization of apoB100 on the surface of low density lipoproteins has been postulated (38).

1.2.2. Apolipoprotein B lipid-binding properties

While precise amino acid sequences within apoB100 that are involved in lipid binding have not been yet identified, the hydrophobic face of the β domains within apoB is thought to give the irreversible lipid-binding ability. The regions enriched in amphipathic β-strands are thought to interact directly with the lipoprotein neutral lipid core. On the other hand, the regions rich in amphipathic α-helices are less tightly associated with lipid, and these α-helical domains are thought to confer the reversible association with the lipoprotein surface (38). The minimum length of apoB that is required for the assembly of a neutral lipid core is between 23-28% of the N-terminal portion of apoB100 (39-41).

On the basis of the conservation of the tertiary structures between the N-terminal β-barrel and α-helical domains of lamprey LV and those of apoB, the amphipathic β-sheets within apoB100 were postulated to form a "lipid-binding" cavity during lipoprotein assembly (32). In lamprey LV, the C-terminal lipid-binding domain of is enriched in β-sheets (36). A triangular "lipid cavity" of lamprey LV is lined on its two major sides by antiparallel β-sheets, namely βA:LV and βB:LV, and capped at the bottom by a third antiparalled β-sheet, namely βD:LV (Fig. 1.4*A*). A fourth antiparallel β-sheet of lamprey LV, namely βC:LV, derived from the N-terminal β-barrel, and the double-layered α-

helical structure containing 17 helices are attached to the top of the triangular "lipid cavity". This configuration of LV is thought to allow accommodation of the total of 38 molecules of lipid (36).

In the case of apoB, the "lipid-cavity" was postulated to form following interaction of apoB with a homologous protein, MTP, which has also been identified as member of the vitellogenin superfamily (32). Unlike that of LV, the "lipid-cavity" of an apoB-containing particle is surrounded by three β-sheets, two are from apoB and one from MTP (Fig.1.4*B*). ApoB contains amphipathic β-sheets that are over 3000 amino acid residues in length. Thus, apoB has been postulated to form a "lipid-cavity" that can accommodate larger amount of lipid than that formed by LV. The "lipid-cavity" model supports the hypothesized co-translational lipoprotein assembly model, in which lipid recruitment is achieved through an expansion of the "lipid cavity" of apoB as additional amphipathic β-strands are being synthesized (Fig. 1.4*C*) (32).

1.2.3. Unique features associated with apolipoprotein B biogenesis

ApoB is an unusually large secretory protein. Translation of the full-length apoB100 molecule takes 15-20 minutes and secretion of apoB from the cell occurs after approximately 30 minutes (42). Early studies have shown that apoB mRNA is quite stable, and that apoB biosynthesis is regulated mostly at the post-transcriptional and post-translational levels (43-45). The mRNA editing process, as well as, translocation of apoB into the microsomal lumen, has been shown to be under tight regulation. Possible "pause-transfer" motifs identified within apoB were postulated to uncouple translocation of apoB

across ER membranes from its translation (46, 47). Furthermore, evidence from numerous studies suggested that the lipid association with apoB is highly regulated and is important in determining the fate of the newly synthesized apoB. Thus, inadequate lipid association during apoB translocation may target apoB for degradation.

As mentioned, the apoB100 mRNA editing results in synthesis of apoB48 in the intestine of humans, and in the liver and intestine of some rodents (Section 1.2.) (6,7). Hepatic apoB mRNA editing is under hormonal regulation and can also be regulated by fasting, diet, and ethanol (48). The apoB mRNA editing occurs with great precision, and is mediated through a multicomponent enzyme complex containing a homodimer of the zinc-coordinating cytidine deaminase, APOBEC-1 (49), and yet unidentified protein components. Some of the identified *cis*-acting elements required for apoB mRNA editing have been identified. They include the recognition ("mooring") sequence of 11 nucleotide, an AU-rich sequence upstream and downstream of the mooring sequence, the stem-loop structure in the region surrounding the edited cytidine, and also the presence of 5' and 3 distal "efficiency sequence" (48). Overexpression of APOBEC-1 in transgenic mice results in development of hepatocellular carcinoma (50). The cancer phenotype is likely associated with observed mRNA editing of two other proteins, a tyrosine kinase and a homologue of translation initiation factor RNA, following overexpression of APOBEC-1 in transgenic animals, suggesting that apoB may not be the only substrate for APOBEC-1 (50).

Studies of translocation of apoB into the ER lumen have revealed several unique features. In mammalian cells, translocation of proteins across the ER membrane usually occurs co-translationally through the translocon, a proteinaceous channel whose minimum components are the signal recognition particle (SRP) receptor and the Sec61p complex (51, 52). For most proteins, tight association of the ribosome with the translocon has been suggested to prevent exposure of the translocating polypeptide to the cytosol (53). However, in the case of apoB, it has been found that a large proportion of the newly synthesized apoB is exposed to the cytosol during translation (43, 54-57). Incompletely translocated apoB on the cytosolic side of the microsomal membrane has been detected in various cell models, including rat hepatocytes (58), chicken and rabbit hepatocytes (59), as well as, rat hepatoma McA-RH7777 cells (40).

The topology of apoB with respect to the ER membrane is still unclear. The primary amino acid sequence of apoB does not reveal obvious topogenic sequences that confer transmembrane topology (60). Some researchers claim that the transmembrane topology of apoB could only be observed as a result of translational pausing (61, 62). On the other hand, other groups have proposed that the multiple amphipathic β-sheets of apoB may cluster together forming a membrane-spanning configuration, similar to that observed in porin, an ion-conducting channel protein (63). Porin also lacks classical membrane-spanning sequences, and the amphipathic β-sheets of porin, interestingly, show 43% homology to those found in apoB (64). Studies using chimeric proteins containing putative amphipathic β-sheets of apoB suggested these sequences are able to confer a transmembrane topology (65).

Multiple *in vitro* translocation studies provided evidence that translocation of the nascent apoB polypeptides occurs discontinuously (47), thus translocation undergoes stop and restart at several discrete points during the apoB chain elongation. While efficient translocation has been observed for the first ~85 kDa of apoB, the translocation pausing of the downstream sequence of apoB is thought to be mediated by so-called "pause transfer" sequences. The consensus motif of the pause transfer sequence is LKK-T----N-A (or LKK---SE), and at least 41 candidate pause transfer sequences can be found within the apoB polypeptide (47). Studies of a single pause transfer motif led to observations that the junction between ribosome and the translocon is open during translocational pausing of apoB. Based on these studies, it has been postulated that certain *cis*-acting elements within apoB that contain pause transfer motifs may serve to regulate the rate of apoB translocation (66, 67). The physiological significance of translocational pausing of apoB remains unknown, but it has been hypothesized that the complete translocation of apoB may depend upon the availability of sufficient amount of secretion-coupled lipid (46). Prolonged translocational pausing of apoB in the absence of "lipid-facilitated translocation" may lead to an arrest in translocation that results in delivery of apoB to the proteasome for degradation (68).

1.2.4. Apolipoprotein B degradation mechanisms

In cell culture models, a large proportion of newly synthesized apoB undergoes extensive pre-secretory degradation. Pulse-chase studies with cultured rat hepatocytes showed that a significant amount of apoB was not recovered from cells or media (69).

This was subsequently confirmed in other cell models including HepG2 cells (70) and also, in McA-RH7777 cells (71). Numerous studies have suggested that the rate of apoB production is dependent upon a balance of lipid availability and degradation. In cell culture models, where the lipid availability is likely rate limiting, extensive degradation of the newly synthesized apoB has been observed. However, *in vivo*, the lipid availability may not be limiting, and thus, apoB degradation may play a regulatory role in apoB production only under certain abnormal physiological conditions, such as dyslipidemia.

The close relationship between lipid availability and apoB degradation can be demonstrated by examining the role of oleate in the biogenesis of apoB. Oleate is known to stimulate lipid synthesis and turnover (43, 45, 72). Pulse-chase studies have shown that supplementation with exogenous oleate to HepG2 cell medium results in diminished apoB degradation (70, 73). Since translocation of apoB may be affected by lipid availability (74-76), oleate is thought to act to decrease apoB degradation by increasing the efficiency of apoB translocation. The limited lipid availability in the absence of exogenous oleate of cells in cell culture models, likely results in arrested apoB translocation, and confinement of apoB to a degradative compartment.

Multiple degradative mechanisms have been observed for apoB, ranging from ubiquitin-proteasome mediated co-translational degradation (77), to proteolysis in the ER (78) and post-ER compartments (79, 80). Mechanism of ubiquitin-proteasome mediated apoB degradation has been extensively studied in HepG2 cells, a cell line where intracellular degradation is very active (81). Lactacystin, acetyl-leu-leu-norleucinal

(ALLN), and CBZ-leu-leu-leucinal (MG132), are effective inhibitors of proteasomes, large multi-subunit complexes in the cytosol responsible for much of the intracellular ER-associated degradation (ERAD) (82, 83). The proteasome-mediated degradation of apoB is associated with "retro-translocation" of the newly synthesized apoB across the ER membrane (84). While the ubiquitin-proteasome mediated degradation has been studied in HepG2 cell models (76, 77), it is unclear whether this pathway is responsible for apoB degradation in other cell systems.

Degradation of apoB has also been shown to occur after apoB is fully translocated into the ER lumen. At least two resident candidate ER proteases, ER-60 and ER-70, that may act to mediate apoB degradation in the ER, have been identified in the rat liver and characterized (85-87). Studies also show evidence of an intracellular pathway(s) that can mediate apoB degradation late in the secretory pathway (79, 88). The late degradation pathway involves reduction in secretion of large, already assembled apoB-containing lipoproteins in a post-ER compartment, and involves signaling via phosphoinositide-3 kinase (79).

1.3. Assembly and secretion of apolipoprotein B-containing very low density lipoproteins

The assembly of apoB-containing very low density lipoproteins involves incorporation of neutral lipid by apoB, in a process initiated co-translationally while apoB is still being translocated into the ER lumen (89). Accumulating data suggests that while the C-terminal portion of apoB is still being translated on the ribosome, the N-

terminal portion that has been translocated across the ER membrane has assembled into a lipopoprotein particle (90, 91). An inverse relationship exists between the length of the growing apoB polypeptide and the density of the forming lipoprotein during the assembly of the apoB-containing lipoproteins, as evidenced in multiple studies using C-terminally truncated apoB variants (39, 41, 89, 91, 92). The assembly of large, TG-rich apoB48 and apoB100-containing VLDL is likely achieved by additional mechanism(s).

1.3.1. Assembly of very low density lipoproteins

While much progress has been made toward understanding the mechanism of assembly of the TG-rich VLDL, whether the assembly of TG-rich VLDL is achieved in one step or in two steps has been a matter of debate over the past few decades. The one-step model theorizes co-translational incorporation of bulk TG into growing apoB polypeptide as it emerges from the translocon (93, 94). The two step model of TG-rich VLDL assembly involves both co-translational and post-translational lipid recruitment (95). The latter "two-step" model has taken more precedence (54, 95-100). According to the "two-step " model, the first-step of VLDL assembly involves the co-translational/co-translocational lipid recruitment and the formation of small, dense apoB-containing lipoproteins, while the second step occurs post-translationally with incorporation of bulk TG into primordial particles and maturation into a TG-rich VLDL. The debate still exists, however, over the issue whether the second step occurs in "quantum" fashion involving fusion with a large "apoB-free" lipid droplet, or "continuously" involving sequential addition of TG as the growing lipoproteins traverse the secretory pathway.

According to the "two step" model, during the first step, increasing amount of lipid is recruited with elongation of the growing apoB chain, until a full-length apoB-containing particle is released into the ER lumen. This model is consistent with the two models of lipoprotein assembly mentioned earlier (Section 1.2.1.), the "ribbon and bow" model (28) and the "lipid cavity" model (32). While the N-terminal 22% of apoB100 contains the βα1 domain likely forming a globular structure, the sequence downstream of the N-terminal 22% of full-length apoB100 coincides with the first lipid-associating domain of apoB, the β1 domain. The globular βα1 domain is not involved in lipid recruitment. However, numerous studies have shown a requirement of the βα1 domain for efficient VLDL assembly and secretion (32, 37, 40, 101-106). It has been postulated that the βα1 domain of the nascent apoB associates with the inner leaflet of the ER membrane during the translation and translocation of the downstream C-terminal sequences responsible for lipid recruitment (38).

The second step of the "two-step" model of VLDL assembly is supported largely by evidence from studies showing a "precursor-product" relationship between a primordial lipid-poor particle and mature TG-rich VLDL. From pulse-chase studies of apoB48 performed in rat hepatoma McA-RH7777 cells, a cell line that retains the ability to form VLDL following supplementation with exogenous oleate, it was shown that the lumenal dense, "HDL-like" apoB48-containing lipoproteins are a precursor of the apoB48-containing VLDL particles (90). Furthermore, experiments with increased extraction efficiency of apoB from the membranes have demonstrated that the membrane-associated apoB48 is a precursor of both secreted apoB48-HDL and apoB48-VLDL (107, 108).

Studies of the assembly of apoB100-containing VLDL in McA-RH7777 cells have suggested that the apoB100-containing HDL, significant amount of which being found in the microsomal lumen but not secreted from the cells, may represent a precursor for the secreted apoB100-containing VLDL particles (108).

1.3.2. Origin of triglyceride substrate for assembly of very low density lipoproteins

Under conditions that stimulate the assembly of TG-rich VLDL, the TG substrate utilized for assembly is not the newly synthesized TG. Instead, some evidence exists that the TG stored in the cytosol is mobilized to undergo a "hydrolysis-re-esterification" cycle that results in formation of a "new" TG species that is subsequently a substrate for VLDL assembly (109, 110). The experimental data concerning TG hydrolysis, however, are still inconclusive. The candidate hydrolase(s) responsible for TG hydrolysis identified so far are the microsomal triacylglycerol hydrolase (111, 112) and hormone-sensitive lipase (113). It is not clear whether cytosolic TG is hydrolyzed primarily to DG (114, 115) or completely to glycerol and acyl moieties (116). The low rate of TG hydrolysis in HepG2 cells has been suggested to reflect a possible defect underlying the inability of HepG2 cells to form TG-rich VLDL (117, 118).

The enzyme responsible for re-esterification of the substrates during "hydrolysis-re-esterification" cycle that are used for VLDL assembly is likely mediated by diacylglycerol acyl transferase (DGAT) (119). Two distinct forms of DGAT have been identified with different topology across the ER membrane. The DGAT form whose active site is facing the cytosol may be involved in *de novo* synthesis of TG to be stored

in the cytosol, while the other form of DGAT, whose active site is facing the ER lumen, may be the form responsible for re-esterification of "new" TG. The function of this latter form of DGAT form has been linked to VLDL maturation, whereby DG and fatty acids released through lipolysis are incorporated into TG and used as substrate during VLDL maturation (120, 121).

An important contribution towards TG incorporation during TG-rich VLDL assembly may be provided through phospholipid remodeling (122). Studies with cultured fibroblasts and smooth muscle cells, as well as rat hepatocytes, have demonstrated that the fatty acyl moieties of membrane phospholipids may act as the precursor for the synthesis of TG used as substrate for VLDL assembly (123, 124). The requirement for active synthesis of PC in VLDL assembly and secretion, as observed in rat hepatocytes (125), suggests that, in addition to already known role(s) of PC in lipoprotein metabolism, PC may serve as a key component of the "hydrolysis-re-esterification" cycle. Moreover, other enzymes of lipid metabolism that may be involved in the regulation of lipid availability during VLDL assembly are ACAT (126), 7α-hydroxylase (127,128), and MTP. Overexpression of 7α-hydroxylase in transgenic mice was shown to be associated with coordinate induction of VLDL assembly and secretion (128). The role of MTP in VLDL assembly and secretion will be extensively discussed in Section 1.3.4.

1.3.3. Subcellular location of very low density lipoprotein maturation

Over the past decade or so, conflicting results have been obtained following attempts to determine the exact subcellular compartment of TG-rich VLDL assembly and

maturation along the secretory pathway. Some studies show evidence of maturation in the early secretory pathway while other studies suggest that maturation of TG-rich VLDL occurs late in the secretory pathway. Evidence that mature VLDL can be formed within rough ER came from studies with rat hepatocytes demonstrating VLDL size, density, and lipid composition of the particles isolated from the lumen of the rough ER are similar to VLDL secreted from the same cells (93). Independently, radiolabeled apoB100 and apoB48 proteins were shown to associate with the VLDL fractions in the lumen of the rough ER (94).

On the other hand, experimental evidence abounds indicating that VLDL maturation may not be confined to the rough ER compartment. Early electron microscopic studies did not detect VLDL particles within rough ER *per se* (100). Similarly, immunoperoxidase studies with rat hepatocytes detected apoB immunostaining in the rough ER, while VLDL-sized lipoproteins that were "free" of apoB were observed in the smooth ER (95). These observations led to the proposal that the apoB-free lipid particles are formed in the smooth ER and that they associate with apoB polypeptides synthesized in rough ER at the junction of the rough and smooth ER (95).

Supporting data suggesting that VLDL maturation may not be confined to rough ER were provided by studies addressing the degree of TG recruitment by apoB along the secretory pathway. Studies with isolated rabbit (98) and rat (97, 99) livers showed increased overall association of TG with apoB in the Golgi (over 70%) than that seen in the rough ER (about 30%). Similarly, metabolic labeling studies with chicken

hepatocytes also suggested Golgi may be the primary site for lipid incorporation and VLDL maturation (54, 96).

More recently, evidence that the maturation of TG-rich apoB100-containing VLDL may be achieved through a stepwise process within post-ER compartments was provided by studies using subcellular fractionation and isolation of the distal Golgi, *cis*/medial Golgi and ER by ultracentrifugation (Tran *et al.*, 2002, unpublished observation). No VLDL was detected in the lumen of the ER and *cis*/medial Golgi following pulse-chase analysis and subcellular fractionation, and in these fractions most apoB was found to be membrane-associated. In contrast, VLDL particles could be detected in the lumen of the distal Golgi, suggesting that the distal Golgi may be the site of VLDL maturation.

1.3.4. Microsomal triglyceride transfer protein

Molecular studies and the underlying phenotypes behind the genetic disorder of abetalipoproteinemia have established the requirement of lipid transfer activity of MTP in the assembly of apoB-containing lipoproteins. The protein-protein interaction between apoB and MTP has been postulated to be crucial for lipid recruitment by apoB during the lipoprotein assembly. Multiple functions have been proposed for MTP during apoB-containing lipoprotein assembly. They include the role of MTP during apoB translocation (42), the role of MTP during partitioning of TG between cytosol and microsomal lumen (129), and the chaperone-like activity of MTP during apoB folding (42).

Microsomal triglyceride transfer protein (MTP) was originally isolated from bovine liver microsomal fraction as a protein that catalyzes *in vitro* transfer of TG, CE, and PL between membranes (130). MTP is expressed predominantly in liver and intestine, and to lesser extent, in other tissues (131). On the basis of its tissue distribution, its subcellular localization and ability to transfer lipid, MTP has been implicated in VLDL and chylomicron assembly. MTP is a heterodimer of a large subunit (97 kDa) that contains the lipid transfer activity and of a small subunit (58 kDa) identified as protein disulfide isomerase (PDI) (132). PDI is involved in formation of disulfide bonds within the ER lumen and is implicated in the ER quality control mechanism (133). Mutation of catalytic sites of PDI did not alter the lipid transfer ability of MTP suggesting that the disulfide isomerase activity of PDI is not required for MTP-mediated transfer activity (134). However, some studies suggest that the role of PDI in the complex is to provide solubility (135). In addition, the KDEL sequence found at the C-terminus of PDI but absent in the large subunit of the MTP complex may allow retention of the MTP heterodimer within the ER (136).

In vitro, MTP promotes TG exchange between membranes of vesicles containing equal amounts of TG in membranes of donor and acceptor vesicles. When the amount of TG is drastically different between membranes of donor and acceptor vesicles, MTP promotes net TG transfer (137). MTP has been shown to form a stable complex with both neutral lipids and phospholipids, and the MTP-lipid complex may be an intermediate during lipid transfer process (137). Under similar *in vitro* conditions MTP preferentially transfers neutral lipid as compared with phospholipids, such that the calculated rate of

transfer of TG, CE, and DG is at least 24-, 16-, and 2.5-fold higher than that of PC, respectively (138). Whether MTP performs similar function *in vivo* has not been determined.

Mutations in the large subunit of MTP are a cause of abetalipoproteinemia, a disease manifested by the inability to produce chylomicrons or VLDL in the intestine and liver, respectively. The downstream effects of abetalipoproteinemia in humans include malnutrition, very low plasma cholesterol and TG, and vitamin deficiency (5). MTP was implicated in lipid and lipoprotein metabolism following hepatic inactivation of MTP by gene targeting in transgenic mice, resulting in complete absence of lipid droplets within the secretory compartment (139). The role of MTP in lipoprotein biogenesis was also demonstrated in studies using adenovirus-mediated overexpression of MTP *in vivo* (140).

MTP is a member of the vitellogenin gene family (35). The modeled structure of MTP, based on the coordinates of the lamprey LV crystal structure, suggested that the N-terminus of MTP, like that of apoB, contains a β-barrel region composed of 13-stranded β-sheets (Fig. 1.3*A*) followed by a double layered α-helical structure (Fig. 1.3*C*) (37). Evidence suggests physical interaction of MTP with the βα1 domain of apoB. Multiple MTP-binding sites have been identified within the N-terminal 18% of apoB, including regions that encompass amino acid residues 430-570 (105), 512-721 (103), and likely 2-154 (37). The apoB-binding site on MTP has also been located within helices 13-17 of the predicted α-helical domain of MTP, in close proximity to the PDI binding site on MTP (37, 103).

1.3.5. Role of microsomal triglyceride transfer protein in assembly of very low density lipoproteins

The role of MTP during co-translational apoB-containing lipoprotein assembly has been established following studies with cells dually transfected with apoB and MTP (40, 141-143). This role of MTP was further confirmed in studies with hepatic cells treated with specific MTP inhibitors (75, 144, 145). In these studies, the MTP activity was demonstrated to be essential for the elongation of the apoB polypeptide chain during translation, translocation of apoB across the ER membrane, and for the assembly and secretion of the products of the first step. It has also been suggested that the requirement of MTP activity at the initial stage of apoB-containing lipoprotein assembly is positively correlated with the extent of lipid recruitment.

The role of MTP during post-translational lipid recruitment in the assembly of VLDL has been unclear. Some studies provided evidence that MTP may not be required for the bulk TG incorporation during the "second step" of assembly of the TG-rich apoB100-containing VLDL (108, 146). Since MTP inactivation is known to inhibit TG secretion but not TG synthesis, decreased influx of TG into the microsomal lumen following MTP inactivation led to the postulate that MTP is the factor that mobilizes TG into the microsomal lumen (129). Hence, MTP may be acting as a switch involved in the intracellular TG partitioning between microsomal lumen and the cytosol that occurs independently of VLDL assembly. Recently, an active MTP co-localized with apoB has been detected in the Golgi compartment, the role of which remains to be determined (147) (Fig.1.5.).

1.3.6. Additional factors in maturation of very low density lipoproteins

Multiple factors are likely involved in regulation of the complex VLDL assembly and secretion process (Table I). Stimulation with n-3 fatty acids, insulin, and apoE, to name just a few, has been shown to regulate VLDL assembly and secretion. The n-3 fatty acids have been shown to decrease hepatic VLDL production (148-150). Insulin (151-153) has been shown to be an important negative regulator of apoB and apoB-containing VLDL secretion. Intracellular apoE has been found to up-regulate VLDL secretion (154). In addition, a brefeldin A (BfA)-sensitive factor has been shown to be required for bulk TG incorporation into apoB (155). Brefeldin A is a fungal metabolite that blocks protein trafficking from ER to Golgi. The blockage is caused by inactivation of a guanine nucleotide exchange factor that is essential for binding (via GDP/GTP exchange) of the small ARF (ADP ribosylation factor) GTPase to membranes, a prerequisite for the formation and budding of coated vesicles (156). In McA-RH7777 cells, the assembly and secretion of both B48-VLDL and B100-VLDL is inhibited using low dose of BfA (0.2 μg/ml) (155). While it is not known how BfA inhibits VLDL assembly, it has been postulated that an unknown GTPase, reversibly inhibitable by low dose of BfA, may be responsible for budding or transport of vesicles carrying bulk TG or immature apoB-containing lipoprotein particles.

Further indication that the process of VLDL assembly may involve a GTP- or ATP-binding protein came from studies with rats fed with orotic acid (pyrimidine precursor), resulting in impaired secretion of VLDL (but not HDL) from the liver of these rats, increased hepatic lipids, and fatty liver (157-161). The effect of orotic acid could be

rapidly reversed or prevented by the addition of adenine or adenosine to the diet, as well as by withdrawal of orotic acid from the diet, suggesting the involvement of a GTP- or ATP-binding protein. Recent studies implicated further requirement for small GTP binding proteins and phospholipase D in the later stages of VLDL assembly (162).

Membrane phospholipid remodeling may play an important role in regulation of VLDL assembly. The remodeling of phospholipids in oleate-treated McA-RH7777 cells is mediated primarily by Ca^{2+}-independent phospholipase A_2 (163). The importance of phospholipid species remodeling is still unclear. However, the phospholipid remodeling mediated by phospholipase A_2 may serve to generate oleoyl-enriched membrane phospholipids that could facilitate correct folding of apoB, modulate apoB interaction with various molecular chaperones, or possibly facilitate the acquisition of bulk neutral lipids in the distal Golgi.

1.4. Post-translational modifications of apolipoprotein B

Modifications of the apoB structure that regulate its biosynthesis, in turn, may represent important regulators of efficient VLDL assembly and secretion. Multiple evidence points out that biosynthesis of apoB is regulated at a post-translational level. ApoB is modified by disulfide bonding at the N-terminus (19), phosphorylation (24), addition and subsequent processing of N-linked oligosaccharides along the secretory pathway (18), and palmitoylation (20-23). Post-translational modifications of apoB, such as disulfide bond formation (102, 106) and palmitoylation (164), have been shown to be required for the assembly and secretion of apoB-containing lipoproteins. However, clear

biochemical evidence for a precise role for some of these, particularly, palmitoylation and the addition of N-linked oligosaccharides, in the assembly and secretion of apoB-containing VLDL has not been obtained.

1.4.1. Phosphorylation of apolipoprotein B

Phosphorylation of proteins regulates rapid and reversible alteration of the protein enzyme activity and protein-protein interactions. Phosphorylation has been proposed to play a role in the mechanism of apoB mRNA editing (165). The editing of apoB mRNA can be significantly modulated by protein kinase inhibitors or activators altering cellular phosphorylation, and also, the editing activity of human APOBEC-1 can be significantly altered by eliminating potential phosphorylation sites (165).

That apoB itself is a phosphorylated protein was shown in studies of secreted apoB48 from hepatocytes of sucrose-fed rats where phosphorylated apoB48 but not apoB100 was found in rat plasma (24). Subsequently, it has been shown that both apoB48 and apoB100 are secreted as phosphoproteins from hepatocytes of rats on normal diets. However, in the same studies, increased apoB phosphorylation was observed in hepatocytes from diabetic rat (166). Additional studies have suggested that phosphorylation may play a role in regulating secretion and degradation of apoB (167). In recent studies, it has been suggested that Golgi may be the intracellular site of apoB phosphorylation (168). In an *in vitro* system utilizing rat hepatic Golgi fractions, phosphorylated apoB100 was found mostly associated with the membrane fraction while phosphorylated apoB48 was found in the lumenal contents. Moreover, these studies

suggested that cAMP dependent protein kinase is not involved in the phosphorylation process (168).

Phosphorylation may play a role in the events regulating secretion of apoB-containing lipoproteins, and thus, it is thought to occur late in the secretory pathway in much the same way as the phosphorylation of vitellogenin has been shown to be a late event during its secretion (169). Phosphorylation may also act in signaling the movement of apoB away from the membrane during apoB-containing VLDL assembly. Yet another possibility is that the function of phosphorylation may be to target or to protect apoB from degradation.

Phosphorylation of apoB has been proposed to be the vehicle by which insulin regulates secretion of apoB-containing VLDL (170). Insulin can regulate VLDL secretion via multiple mechanisms including effects on apoB synthesis and degradation (170), and modulation of MTP expression (171). Studies in primary rat hepatocytes indicated that the inhibition of apoB secretion by insulin is a result of enhanced intracellular degradation of newly synthesized apoB (172), and that the effect is mediated by the action of the insulin receptor (173). Studies have also shown that the downstream effects of insulin action result in activation of phosphoinositide 3-kinase, a downstream effector protein known to phosphorylate phosphatidylinositols (174, 175). Furthermore, insulin has been shown to decrease apoB phosphorylation (167). The detailed role of phosphorylation of apoB during apoB-containing assembly and secretion remains to be determined.

1.4.2. The importance of disulfide bonds at the amino terminus of apolipoprotein B in very low density lipoprotein assembly and secretion

Proper folding of most secretory proteins requires formation of disulfide bonds as the proteins co-translationally translocate across the ER membranes. Disulfide bond formation is mediated by the enzyme protein disulfide isomerase (PDI), which exists as an ER resident tetramer complex (α_2/β_2). The β subunit contains a C-terminal KDEL sequence responsible for ER retention (133). The β subunit of PDI mediates disulfide exchange that involves cleavage and reformation of disulfide bonds. PDI forms a heterocomplex with MTP, as well as, with another enzyme, isoprolyl hydroxylase (133). As mentioned earlier (Section 1.3.4.), while the activity of PDI is not required in the complex, it is thought that PDI renders solubility to these complexes (134). In the absence of proper disulfide formation, most proteins are misfolded, retained in the ER through interaction with molecular chaperones, and targeted for degradation.

Of the total 25 cysteine residues that are present in full length apoB100, 16 are involved in the formation of disulfide bonds, 7 are known to be free, while status of the remaining two, at cysteine residues 2906 and 4326, respectively, is unknown (19). Interestingly, seven of the total of eight disulfide bonds are clustered within the N-terminal 500 amino acids of the apoB βα1 domain (Fig.1.1*C*), a region of apoB thought to fold into a globular structure (19). As mentioned earlier (Section 1.3.1.), even though the compact structure yields low affinity for binding to the lipids (176), the N-terminal region of apoB has been shown crucial for proper formation and secretion of VLDL (40,

104). That folding of this N-terminal region of apoB requires proper disulfide bond formation and, in turn, is required for VLDL assembly, was shown in experiments using ditheothreiol (DTT) to perturb formation of disulfide bonds, resulting in impaired secretion of apoB (177). Disulfide bonds at the N-terminus of apoB are important for proper folding and secretion competence of apoB regardless of the lipidation state, as shown using DTT-treated C127 cells that are devoid of MTP expression and are capable of secreting only the dense "HDL-like" particles (178).

The importance of each of the seven disulfide linkages located within the N-terminal 500 amino acids of apoB was studied by using site-specific mutagenesis (Cys-to-Ala or Cys-to-Ser substitutions) that disrupted normal disulfide bond formation (102, 106). Disruption of some of these disulfide bonds had little or no effect on secretion of apoB. However, two of the disulfide clusters, namely the second and fourth linkage from the N-terminus, have been shown to be crucial for secretion of the C-terminally truncated B29 protein, as well as, for the efficient assembly and secretion of apoB50-containing VLDL (106).

Perturbation of disulfide bond formation may lead to apoB misfolding and increased apoB proteasomal degradation, as suggested by studies using DTT treatment resulting in decreased apoB100 translocation across ER membrane and increased ubiquitination and association with Sec61-component of the translocon (179). Furthermore, ubiquitin-mediated proteasomal degradation of apoB has been linked to association of apoB100 with immunoglobulin binding protein (BiP) (180), a molecular

chaperone that interacts with unshielded regions of misfolded proteins and catalyzes their refolding. While the folding process of apoB itself has not been well defined, it may require the network of molecular chaperones found in the ER. Besides BiP and MTP, multiple ER resident molecular chaperones have been found to associate with apoB, such as calnexin and ERp57, and more recently calreticulin, ERp72, and GRP94 (181, 182). How or if these chaperones participate in regulation of apoB folding, stability, and secretion competence remains to be determined.

1.4.3. Mechanisms of endoplasmic reticulum quality control

The primary function of the quality control system of the ER is to ensure correct folding of the newly synthesized polypeptide (183). This role is fulfilled through the action of multiple enzymes, such as PDI, and molecular chaperones such as BiP, calnexin and calreticulin (183). The role of BiP and PDI in protein folding has been documented (184). BiP has been found associated with many mutant, misfolded, or improperly assembled proteins in the ER with a function to monitor protein folding and prevent ER exit of misfolded proteins (183). BiP protects the misfolded proteins from aggregation by binding to the exposed protein regions in an ATP-dependent fashion (183).

Calnexin, a type I membrane protein, and calreticulin, its soluble ER lumenal paralog, belong to a family of lectins that is conserved across species (185). The lumenal domain of calnexin has been shown to interact with the nascent chains of the newly synthesized N-linked glycoproteins immediately upon their translocation into the ER (186). Recent studies have shown that the presence or absence of a glycosylation site

close to the N-terminal (within 50 amino acids) of the protein determines whether the newly synthesized protein will associate co-translationally with calnexin and calreticulin, or with BiP, respectively (187). Both calnexin and calreticulin have been shown to form heterodimeric complexes with ERp57, a thiol oxidoreductase and a homolog of PDI (188). Partial determination of the tertiary structure of calnexin suggested that calnexin and calreticulin are highly asymmetric molecules containing a long, hydrophilic peptide that is formed by the so-called P-domain, a region composed of proline-rich tandem sequence (189).

The "binding-and-release" cycle of association of calnexin and calreticulin with the oligosaccharide moiety of the proteins has been postulated to play a role in regulating correct protein folding (Fig. 1.6.) (190). Calnexin and calreticulin binding is specific for the monoglucosylated form of the glycans (185, 190). The cycle is driven by the action of two soluble ER enzymes, namely uridine diphosphate (UDP)-glucose:glycoprotein glucosyltransferase (GT), which adds a glucose residue to high-mannose glycans, and the glucosidase II, which catalyzes glucose trimming (185, 191). The GT enzyme is thought to function as the "folding sensor" so that the cycle is repeated until the protein is correctly folded. With correct folding, the protein does not undergo reglucosylation, or interaction with calnexin and calreticulin, and hence, is free to leave the ER (185, 190).

In addition to facilitating correct folding of newly synthesized proteins, the other important function of the ER quality control is to target the terminally misfolded proteins for ER-associated degradation (ERAD) (192). ERAD involves retro-translocation of

misfolded proteins via the ER translocation pore into the cytosol, where they are ubiquitinated and degraded by the proteasome (183, 192). Two distinct ER quality control mechanisms, the retention and the retrieval pathway, have recently been proposed for the sorting of the misfolded protein (193). While the misfolded soluble proteins are transported to the Golgi apparatus, and retrieved back to the ER via the retrograde transport pathway, the misfolded membrane proteins are retained in the ER (193). Function of the recently identified gene in yeast, *BST1*, has been implicated in the transport of misfolded soluble proteins from the ER to Golgi (193).

1.4.4. Mechanisms regulating the unfolded protein response

Accumulation of misfolded proteins leads to ER stress that results in triggering of an important intracellular pathway, designated as the unfolded protein response (UPR). The function of the UPR signaling overlaps with the functions of the ER quality control and ERAD (194). Treatment with agents known to impair protein folding, including inhibition of N-linked glycosylation using tunicamycin, reduction of disulfide bonds using DTT, and disruption of calcium homeostasis (194), have been shown to trigger UPR, resulting in up-regulation of molecular chaperones known to associate with misfolded proteins, BiP (GRP78) and GRP94 (194).

In yeast, the UPR signaling pathway requires only three components, namely Ire1p, Hac1p, and Rlg1p (195). Accumulation of misfolded proteins in the ER leads to ER stress, with subsequent oligomerization of the ER transmembrane protein kinase/endoribonuclease Ire1p, its autophosphorylation and activation of downstream

signaling (195). Under non-stress conditions the luminal domain of Ire1p has been suggested to form stable complexes with GRP78/BiP. ER stress is thought to promote reversible dissociation of GRP78/BiP from the luminal domain of Ire1p, and activation of the Ire1p autophosphorylation and UPR signaling (Fig. 1.7.) (196, 197). The endoribonuclease domain of Ire1p catalyzes splicing of the *HAC1* mRNA, the mRNA encoding basic leucine zipper transcription factor Hac1p, while the activity of Rlg1p, a tRNA ligase, is required to re-ligate the transcript (195). Whereas unspliced *HAC1* mRNA is poorly translated, spliced *HAC1* mRNA is efficiently translated into a functional transcription factor that activates transcription of genes that contain UPR elements (UPRE) in their promoters (195). The UPR signaling in yeast requires only these three components, as shown in an *in vitro* reconstitution system (198).

While the mechanism of UPR signaling in yeast has been well characterized, the UPR signaling pathway in mammalian cells is less clearly defined. Mammalian UPR seems to be more complex than that discovered in yeast and is mediated through multiple pathways. Homologues of Ire1p have been identified recently in higher eukaryotes, including Ire1α (199), Ire1β (200), and PERK (201). Instead of *HAC1* mRNA, the target of Ire1p-mediated splicing in mammalian cells is the recently identified *XBP-1* mRNA (195). Furthermore, activation of the mammalian UPR requires proteolytic cleavage of Ire1p that releases a soluble form into the nucleus (195). What generates complexity in the mammalian UPR is the divergence in the downstream signaling events following a response of Ire1α, Ire1β, and PERK to the inducers (195). Furthermore, an additional

pathway mediated by the activity of the ATF6 transcription factor was found to be essential for induction of the mammalian UPR signaling (195).

The UPR allows cells to elicit multiple downstream effects including transcriptional induction of molecular chaperones, attenuation of translation, and degradation of misfolded proteins. In addition, the volume and capacity of the ER to accommodate misfolded protein increases following UPR-stimulated induction of lipid synthesis (194). Under conditions of long-term accumulation of misfolded protein in the ER, however, cells respond by activation of the apoptotic pathways. Chronic ER stress that was a result of long-term ER accumulation of misfolded proteins has been associated with multiple diseases, such as α1-antitrypsin deficiency, retinis pigmentosa, cystic fibrosis, as well as, the early onset of familial Alzheimer's disease (202). Homocysteine-mediated induction of ER stress and UPR in cultured human hepatocytes has also been shown to result in dysregulation of the cholesterol and triglyceride biosynthetic pathways (203). Hence, UPR signaling pathway(s) may represent an important link between chronic ER stress and the onset of some diseases.

1.4.5. The N-linked oligosaccharides of apolipoprotein B

The asparagine (N)-linked oligosaccharides of proteins are an important component of the quality control mechanisms of eucaryotic cells. However, other roles have been assigned to N-linked oligosaccharides, including protection from proteolytic degradation, intracellular trafficking, secretion, cell surface expression, maintenance of protein conformation, cell-cell recognition, and enzymatic activity (190). N-linked glycosylation

of proteins commences co-translationally with addition of 14 sugars *en bloc* to the newly synthesized polypeptide in the ER (Fig. 1.8.). The assembly of the 14 sugars $(Glc)_3(Man)_9(GlcNAc)_2$, representing the "core oligosaccharide unit", on the dolichylpyrophosphate precursor occurs on the membrane side of the ER, and the completed core is then transferred from the dolichylpyrophosphate precursor and coupled through an N-glycosidic bond to asparagine of the protein (190). The transfer of the core oligosaccharide is catalyzed by oligosaccharyltransferase that recognizes a specific conformation of the protein motif Asn-X-Ser/Thr (204). The presence of the N-linked oligosaccharide is thought to render a compact conformation, such as β turn, to a glycoprotein (205).

The process of N-linked glycosylation involves assembly of the core oligosaccharide that is followed by subsequent post-translational trimming and rebuilding into different forms (Fig. 1.9.). The trimming involves removal of the three terminal glucoses of the core oligosaccharide unit by glucosidase I and II, and the removal of the terminal mannoses by mannosidase (190). The "glucosylation-deglucosylation" or "binding-and-release" (mentioned in Section 1.4.3.) cycles are thought to regulate proper folding of proteins through regulation of their association with calnexin and calreticulin. All glycoproteins undergo similar alterations in the ER, which provides a limited spectrum of glycoforms. The terminal glycosylation pathways may provide significant structural diversification once glycoproteins transit to the Golgi apparatus, where glycoproteins undergo further trimming, and addition of new sugars such as GlcNac, galactose, sialic acid, and fucose (190). Thus, while the role of N-linked glycans in the

ER seems to be mainly involved in regulating protein folding and ER quality control, the highly complex, branched structures present in mature proteins in the Golgi may provide a spectrum of novel, yet unidentified functions.

There are 20 potential N-linked glycosylation sites within apoB100, of which 16 Asn residues are conjugated with oligosaccharides on plasma low-density lipoproteins (LDL) (18). ApoB100 from human LDL has been shown to contain 8-10% carbohydrate, by weight, consisting of galactose, mannose, glucosamine, and sialic acid (206). ApoB has been shown to contain both high mannose and complex carbohydrate chains (207). Previous studies have addressed a possible role of N-linked glycosylation in regulating the binding of LDL to the LDL receptor and LDL particle internalization (208-211). It was shown that desialylated LDL were internalized by cultured human arterial smooth muscle cells more rapidly than native LDL were (210) and also, accumulated in the rabbit aorta more than normal LDL did following injection into the animal (209). Desialylation of LDL was shown to have no effect on degradation in cultured rat hepatocyte (208). Furthermore, the removal of carbohydrate moieties from LDL by digestion with a mixture of glycosidases did not alter its binding to the cultured human fibroblast cells (211). In more recent studies, ectopic expression of an enzyme that regulates branching of N-linked oligosaccharides, N-acetylglucosaminyltransferase III, in transgenic hepatocytes, was found to impair apoB secretion and induce generation of fatty liver in mice (212).

The role for N-linked oligosaccharides of apoB in apoB-containing VLDL assembly and secretion has not been determined. Early studies with rat or chicken hepatocytes suggested that inhibition of N-linked glycosylation of apoB with the chemical inhibitor tunicamycin had no major impact on VLDL secretion (213, 214). However, experiments with human hepatoblastoma HepG2 cells showed that secretion of apoB100 was reduced by the tunicamycin treatment (215). Furthermore, decreased apoB100 secretion in tunicamycin-treated HepG2 cells was found associated with increased apoB degradation (216, 217).

1.4.6. Palmitoylation of apolipoprotein B

Fatty acylation involves covalent attachment of fatty acids, such as myristate and palmitate, onto the protein backbone. Two types of fatty acylation have been characterized based on whether attachment occurs through an amide linkage (N-acylation) or thioester linkage (S-acylation) (218, 219). Myristoylation involves an irreversible co-translational attachment of the 14-carbon myristate onto an N-terminal glycine via amide linkage, and is a well-characterized process catalyzed by an enzyme N-myristoyl transferase (218, 219). Palmitoylation, on the other hand, involves a reversible, post-translational attachment of the 16-carbon palmitate onto a free cysteine via thioester linkage. A candidate enzyme, a membrane-associated palmitoyl transferase (PAT) activity, associated with palmitoylation of myristoylated substrates, has been partially purified from bovine brain (220). Cytosolic acyl protein thioesterase responsible for turnover of thioacyl groups has been identified that together with PAT may represent the

molecular machinery of the regulated thioacylation cycle in the cell (221). While no apparent consensus sequence exists for palmitoylation, some signaling molecules, such as the members of the Src kinase family and the α subunits of the heterotrimeric G proteins, contain the sequence myrGlyCys, where Cys-3 is palmitoylated following myristoylation (218, 219).

Multiple roles have been proposed for palmitoylation of proteins and they range from a role in anchoring proteins to membranes, regulation and stabilization of protein-protein interactions, subcellular localization, and regulation of enzymatic activity in mitochondria (219, 222, 223). Palmitoylation has been shown to play a role in mediating anchoring to membranes for many signaling molecules that translocate between the cytosol and plasma membrane (218, 219). For some of the signaling molecules, dual lipidation, involving myristoylation of the protein that precedes palmitoylation, is the necessary and sufficient targeting signal for the proteins to the plasma membrane (218, 219). Furthermore, palmitoylation of proteins has been shown to be critical for localization of some proteins in detergent-resistant microdomains (DRMs) of the plasma membrane, namely in caveolae, the signaling depots enriched in cholesterol, glycosphingolipids, and glucosyl phosphatidylinositol-anchored proteins (219). More recently, palmitate cycling of a protein PSD-95 at the synapse has been shown to regulate synaptic strength (224).

Apolipoprotein B undergoes covalent fatty acylation whereby palmitate is attached through a thioester bond (20-23). While the role of apoB palmitoylation in apoB-

containing VLDL assembly and secretion has not been addressed, evidence was provided for the role of palmitoylation at a single cysteine at position 1085 in the assembly and secretion of apoB29-containing lipoproteins (164). In this study, it was proposed that palmitoylation might play a structural role during the assembly of B29-containing lipoproteins, as well as, a positional role in the apoB intracellular trafficking (164).

1.5. Thesis objective

The overall hypothesis of this thesis is that post-translational modifications of apolipoprotein B play an important regulatory role during the complex metabolic process of VLDL assembly and secretion. The focus of this thesis will be on determining the role(s) of two types of post-translational modifications, namely N-linked glycosylation and palmitoylation, of human apolipoprotein B in the assembly and secretion of apoB-containing VLDL using rat hepatoma McA-RH7777 cells stably expressing C-terminally truncated human apoB variants. The assembly of apoB48- and apoB100-VLDL in McA-RH7777 cells has been studied extensively (107, 129, 225). In these cells, the VLDL assembly proceeds through a two-step lipidation process. In the first step of lipidation, primordial lipoproteins with density similar to that of HDL (d =1.063-1.21 g/ml) are generated co-translationally. In the presence of sufficient lipid availability, second step lipidation occurs and involves bulk incorporation of lipid into the core of the primordial particle to form mature VLDL (107, 129). Supplementation with exogenous oleate to medium of rat hepatoma McA-RH7777 cells has been shown to lead to stimulation of VLDL production (90). Hence, the well-characterized apoB48-VLDL assembly process in rat hepatoma McA-RH7777 cell line provides a good system for studies of the post-

translational modifications at the amino terminus of human apoB structure in apoB-containing VLDL assembly and secretion.

The following questions will be addressed:

(a) Are N-linked oligosaccharides required for proper synthesis and secretion of human C-terminally truncated apoB variants? If so, are all N-linked oligosaccharides equally important?

(b) Does assembly and secretion of apoB-containing VLDL require proper N-linked glycosylation of apoB?

(c) What role(s) do N-linked oligosaccharides play in apoB biogenesis?

(d) Is palmitoylation required for biosynthesis of the human apolipoprotein B48-containing VLDL?

FIG. 1.1. **Structure of human apolipoprotein B.** *A,* schematic representation of the amino acid residues within human apolipoprotein B. Two forms of apoB synthesized naturally are the full-length apoB100 and the N-terminal 48% of the full-length apoB, designated B48. B, the line depicts position of the N-linked oligosaccharides within human apoB100. There are 20 NxS/T consensus N-linked glycosylation sites within apoB100, 16 of them glycosylated *(closed rectangles)* and 4 of them non-glycosylated *(open rectangles)* (18). *C,* the line depicts position of the cysteine residues within human apoB100. Cysteines that are involved in disulfide linkages are connected (19). *D,* the pentapartite model of the human apoB100 structure (31).

Fig. 1.1.

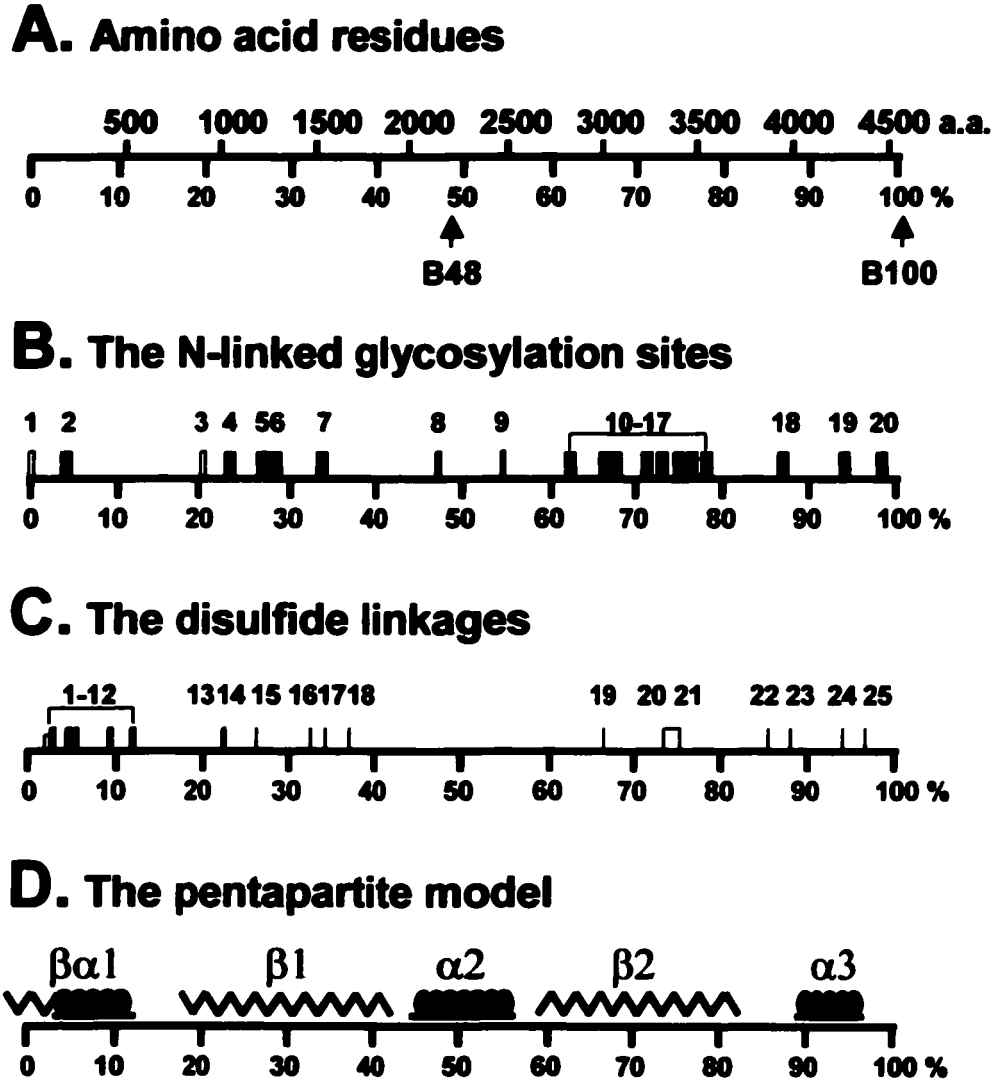
A. Amino acid residues
500 1000 1500 2000 2500 3000 3500 4000 4500 a.a.
0 10 20 30 40 50 60 70 80 90 100 %
B48
B100
B. The N-linked glycosylation sites
1 2 3 4 56 7 8 9 10-17 18 19 20
0 10 20 30 40 50 60 70 80 90 100 %
C. The disulfide linkages
1-12 1314 15 161718 19 20 21 22 23 24 25
0 10 20 30 40 50 60 70 80 90 100 %
D. The pentapartite model
βα1 β1 α2 β2 α3
0 10 20 30 40 50 60 70 80 90 100 %

FIG. 1.2. **Model of the lamprey lipovitellin monomer.** Ribbon diagram of the lamprey lipovitellin monomer. The atomic coordinates of the X-ray crystal structure for lamprey LV (36, 226) were obtained from the Protein Databank, Brookhaven, accesion code 1LLV. Color-coding represents the three domains of LV. The model was created using the program RASMOL.

Fig. 1.2.

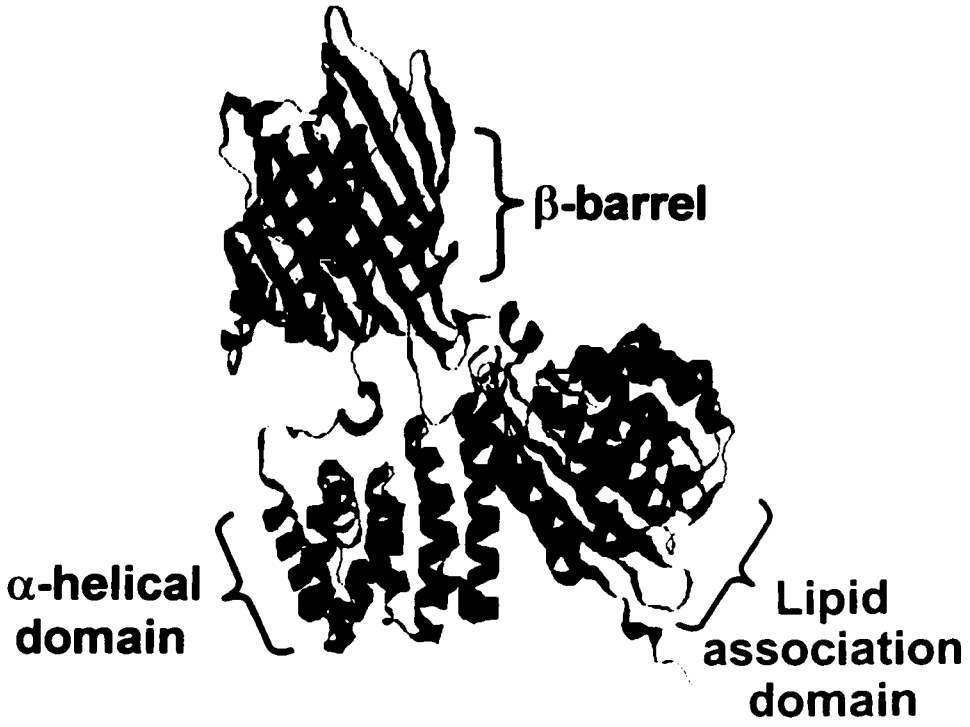

FIG. 1.3. **Molecular models of MTP and apoB.** The models were generated using the atomic coordinates of lamprey lipovitellin. *A*, model of the MTP β-barrel. *B*, model of the apoB β-barrel. *C*, the predicted α-helical bundle of MTP. *D*, the predicted α-helical bundle of apoB. The α-helices are depicted as blue cylinders, disulfide bonds are red, loops are gray and β-strands are yellow, except for those that correspond to the homodimerization interface of lamprey lipovitellin, which are shown in green (adapted with permission from (37)).

Fig. 1.3.

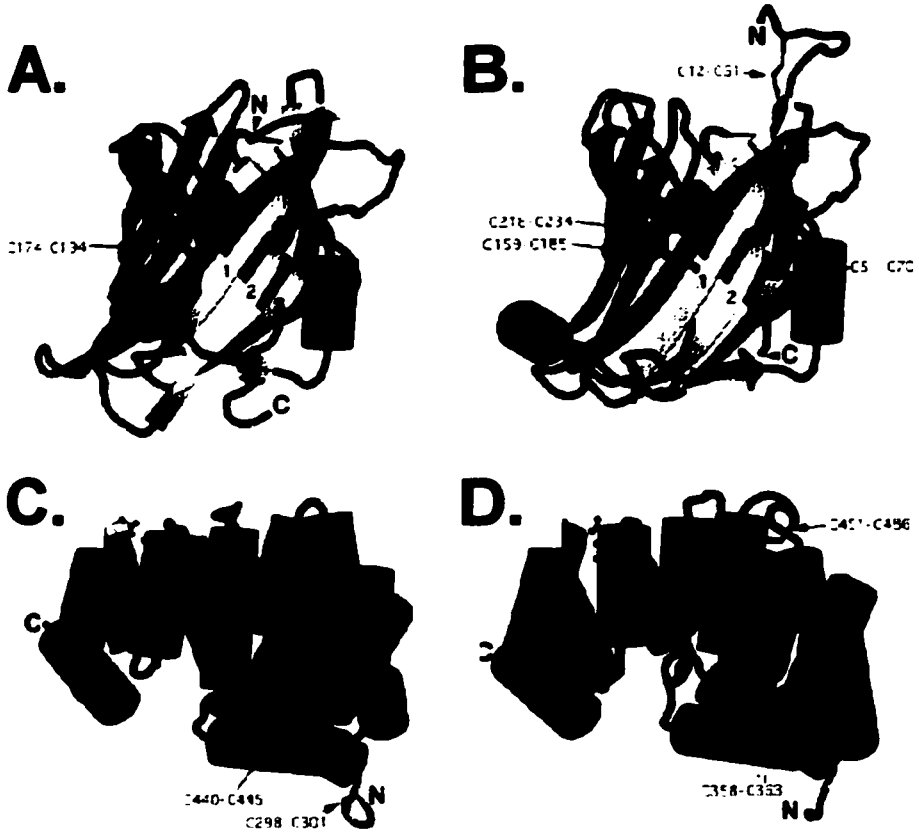

FIG. 1.4. **"Lipid-cavity" model for assembly of apolipoprotein B-containing lipoprotein particles.** *A,* model of the lamprey lipovitellin "lipid cavity" viewed from above. Green circles represent phospholipid headgroups. Lipovitellin consists of four β-sheets, namely βC:LV, βA:LV, βB:LV, and βD:LV, and an α-helical cluster, α:LV (α-helices are represented with cylinders and antiparallel β-sheets with arrows). *B,* the proposed "lipid cavity" model of apoB. To complete the "lipid cavity" (compare with *A*) βA:B and βB:B require the contribution of the βB:MTP and the α-helical cluster α:MTP ApoB structure is represented by blue while MTP is represented by red. C, the amphipathic β strands (blue dashes) located in the α_1 domain of apoB form an incomplete "lipid pocket". In presence of MTP, the pocket fills up with lipid (shown by yellow, green, and black). Elongation of the apoB chain results in addition of more amphipathic β strands from the β_1 domain of apoB, allowing the expansion of the "lipid-cavity" until lipoprotein particles with HDL-like and VLDL density are formed (adapted with permission from (32)).

Fig. 1.4.

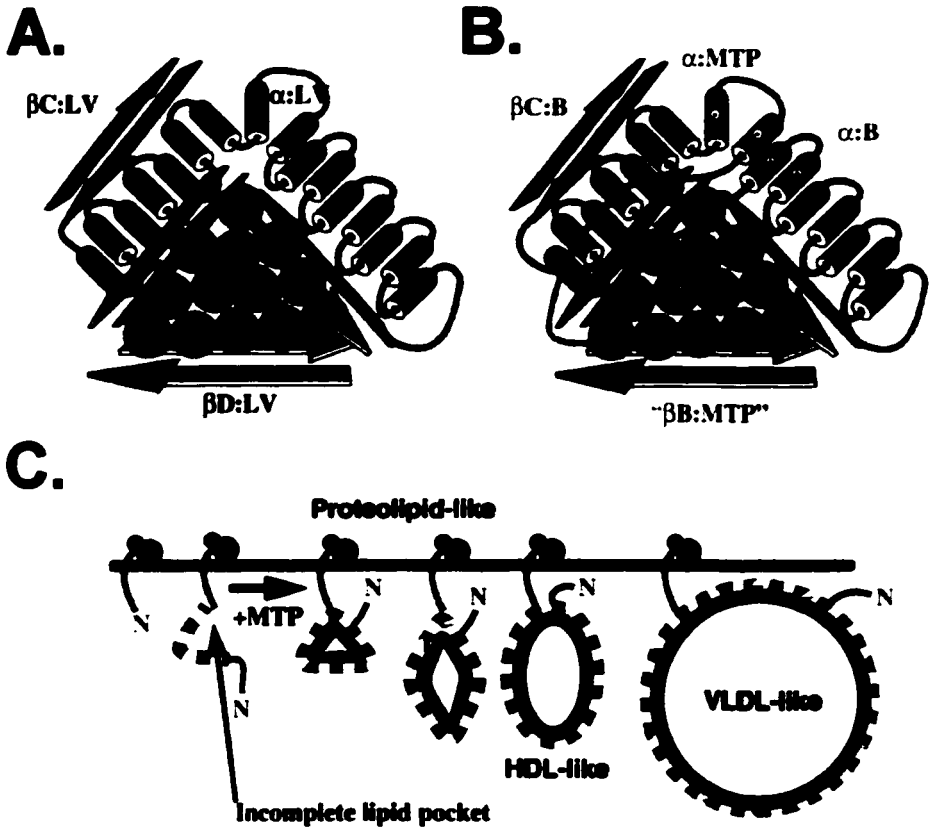
A.
βC:LV
α:L
βD:LV
B.
α:MTP
βC:B
α:B
"βB:MTP"
C.
Proteolipid-like
N
+MTP
N
N
N
N
N
HDL-like
VLDL-like
Incomplete lipid pocket

FIG. 1.5. **Model for the assembly of apolipoprotein B-containing VLDL.** The assembly of apoB-containing very low density lipoproteins involves incorporation of neutral lipid by apoB along the intracellular secretory route (depicted by black arrows between the intracellular compartments). The assembly process is initiated co-translationally while synthesizing apoB (red lines), still associated with ribosomes (black circles), is translocating into the ER lumen. The assembly is achieved in a two-step lipidation process. The first step requires co-translational lipid (yellow) recruitment by apoB (red) to form dense, primordial particles that are membrane-associated. The MTP (blue) activity may be required for the elongation of the apoB polypeptide chain during translation, translocation of apoB across the ER membrane, and for the assembly of the products of the first step. The second step involves bulk lipid recruitment by apoB, and maturation of particles into TG-rich VLDL that are soluble and secretion-competent. Distant Golgi is the likely intracellular site of VLDL maturation. MTP may not be required for bulk TG incorporation during the "second step" of assembly of VLDL, but may be acting as a switch that mediates the intracellular TG partitioning between the microsomal lumen and the cytosol (represented by blue arrows outside of the *cis*-Golgi).

Fig. 1.5.

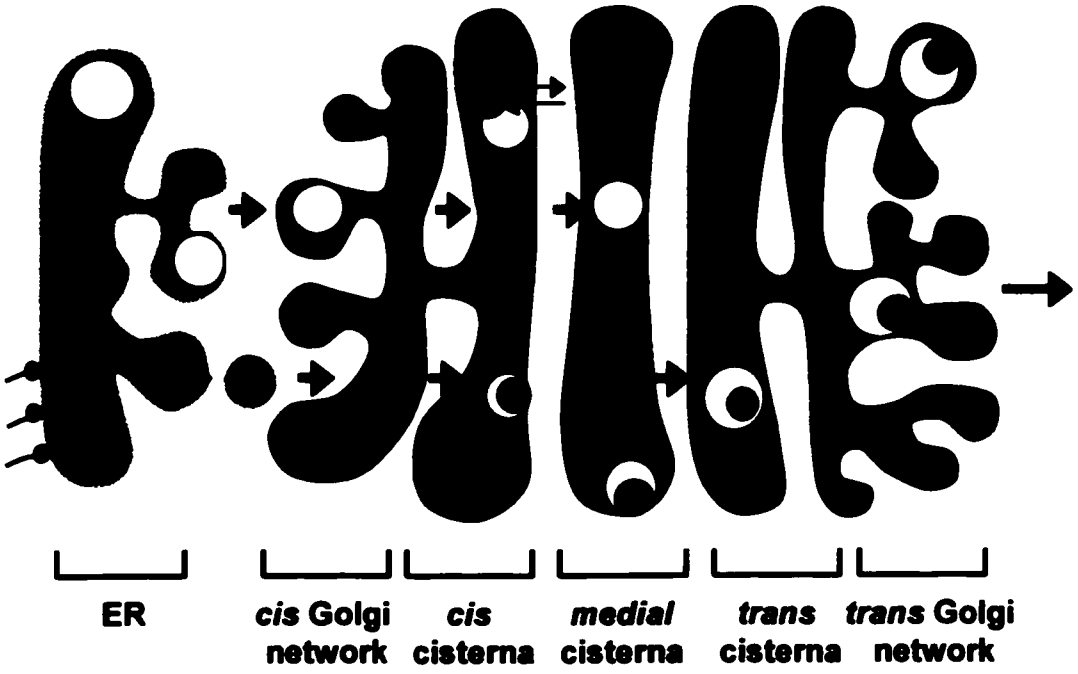
ER
cis Golgi network
cis cisterna
medial cisterna
trans cisterna
trans Golgi network

FIG. 1.6. **The calnexin-calreticulin cycle.** The nascent or newly synthesized glycoproteins interact with calnexin (CNX) or calreticulin (CRT), ER chaperones that recognize monoglucosylated core oligosaccharides (glucose residues are represented by red triangles), and another folding factor ERp57, that binds to both CNX and CRT. Trimming of the last glucose residue by glucosidase II leads to dissociation of the complexes. If the glycoprotein is not folded at this time, the oligosaccharides are reglucosylated by an ER glucosyltransferase, and the protein reassociates with CNX or CRT. The cycle is repeated until the glycoprotein is either folded or degraded. Once correctly folded, a glycoprotein is no longer recognized by the glucosyltransferase, or by CNX or CRT, and can exit the ER.

Fig. 1.6.

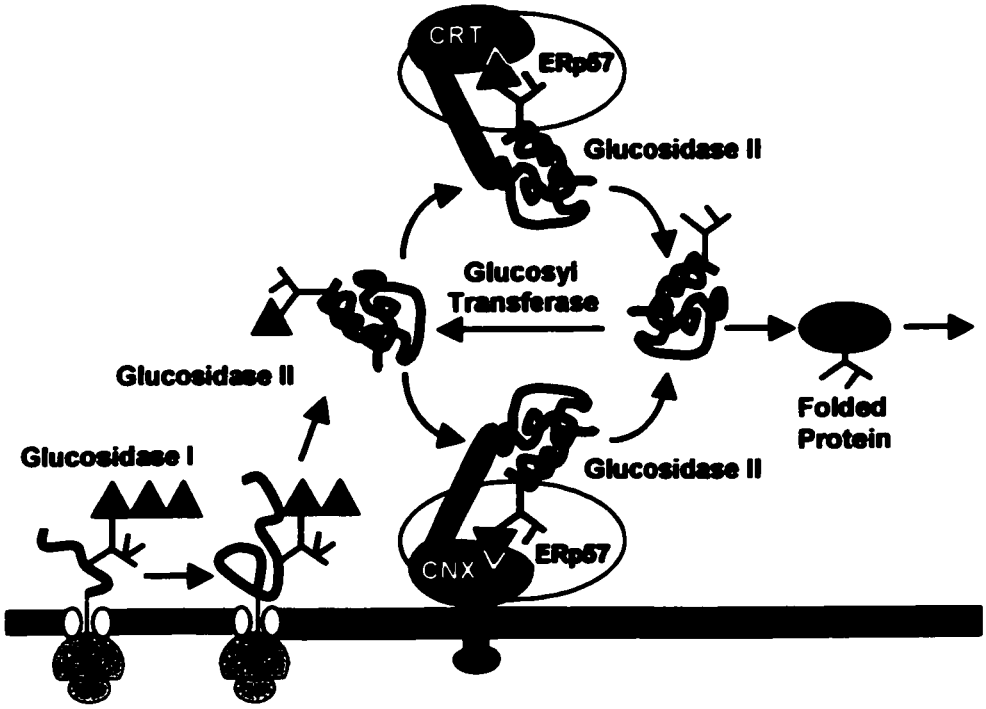
CRT
ERp57
Glucosidase II
Glucosyl
Transferase
Glucosidase II
Folded
Protein
Glucosidase I
Glucosidase II
CNX
ERp57

FIG. 1.7. **The unfolded protein response (UPR).** Under non-stress conditions the endoribonuclease/kinase Ire1 forms stable complexes with GRP78/BiP. Accumulation of misfolded proteins in the ER leads to ER stress and triggers the unfolded protein response (UPR). ER stress is thought to promote reversible dissociation of GRP78/BiP from the luminal domain of Ire1p, activation of Ire1p autophosphorylation, oligomerization, and activation of downstream signaling. In yeast, the endoribonuclease domain of Ire1p catalyzes splicing of the *HAC1* mRNA, encoding the basic leucine zipper transcription factor Hac1p. Whereas unspliced *HAC1* mRNA is poorly translated, spliced *HAC1* mRNA is efficiently translated into a functional transcription factor that activates transcription of genes encoding ER chaperones that contain UPR elements (UPRE) in their promoters.

Fig. 1.7.

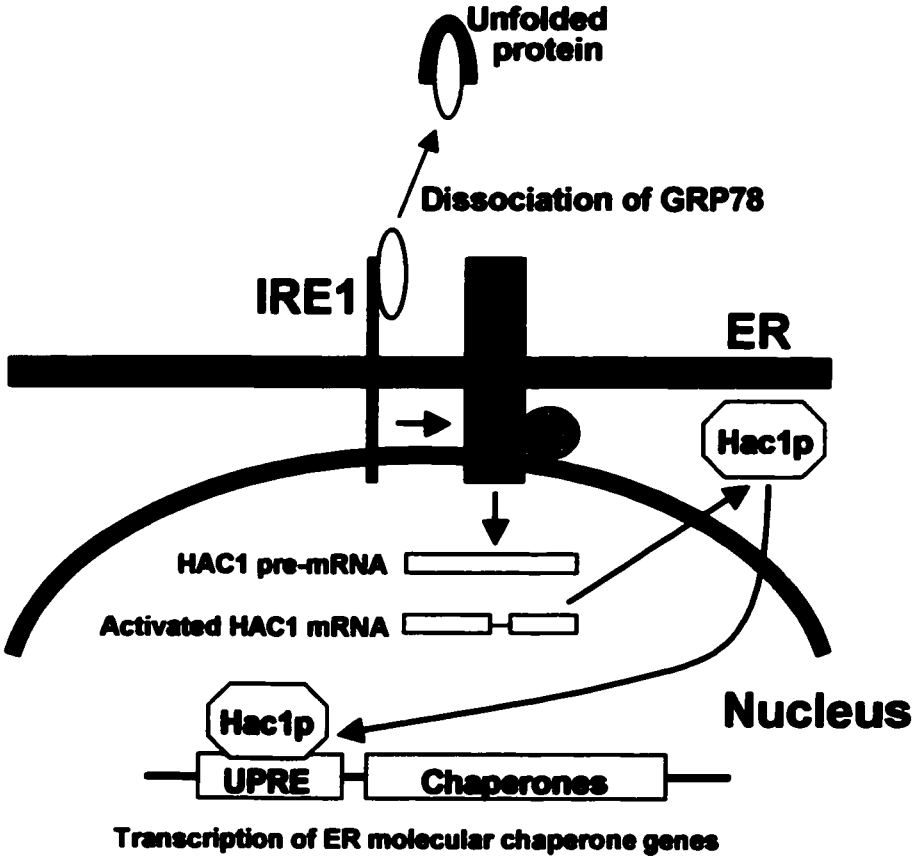
Unfolded protein
Dissociation of GRP78
IRE1
ER
Hac1p
HAC1 pre-mRNA
Activated HAC1 mRNA
Hac1p
Nucleus
UPRE
Chaperones
Transcription of ER molecular chaperone genes

FIG. 1.8. **The N-linked core oligosaccharide.** The N-linked glycosylation of proteins involves co-translational addition of 14 sugars *en bloc* to the newly synthesized polypeptide. Once the assembly of 14 sugars $(Glc)_3(Man)_9(GlcNAc)_2$, representing the "core oligosaccharide unit" is completed, the oligosaccharide is transferred and coupled via an N-glycosidic bond to asparagine of the protein. The transfer of the core oligosaccharide is catalyzed by the oligosaccharyltransferase that recognizes a specific conformation of the protein motif Asn-X-Ser/Thr. The symbols used for the different sugars are shown.

Fig. 1.8

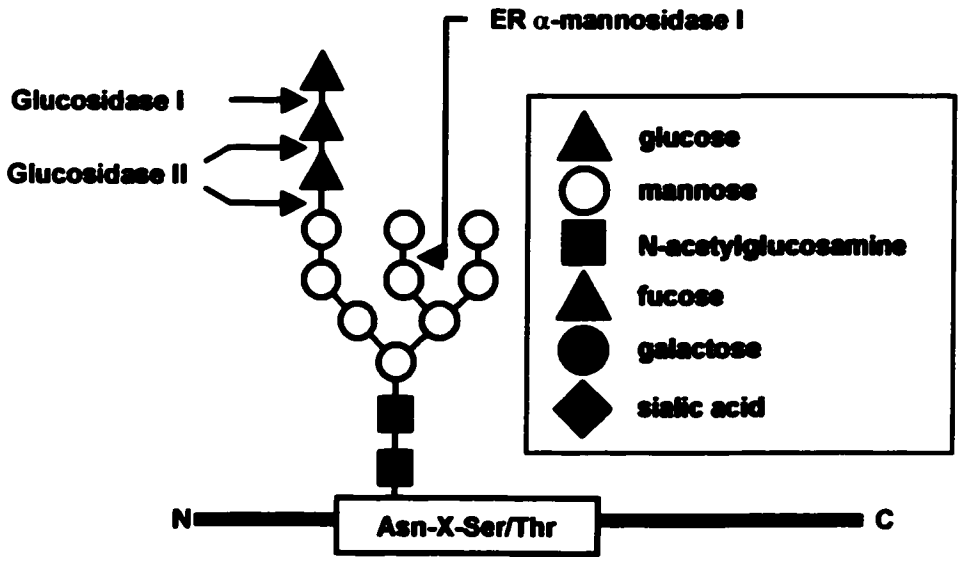
ER α-mannosidase I
Glucosidase I
Glucosidase II
glucose
mannose
N-acetylglucosamine
fucose
galactose
sialic acid
N
Asn-X-Ser/Thr
C

FIG. 1.9. **Biosynthesis and processing of N-linked oligosaccharides.** *A*, biosynthesis of the N-linked core oligosaccharide is initiated on the cytosolic surface of the ER membrane by the addition of sugars to dolichylphosphate. When two N-acetylglucosamines and five mannoses have been added, the oligosaccharide is flipped to the lumenal side of the membrane, and seven further sugars are added from lipid precursors. The transfer of the core oligosaccharide onto the growing polypeptide chain is catalyzed by oligosaccharyltransferase enzyme complex. The three glucoses are trimmed away by glucosidase I and II, and terminal mannose by ER mannosidases. *B*, upon arrival of the glycoprotein in Golgi, further trimming of mannose residues occurs. Subsequent terminal glycosylation involves addition of new terminal sugars including GlcNAc, galactose, sialic acid, and fucose.

Fig. 1.9.

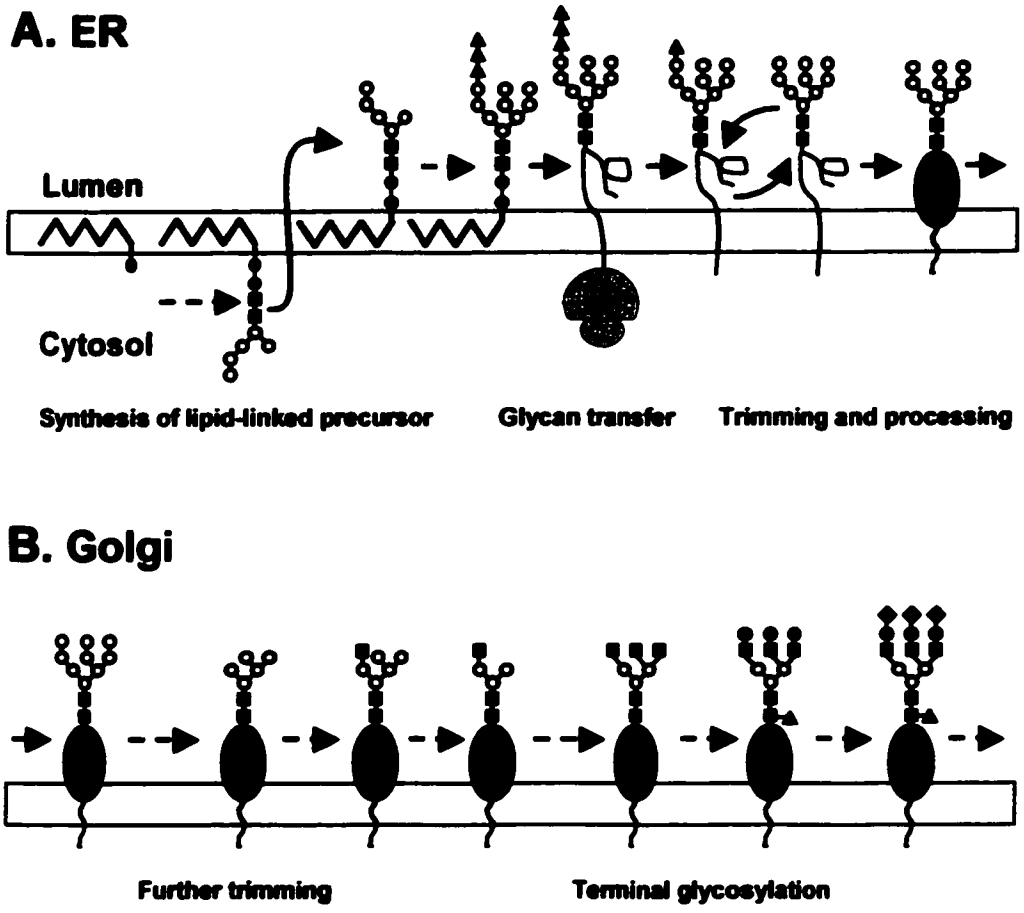
A. ER
Lumen
Cytosol
Synthesis of lipid-linked precursor
Glycan transfer
Trimming and processing
B. Golgi
Further trimming
Terminal glycosylation

Table I

Multiple factors involved in regulation of the assembly and secretion of very low density lipoproteins

	Factor	Functional Role	Ref.
Assembly Initiation	ApoB pause-transfer sequence	Efficient apoB translocation	(46)
	ApoB length, lipid-binding sequences	Regulation of lipid recruitment	(31, 38)
	Disulfide pairs within apoB	ApoB folding	(102, 106)
	MTP	ApoB translocation and first-step lipidation	(144, 227)
	BiP, calnexin	ApoB translocation, folding, degradation	(68, 179, 182)
	PMME	ApoB translocation	(93)
Lipid Regulation	MTP	TG partitioning	(129)
	Oleate	Stimulates lipid synthesis and turnover	(43, 70, 71)
	n-3 fatty acids	Decrease VLDL production	(148-150)
	Ca^{2+}-independent phospholipase A_2	Phospholipid remodeling	(163)
	TG hydrolase, ACAT and DGAT	Regulation of lipid substrate availability	(111, 126,119)
	PC	Regulation of lipid substrate availability	(125)
	7-α-hydroxylase	Regulation of lipid substrate availability	(128)
	ARF, phospholipase D	Formation of PA from PC	(162)
	PE methylation	ApoB48-containing VLDL assembly	(228)
Intracellular Trafficking	Brefeldin A	Inhibits formation and budding of vesicles from ER	(162)
	GTP-binding protein(s)	N/A	
Secretion	Orotic acid	Decreased VLDL production	(160)
	Apolipoprotein E	Increased VLDL production	(154)
	Dexamethasone	Increased VLDL production	(229)
	Insulin	Decreased VLDL production	(153)
	Growth hormone	Increased VLDL secretion	(230)

Chapter 2 Materials and Methods

Materials – QuikChange™ mutagenesis kit was obtained from Stratagene Inc., La Jolla, CA. Primers for mutagenesis, Dulbecco's modified Eagle's medium (DMEM), fetal bovine serum (FBS), and neomycin analog G418 were obtained from Invitrogen. Reagents for polyacrylamide gel electrophoresis (PAGE) and nitrocellulose membrane were obtained from Bio-Rad. Fumed silica, 2-bromopalmitate, oleic acid (OA), and fatty acid free bovine serum albumin (BSA) were obtained from Sigma/Aldrich. ProMix™ (a mixture of [^{35}S]methionine and [^{35}S]cysteine, 1000 Ci/mmol), [2-^{3}H]glycerol (1 Ci/mmol), glycerol tri[1-^{14}C]oleate (80 mCi/mmol), peroxidase-conjugated anti-mouse and anti-rabbit immunoglobulin G antibody, and Amplify solution were obtained from Amersham/Pharmacia. The enhanced chemiluminescence (ECL) immunoblot detection system and tunicamycin were obtained from Roche. Protein A-Sepharose CL-4B beads were obtained from Amersham/Pharmacia LKB Biotechnology Inc. N-acetyl-leucyl-leucyl-norleucinal (ALLN) was obtained from Biomol. Silica Gel 60 thin-layer chromatography (TLC) plates and organic solvents used for TLC were obtained from BDH Chemicals. Monoclonal antibody 1D1 and MB19 raised against human apolipoprotein B were a gift of R. Milne and Y. Marcel (University of Ottawa Heart Institute) and S. Young (Gladstone Institute of Cardiovascular Disease, San Francisco), respectively. The anti-apoA-I antiserum was a gift of J. Vance (University of Alberta). Antibody against α-mannosidase II was a gift of M. Farquhar (University of California, San Diego). The antibodies against calnexin and BiP were obtained from StressGen (Victoria, BC). The anti-microsomal triglyceride transfer protein (MTP) rabbit antiserum was a gift of C. Shoulders (MRC Molecular Medicine Group, London).

Preparation of Apolipoprotein B Expression Plasmids Containing Asparagine-to-Glutamine Substitution – The expression plasmid pB17wt that contained nucleotides 20 to 2555 of the human apoB cDNA was prepared by inserting the coding sequence between *EcoR*I and *Cla*I sites at the polylinker region of pCMV5 vector. The asparagine-to-glutamine (N-to-Q) substitution was introduced into pB17wt at Asn^{158} using the QuikChange™ site-directed mutagenesis kit according to the manufacturer's instructions. The plasmids pB17wt and $pB17N^{158}$ were used to create pB37wt and $pB37N^{158}$, respectively, by inserting a *Hind*III–*Sal*I fragment (nucleotides 2279–5290 of the apoB cDNA) that was derived from pB48 (231). Similarly, plasmid pB17wt and $pB17N^{158}$ were used to create pB48wt and $pB48N^{158}$, respectively, by inserting a *Hind*III-*Hind*III fragment from nucleotides 2279 of the apoB cDNA to the polylinker of pCMV5 that was derived from pB48 (231). In this construct (pB48), the codon CAA for Gln at position 2153 was mutagenized to UAA, thus giving apoB48. Furthermore, $pB37N^{956}$, $-N^{1341}$, $-N^{1350}$, $-N^{1496}$, $-N^{158-956}$, $-N^{158-1341}$, $-N^{158-1350}$, and $-N^{158-1496}$ that contained N-to-Q substitutions at selected or combined Asn^{956}, Asn^{1341}, Asn^{1350}, and Asn^{1496} positions were generated by multiple rounds of mutagenesis using $pB37N^{158}$ as a template. Subsequently, plasmid $pB50N^{158-1496}$ was constructed by inserting a *Sal*I–*Sal*I fragment (from nucleotide 5290 of the apoB cDNA to the polylinker of pCMV5) excised from pB50 into $pB37N^{158-1350}$ that had been digested with *Sal*I followed by mutagenesis using $pB50N^{158-1350}$ as a template. The 3' of the coding sequence in pB50 contains an engineered *Mlu*I site at nucleotide 7010. Sequence of primers used for mutagenesis is

presented in Table II. Resulting plasmids were purified by centrifugation twice in a CsCl gradient, and the apoB coding regions were authenticated using direct sequencing.

Preparation of Apolipoprotein B Expression Plasmids Containing Cysteine-to-Serine Substitution – The cysteine-to-serine (C-to-S) substitution within human pB48 expression plasmid (prepared using the pCMV5 vector) was achieved by four rounds of successive site-specific mutagenesis. The C-to-S substitution was first introduced into pB48wt at Cys^{1085} using the QuikChange™ site-directed mutagenesis kit according to the manufacturer's instructions. Subsequently, C-to-S substitutions at selected Cys^{1395}, Cys^{1479}, and Cys^{1635} positions were generated by multiple rounds of mutagenesis using $pB48C^{1085}$, $pB48C^{1085\text{-}1395}$ and $pB48C^{1085\text{-}1479}$ as template. Sequences of primers used for mutagenesis are presented in Table III. Resulting plasmids were purified by centrifugation twice in a CsCl gradient, and the apoB coding regions were authenticated using restriction enzyme digests. The $pB48C^{1085\text{-}1635}$ cDNA was authenticated using direct sequencing in collaboration with R.Hegele (Western University, London).

Preparation of the Green Fluorescent Tagged Apolipoprotein $B46N^{158\text{-}1496}$ Expression Plasmid – The pGFP-B46wt expression plasmid was a gift from E. Fisher (Columbia University, New York). Gel purified *EcoR*I insert fragment from $pCMV5\text{-}B50N^{158\text{-}1496}$ was ligated with gel purified *EcoR*I vector fragment from pEGFP-B46wt. Resulting plasmid $pEGFP\text{-}B45N^{158\text{-}1496}$ was purified by centrifugation twice in a CsCl gradient. Both plasmids were used in fluorescence microscopy experiments following expression in transiently transfected rat hepatoma McA-RH7777 cells.

Cell Culture, Stock Solution, and Transfection – Rat hepatoma McA-RH7777 cells were cultured in DMEM containing 10% (v/v) FBS and 10% (v/v) horse serum (HS). Cells were split in a ratio of 1:8 every three days (defined as one passage). Transfection of the cells with expression plasmids encoding wild type or mutant forms of B17, B37, B45, B48 or B50 was achieved using the previously described calcium phosphate precipitation method (232). Plated cells (100 mm dishes) of approximate 80% confluency were used for transient transfection, whereas cells of 20-30% confluence were used for stable transfection. For transient transfection, cells were transfected with 10 μg of the apoB expression plasmid. For stable transfection, 15 μg of human apoB constructs was co-transfected with pSV2neo at a molar ratio of 20:1. At least four hours after transfection cells were subjected to glycerol shock. Transiently transfected cells were used for experiments within 48 hours of transfection. Selection of stable transformants was initiated by adding 400 μg/ml G418 to the culture media two weeks following transfection with subsequent maintenance of individually picked colonies in culture media containing 200 μg/ml G418. For experiments, cells were grown no more than 10 passages after revival from liquid nitrogen. All experiments, unless specified, were carried out on cells of approximate 80% confluence (about 1.2 mg protein/dish) plated in 60 mm Primaria dishes.

A stock solution of tunicamycin (5 mg/ml) and 2-bromopalmitate (100 mM) were prepared in dimethylsulfoxide.

Expression of the recombinant human apoB was verified by immunoblotting of the conditioned media using monoclonal antibody 1D1 (25). Experiments described below with apoB recombinants containing N-to-Q substitution were performed using transiently transfected McA-RH7777 cells as well as mixed culture of G418-resistant transfectants, except with apoB50-expressing cells where individual G418-resistant colonies were used. Experiments described below with apoB48 containing C-to-S substitutions were performed using multiple G418-resistant colonies of stably transfected McA-RH7777 cells.

Analysis of ApoB Proteins – The rabbit anti-human apoB polyclonal antibody that cross-reacts with both rat apoB100 and rat apoB48 was used for immunoprecipitation. The immunoprecipitated apoB were recovered using protein A-Sepharose CL-4B. ApoB proteins were eluted from the beads, and subjected to electrophoresis on 3-15% (w/v) gradient polyacrylamide gels with 0.1% (w/v) sodium dodecyl sulphate (SDS), as previously described (39). For radiolabeled apoB proteins, the gels were treated with Amplify solution for 30 min, dried, and apoB proteins were detected by fluorography. For non-radiolabeled apoB proteins, after electrophoresis apoB proteins were transferred onto nitrocellulose membranes at 125V for 6 h with a transfer buffer (190 mM glycine, 25 mM Tris base, 20% methanol) at –10 °C, and detected by immunoblotting with 1D1.

Biosynthetic Labeling - Cells stably transfected with pB48wt and pB48 constructs containing C-to-S substitutions were labeled with [^{125}I]palmitate, as previously described (164).

Protein Metabolic Labeling – Cells were labeled using two methods. (i) *Continuous labeling experiments.* Cells were labeled with [^{35}S]methionine/cysteine (200 μCi/ml) for up to 60 minutes to measure the synthesis rates of apoB. At different time points cell-associated ^{35}S-apoB was immunoprecipitated and analyzed by SDS-PAGE and fluorography. (ii) *Pulse-chase experiments.* Cells were pre-treated in the presence or absence of 5 μg/ml tunicamycin for 3 h, labeled with [^{35}S]methionine/cysteine (200 μCi/ml) for an hour, and chased for up to 3 h in the presence or absence of tunicamycin treatment. At different time points of the chase, both cell- and medium-associated ^{35}S-apoB (and ^{35}S-apoA-I) were immunoprecipitated and analyzed by SDS-PAGE and fluorography.

Protein Assay - Protein concentration was determined according to Lowry method, as previously described (233), using bovine serum albumin as a standard.

Separation of Lipoproteins – ApoB-containing lipoproteins were separated using three methods. (i) S*ucrose density gradient ultracentrifugation.* Cells were labeled with [^{35}S]methionine/cysteine for 1 h and chased for 2 h in DMEM containing 20% FBS and 0.4 mM oleate as described previously (163). At the end of chase, the media and microsomal content were fractionated in a sucrose density gradient as described previously (89). Gradient was loaded by layering from the bottom of the tube: 2 ml of 47% sucrose, 2 ml of 25% sucrose, 5 ml of sample in 12.5% sucrose, and 3 ml phosphate-buffered saline (PBS) pH 7.4. The gradient was formed following

centrifugation at 35, 000 rpm in a Beckman SW41 rotor for 65 h at 12 °C. Twelve fractions (1 ml each) were collected from the top, of which fractions 1 and 2 represent very low density lipoproteins (VLDL) (d < 1.02 g/ml) and fractions 8-10 represent lipoproteins of densities similar to that of high density lipoproteins (HDL) (d = 1.08 – 1.13 g/ml). The apoB proteins in each fraction were immunoprecipitated and subjected to SDS–PAGE and fluorography or immunoblotting with 1D1. (ii) *Ultracentrifugation at fixed density*. To isolate apoB50-containing lipoproteins, the chase media were separated into *d* <1.02 and *d* > 1.02 g/ml fractions. (iii) *Ultracentrifugation using potassium bromide gradient*. The conditioned media were incubated with 0.7 g of KBr. The dissolved samples were loaded into quick-seal tubes containing 0.9% sodium chloride solution, and subjected to ultracentrifugation in the bench top Beckman TLA 110 rotor, at 65, 000 rpm for 1h at 4 °C. The gradient was unloaded in 19 fractions from the bottom of the tube. The apoB proteins in each fraction were immunoprecipitated, subjected to SDS–PAGE and immunoblotting with 1D1.

Isolation of Lumenal Contents - Metabolically labeled cells (100 mm dish) were resuspended in 2 ml of Tris-sucrose buffer (10 mM Tris-HCl, pH 7.4, and 250 mM sucrose) that was supplemented with protease inhibitors. The cells were homogenized using 10 passages with a ball-bearing homogenizer and the total microsomes were obtained by centrifugation at 10, 000 x g, 4 °C, for 10 min. The lumenal contents were released from total microsomes with 0.1 mM sodium carbonate, pH 11.3, by gentle mixing using a nutator for 30 min at room temperature. The lumenal contents were

separated from microsomal membranes by ultracentrifugation at 400, 000 x *g*, 4 °C, for 16 min, and subjected to cumulative rate flotation as described below.

Cumulative Rate Flotation - The density of the microsomal lumenal contents was adjusted to d = 1.10 g/ml with KBr, and loaded onto the bottom of Beckman SW41 centrifuge tube. The sample was overlaid with 3 ml of d = 1.065 g/ml NaBr, 3 ml of d = 1.02 g/ml NaBr, and 3 ml of d = 1.006 g /ml NaCl. After ultracentrifugation at 40, 000 rpm (20 °C, 148 min), $VLDL_1$ ($S_f > 100$) was collected from the top of the gradient. Following additional ultracentrifugation at 37, 000 rpm (15 °C, 18 h), $VLDL_2$ (S_f 20-100) and other lipoproteins were collected from top to bottom into twelve fractions. The apoB proteins in each fraction were immunoprecipitated and subjected to SDS-PAGE and fluorography.

Subcellular Fractionation Using Nycodenz Gradient – Cells were homogenized using a ball-bearing homogenizer. The post nuclear supernatant was prepared and fractionated on preformed Nycodenz gradients, as described previously by ultracentrifugation in an SW41 rotor (4 °C, 90 min, 37,000 × *g*) (234, 235). A total of 19 fractions (600 µl/fraction) were collected, and an aliquot of each fraction was subjected to SDS-PAGE and immunoblotting to detect α-mannosidase II, calnexin, and apoB.

Lipid Assay – Cells, plated into two 6-well plates a day before the experiment, were labeled with 5 µCi/ml [^{3}H]glycerol for up to 2 hours. At different time points, lipids were extracted from the cells with chloroform/methanol/acetic acid/saturated $NaCl/H_2O$

(4:2:0.01:1:2, by volume), and resolved on Silica Gel 60 plates by thin-layer chromatography using egg yolk lipids as a carrier. The solvent system chloroform/methanol/acetic acid/formic acid/H_2O (70:30:12:4:2, by volume) was used for separation of phosphatidylcholine (PC) and phosphatidylethanolamine (PE), whereas hexane/diethyl ether/acetic acid (70:30:1, by volume) was used for separation of fatty acids and triacylglycerol (TG), as described previously (129). TG and PC bands were identified and the radioactivity for each sample was quantified using liquid scintillation counting.

TG Mass Assay – Lipids were extracted from cells using chloroform/methanol/H_2O, and TG was separated by thin-layer chromatography. Lipids were dried, resuspended in isopropanol, and TG mass was measured using the previously described colorimetric assay (236).

Microsomal Triglyceride Transfer Protein Assay - The TG transfer activity of MTP was measured using [^{14}C]triolein as substrate, as previously described (5). Donor and acceptor small unilamellar vesicles (SUVs) were prepared by bath sonication in assay buffer (15 mM Tris-HCl, pH 7.5, 40 mM NaCl, 1 mM EDTA). The lipid transfer mixture contained donor membranes (40 nmol of egg PC, 7.5 mol % cardiolipin, and 0.25 mol % [^{14}C]triolein), acceptor membranes (240 nmol of egg PC, unlabeled TG), and 5.0 mg of BSA in a total volume of 0.68 ml of assay buffer. The reaction was started by the addition of various amounts of post-nuclear supernatant containing MTP activity. After 60 min, the reaction was terminated by the addition of 0.5 ml of DE52-cellulose pre-

equilibrated in assay buffer. The mixture was nutated for 5 minutes and centrifuged in a microfuge at maximum speed for 3 min to pellet the DE52 containing bound donor vesicles. To quantitate lipid transfer, radioactivity from 0.5 ml of the supernatant was measured.

Microscopy – The cells were plated on cover slips for 24 h, fixed with 3% paraformadehyde (in PBS) for 20 min, followed by quenching with 50 mM ammonium chloride. Cells were permeabilized using 0.1% Triton X-100 (in PBS) for 3 min and incubated with 10% FBS (in PBS) for 20 min. Monoclonal antibody 1D1 was used to probe the recombinant human apoB for 1 h with goat anti-mouse IgG Alexa Fluro 488 conjugate (Molecular Probes, #A-6440) as secondary antibody. The endoplasmic reticulum and Golgi were probed with anti-calnexin and anti-α-mannosidase II antibodies, respectively, with Alexa Fluro 594 conjugated anti-rabbit IgG (Molecular Probes, #R-6394) as secondary antibody. Between all steps, cells were washed three times with PBS. All incubation and washing were performed at room temperature. After staining, cells were mounted onto the glass slide using SlowFade Antifade kits (Molecular Probes, #S-7461). The images were captured using the MRC-1024 laser scanning confocal imaging system (Bio-Rad).

TABLE II

Sequence of oligonucleotides used for site-directed mutagenesis of N-linked glycosylation sites within human apolipoprotein B

The oligonucleotides correspond to the complementary sequences of the human apolipoprotein B cDNA. The mutant codons are underlined while additional nucleotides mutagenized for the purposes of introducing or deleting restriction enzyme sites are highlighted in bold. Site-directed mutagenesis was performed using QuikChange™ mutagenesis kit (Stratagene).

Amino acid change	Mutagenic oligonucleotide
Asn^{158}-Gln	5'-GAT ACC GTA TAC GGA CAA TGC TCC ACT CAC TTT ACC-3' 3'-GGT AAA GTG AGT GGA GCA TTG TCC GTA TAC GGT ATC-5'
Asn^{956}-Gln	5'-GGC GCT TAC TCC CAA GCT TCC TCC ACA GAC TCC GCC-3' 3'-GGC GGA GTC TGT GGA GGA AGC TTG GGA GTA AGC GCC-5'
Asn^{1341}-Gln	5'-CAG CAA CTT GTA CCA ATG GTC CGC CTC CTA CAG TGG-3' 3'-CCA CTG TAG GAG GCG GAC CAT TGG TAC AAG TTG CTG-5'
Asn^{1350}-Gln	5'-CTA CAG TGG TGG CCA AAC TAG TAC AGA CCA TTT CAG-3' 3'-CTG AAA TGG TCT GTA CTA GTT TGG CCA CCA CTG TAG-5'
Asn^{1496}-Gln	5'-TCC AAC CTG CGG TTT CAA TCC TCC TAC CTC CAA GGC-3' 3'-GCC TTG GAG GTA GGA GGA TTG AAA CCG CAG GTT GGA-5'

TABLE III

Sequence of oligonucleotides used for site-directed mutagenesis of potential palmitoylation sites within human apolipoprotein B48

The oligonucleotides correspond to the complementary sequences of the human apolipoprotein B cDNA. The mutant codons are underlined while additional nucleotides mutagenized for the purposes of introducing or deleting restriction enzyme sites are highlighted in bold. Site-directed mutagenesis was performed using QuikChange™ mutagenesis kit (Stratagene).

Amino acid change	Mutagenic oligonucleotide
Cys^{1085}-Ser	5'-CCC TCA TGG GCC ACC **TCT CGA** GTG ACA CAA AGG AAG-3'
	3'-CTT CCT TTG TGT CA**C TCG AGA** GGT GGC CCA TGA GGG-5'
Cys^{1395}-Ser	5'-GAA TAC GTT CAC ACT **CTC GAG** TGA TGG GTC TCT ACG-3'
	3'-CGT AGA GAC CCA TCA **CTC GAG** AGT GTG AAC GTA TTC-5'
Cys^{1479}-Ser	5'-GGC ACA TAT GGC CTG **AGC TCT** CAG AGG GAT CCT AAC-3'
	3'-GTT AGG ATC CCT CTG A**GA GCT** CAG GCC ATA TGT GCC-5'
Cys^{1635}-Ser	5'-GCA ACG ACC AAC TTG AA**G AGC TCT** CTC CTG GTG CTG-3'
	3'-CAG CAC CAG GAG A**GA GCT C**TT CAA GTT GGT CGT TGC-5'

FIG. 2.1. **Schematic diagram of apolipoprotein B constructs containing N-to-Q substitution.** *Closed circles* represent utilized N-linked glycosylation site(s); *open circles* represent N-linked glycosylation site(s) mutagenized using N-to-Q substitution. *A,* preparation of human apoB17, -B37, and –B48 constructs containing the N^{158}-to-Q substitution. *B,* preparation of human apoB37 and –B50 constructs containing multiple N-to-Q substitution at five residues (Asn^{158}, Asn^{956}, Asn^{1341}, Asn^{1350}, and Asn^{1496}, respectively). *C,* preparation of green fluorescent protein-tagged human apoB45 construct containing multiple N-to-Q substitution at five residues (Asn^{158}, Asn^{956}, Asn^{1341}, Asn^{1350}, and Asn^{1496}, respectively).

Fig. 2.1.

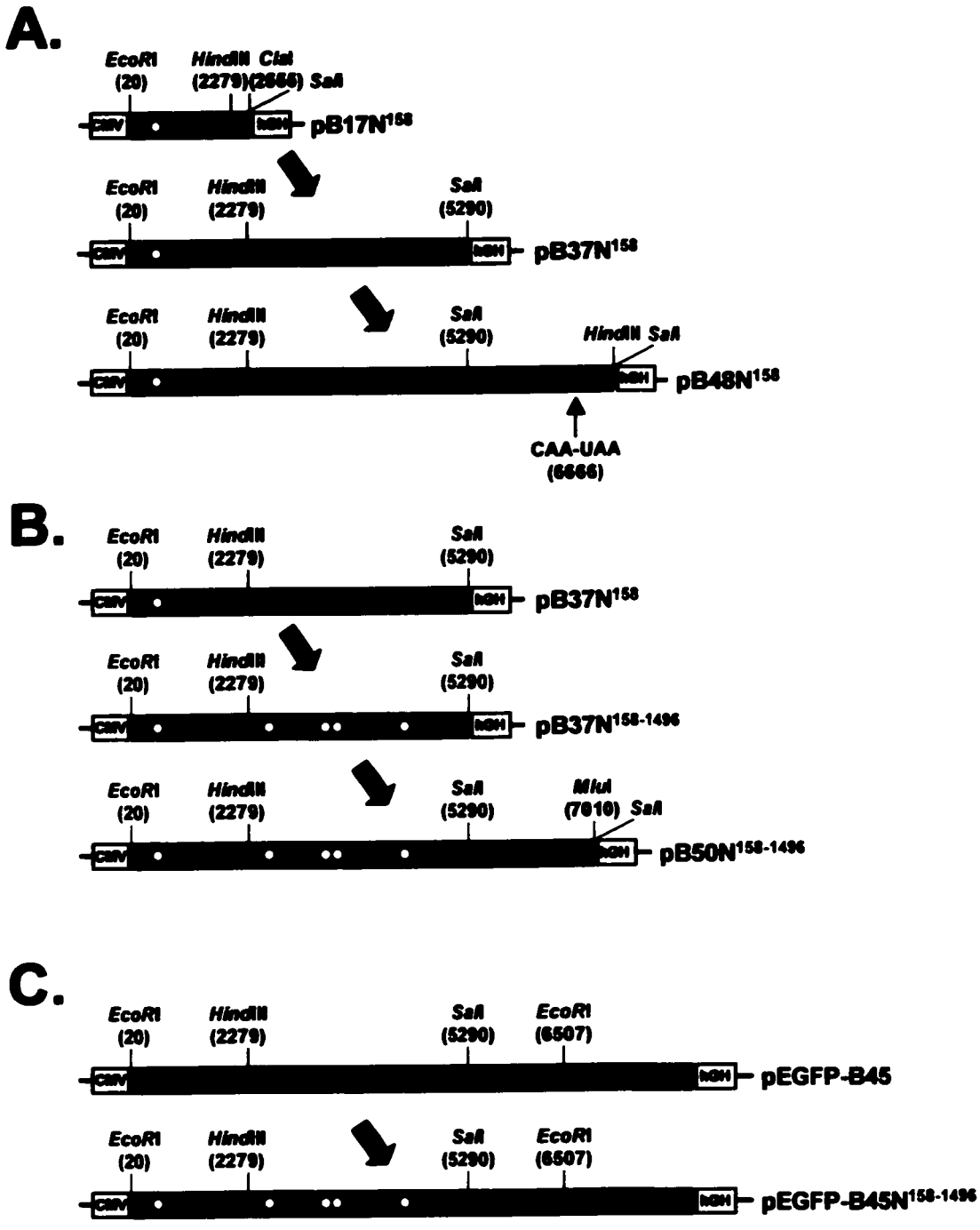
A.
EcoR1 (20)
HindIII (2279)
ClaI (2666)
SalI
pB17N158
EcoR1 (20)
HindIII (2279)
SalI (5290)
pB37N158
EcoR1 (20)
HindIII (2279)
SalI (5290)
HindIII SalI
pB48N158
CAA-UAA (6666)
B.
EcoR1 (20)
HindIII (2279)
SalI (5290)
pB37N158
EcoR1 (20)
HindIII (2279)
SalI (5290)
pB37N158-1496
EcoR1 (20)
HindIII (2279)
SalI (5290)
MluI (7010)
SalI
pB50N158-1496
C.
EcoR1 (20)
HindIII (2279)
SalI (5290)
EcoR1 (6507)
pEGFP-B45
EcoR1 (20)
HindIII (2279)
SalI (5290)
EcoR1 (6507)
pEGFP-B45N158-1496

FIG. 2.2. **Schematic diagram of apolipoprotein B constructs containing C-to-S substitution.** *Closed circles* represent potential palmitoylation site(s); *open circles* represent palmitoylation site(s) mutagenized using C-to-S substitution. Preparation of human apoB48 constructs containing C-to-S substitution at four Cys residues (Cys^{1085}, Cys^{1395}, Cys^{1479}, and Cys^{1635}, respectively).

Fig. 2.2.

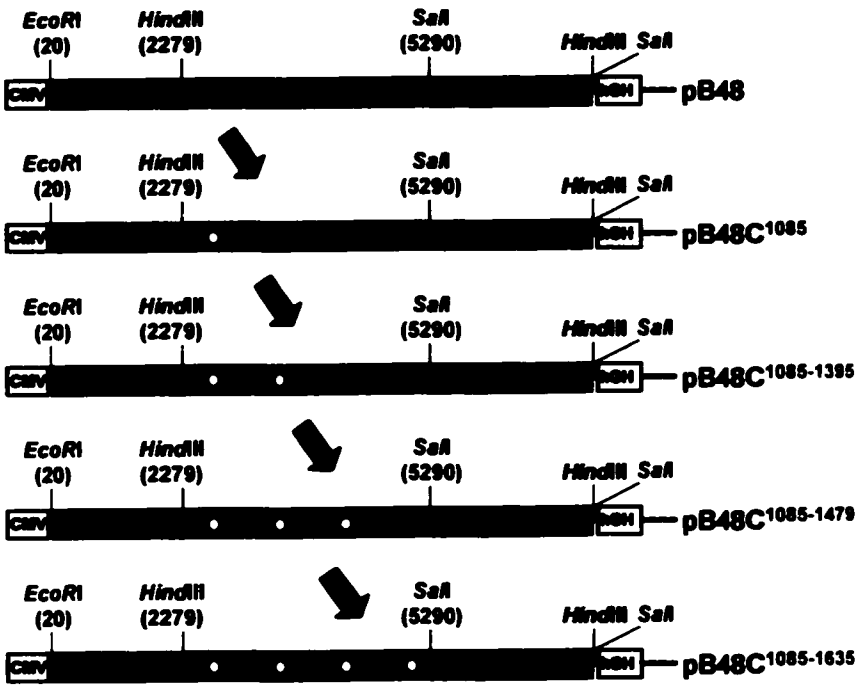
EcoR1
(20)
HindIII
(2279)
Sal
(5290)
HindIII Sal
pB48
pB48C1085
pB48C1085-1395
pB48C1085-1479
pB48C1085-1635

Chapter 3 The Role of N-linked Glycosylation of Apolipoprotein B

3.1. N-linked oligosaccharides are important for efficient secretion of the apolipoprotein B polypeptide

As discussed in Section 1.4.5., conflicting results regarding the role of N-linked oligosaccharides of apoB in apoB and apoB-containing lipoproteins secretion exist in the literature, which prompted us to re-examine this post-translational modification of apoB. The conjugation of oligosaccharide with the asparagine residue of the newly synthesized polypeptide can be prevented using tunicamycin, a fungal antibiotic that inhibits the formation of GlcNAc-P-P-Dol (237). Following inhibition of N-linked glycosylation using tunicamycin treatment, impaired secretion of human apoB from rat hepatoma McA-RH7777 cells was observed (Fig. 3.1.1.). Human apoB100 contains 20 potential N-linked glycosylation sites, of which 16 are conjugated with oligosaccharides (Fig. 3.1.1*A*). In McA-RH7777 cells expressing recombinant human B17, B37, or B50, tunicamycin treatment decreased secretion efficiency of the nonglycosylated apoBs by varied extents as compared with the controls (*i.e.* no tunicamycin treatment) (Fig. 3.1.1*B*). The secretion of endogenous apoB100 in these cells was also decreased by tunicamycin treatment (Fig. 3.1.1*C*). Similar inhibitory effect of tunicamycin treatment on secretion of rat apoB100 was observed in primary rat hepatocytes (data not shown). Tunicamycin treatment affected the incorporation of ^{35}S-label into rat B100 but had no effect on the incorporation of ^{35}S-label into truncated apoB forms (Fig. 3.1.1*D*). These results confirmed that the lack of N-linked oligosaccharides is associated with impaired secretion but not synthesis (at least the N-terminal half) of apoB.

In light of this evidence, we decided to analyze in more detail the role of N-linked oligosaccharides present within the amino terminus of apoB in the efficient secretion of the apoB polypeptide. We raised the following questions: (a) Does the inhibition of apoB N-linked glycosylation using site-specific mutagenesis (N-to-Q substitution) impair the secretion efficiency of the apoB polypeptide? (b) Does the effect of N-to-Q substitution on the apoB secretion efficiency vary among apoB polypeptides having a different lipid-binding ability? (c) Are some N-linked glycosylation site(s) more important than others for the efficient secretion of the apoB polypeptide? We addressed these questions using transfected McA-RH7777 cells expressing four C-terminally truncated forms of human apoB100, namely B17, B37, B48, or B50, that contain N-to-Q substitution at consensus N-linked glycosylation site(s).

3.1.1. Effect of N^{158}-to-Q substitution on secretion efficiency of human apolipoprotein B17

To test the role of N-linked oligosaccharides in the secretion of the apoB polypeptide, we performed N-to-Q substitution at the single N-linked glycosylation site (N^{158}) within human B17 (Fig. 3.1.2*A*). Media was collected at different time points from McA-RH7777 cells stably transfected with wild type (B17wt) or mutant B17 containing the N^{158}-to-Q substitution (designated B17N^{158}), and the apoB signal was detected using monoclonal antibody 1D1 specific for human apoB. The time-course of secretion from this experiment suggested impaired secretion of B17N^{158} (Fig. 3.1.2*B*). Furthermore, pulse-chase analysis showed quantitatively that the secretion efficiency of the B17N^{158} was decreased by 50% as compared to B17wt (Fig. 3.1.3*A*). The inhibitory effect of N^{158}–

to-Q substitution on B17 secretion was almost equivalent to that of tunicamycin treatment. The level of expression of B17wt and B17N^{158} was similar in the two cell cultures (as judged by ^{35}S incorporation in Fig. 3.1.4). The amount of cell-associated ^{35}S-B17 during chase was similar between the two transfectants (Fig. 3.1.3*B*), suggesting the impaired secretion of B17N^{158} was not associated with intracellular accumulation but with degradation.

Several mechanisms exist in the hepatic cells by which newly synthesized apoB can be degraded, either at the stage after apoB translation or else during apoB polypeptide chain elongation (238). Rapid degradation of apoB during or immediately after apoB translation is mediated by proteasomes, which can be prevented by inhibitors ALLN or MG132 in McARH7777 cells (106). To test the possible role of proteasome in B17N^{158} degradation, proteasomal inhibitors ALLN and MG132 were included during metabolic labeling (Fig. 3.1.4). While inhibition of proteasome elevated the intracellular levels of endogenous rB100 by 1.5-fold at the end of 30-min labeling, no significant change in the intracellular levels of B17wt or B17N^{158} was observed. Thus, the B17N^{158} degradation was unlikely degraded by proteasome during translation.

Whether or not N^{158}-to-Q substitution has an effect on B17 conformation was tested using a conformation-specific antibody MB19 that detects cell-associated apoB. Under non-reducing conditions, immunoblotting using the MB19 antibody following non-reducing SDS-PAGE detected both B17wt and B17N^{158}, suggesting no detectable change in B17N^{158} conformation (Fig. 3.1.5*B*). An additional band of molecular weight greater

than that of B17 was observed for both B17wt and B17N^{158}, as pointed by arrow (Fig. 3.1.5*B*). This band was absent following immunoblotting with monoclonal antibody 1D1 that has an epitope located within amino acids 474-539 under reducing conditions (Fig. 3.1.5*C*). It is possible that the additional band may be due to non-specific binding of MB19. It may be possible, however, based on the estimated molecular weight, that B17 dimerizes or interacts with other proteins through disulfide bonding that is sensitive to reduction following reducing SDS-PAGE.

3.1.2. Decreased effect of N^{158}-to-Q substitution on secretion efficiency of human apolipoprotein B37 and apolipoprotein B48 polypeptides

The above results demonstrated the importance of N-linked oligosaccharides in the secretion of B17, a polypeptide that has limited ability to assemble lipids. To determine the effect of the N^{158}-to-Q substitution on secretion of apoB peptides with lipid-binding ability, we introduced the N^{158}-to-Q substitution into C-terminally truncated apoBs that contain some lipid-binding sequence (31), namely B37 and B48 (Fig. 3.1.6*A*). Pulse-chase analysis was performed with McA-RH7777 cells stably expressing wild type B17, B37, and B48 or mutant B17, B37, and B48 containing N^{158}-to-Q substitution (Fig. 3.1.6*B*). Calculated secretion efficiency suggested that, in comparison with B17N^{158}, the inhibitory effect of the N^{158}-to-Q substitution on B37 and B48 secretion efficiency diminished gradually as the length of apoB increased (43% vs 62% for B37; 57% vs 53% for B48) (Table IV).

3.1.3. Effect of selective versus combined N-to-Q substitution on secretion efficiency of human apolipoprotein B37

To determine the role of N-linked oligosaccharides in the secretion of apoB-containing lipoproteins, we used B37 as a model that contains lipid-binding sequences and four additional N-linked glycosylation sites at N^{956}, N^{1341}, N^{1350}, and N^{1496} (Fig. 3.1.7.). The lack of significant effect of N^{158}-to-Q substitution on the secretion of B37 or B48 could be explained to the existence of N-linked oligosaccharides at the other four N-linked glycosylation site(s). Or, it could be attributable to the lipid-binding sequences downstream of B17, which can be important for the efficient secretion of the apoB polypeptide. To test these possibilities, we performed selective or combined site-specific N-to-Q substitution at the other four N-linked glycosylation sites, at N^{956}, N^{1341}, N^{1350}, and N^{1496}, respectively (Fig. 3.1.8). An additional purpose for introducing N-to-Q substitution at a single glycosylation site (*i.e.* N^{158}, N^{956}, N^{1341}, N^{1350}, or N^{1496}) was to help us determine if there is a critical N-linked glycan that is important for lipoprotein synthesis.

Preliminary experiments showed that the transient transfection with various B37 constructs resulted in different levels of apoB expression, as shown by varied incorporation of ^{35}S-amino acid (Fig. 3.1.8*A*). However, expression of various B37 constructs had no marked effect on the synthesis of endogenous apoA-I or B100 in different cells (Fig. 3.1.8*A*). The N-to-Q substitution at each single glycosylation site had a different effect on B37 secretion efficiency. Thus, while secretion of $B37N^{158}$ and $B37N^{1350}$ was not different from B37wt, secretion of $B37N^{956}$, $B37N^{1341}$ and $B37N^{1496}$

decreased by 30-40% compared to B37wt (Fig. 3.1.8*B*). These data suggest that N-to-Q substitution at a single N-linked glycosylation site exerted no or partial inhibition on B37 secretion. On the other hand, introducing N-to-Q substitution at multiple glycosylation sites (*i.e.* $N^{158\text{-}956}$, $N^{158\text{-}1341}$, $N^{158\text{-}1350}$, and $N^{158\text{-}1496}$) progressively and consistently decreased B37 secretion efficiency. Thus, when all five glycosylation sites were mutated, the secretion efficiency of $B37N^{158\text{-}1496}$ was decreased to 40% of B37wt, a level almost equivalent to that of B37wt treated with tunicamycin (Fig. 3.1.8*B*). The secretion efficiency of endogenous apoA-I (Fig. 3.1.8*B*) or B100 (data not shown) was not altered among cells transiently transfected with various B37 forms.

Notably, N-to-Q substitution at N^{1496} resulted in increased electrophoretic mobility of $B37N^{1496}$ and $B37N^{158\text{-}1496}$ (indicated by "x" in Fig. 3. 1.8*B*). Sequencing analysis of the expression plasmid DNA excluded the possibility of deletions within the coding sequence. To determine if the aberrant electrophoretic mobility was caused by proteolytic cleavage at the carboxyl terminus of the mutant B37, epitope mapping was performed with a panel of monoclonal antibodies (data not shown). The mutant $B37N^{158\text{-}1496}$ reacted normally with most antibodies but lost its reactivity with antibody 2D8 (epitope residues 1438-1481). Thus, it is likely that mutation at residue N^{1496} rendered B37 susceptible to proteolysis at amino acid residues approximately 1440 (~ 32% of B100). These data suggest an important role of glycosylation at residue N^{1496} for the stability of B37. Loss of N-linked oligosaccharide resulting in proteolytic cleavage has been reported for other proteins (239).

3.1.4. Effect of combined N-to-Q substitution on the secretion efficiency of apolipoprotein B37 and apolipoprotein B50

The effect of N-to-Q substitution at all five N-linked glycosylation sites within B37 was determined further using mixed cultures of stable transfectants. Again, the aberrant mobility of $B37N^{158\text{-}1496}$ was observed (indicated by "x" in Fig. 3.1.9.). Pulse-chase analysis showed that the secretion efficiency of $B37N^{158\text{-}1496}$ was decreased by more than 2-fold as compared to that of B37wt, which was similar to the effect of tunicamycin treatment on B37wt secretion (Fig. 3.1.9*B*). However, there was no difference in the amount of intracellular $B37N^{158\text{-}1496}$ during chase as compared with B37wt (Fig. 3.1.9*A*).

The studies with B37 suggest strongly that appropriate glycosylation is required for efficient secretion of the apoB polypeptide. However, the unexpected proteolytic cleavage of $B37^{158\text{-}1496}$ that removed approximately 5% apoB sequences from the carboxyl terminus of B37 made the above data less conclusive. To ascertain whether N-glycan of apoB play a role in efficient biosynthesis of apoB and apoB-containing lipoproteins, we extended the mutagenesis studies to B50 that has the same number of N-glycan sites as B37 but contains more lipid-binding sequences (31). Pulse-chase experiments were performed in two stable cell lines that expressed similar level of B50wt or $B50N^{158\text{-}1496}$.

The amount of cell-associated $^{35}S\text{-}B50N^{158\text{-}1496}$ during chase was greater than that of B50wt, which suggested that, unlike $B17N^{158}$ or $B37N^{158\text{-}1496}$, the mutant B50 was not rapidly degraded intracellularly (Fig. 3.1.10*A*). Between the two stably transfected cells,

the secretion efficiency of endogenous apoA-I was comparable as determined by pulse-chase analysis in two independent experiments (Fig. 3.1.10*B*). The combined N-to-Q substitution impaired the secretion efficiency of B50 to a lesser extent than that of B37 (Fig. 3.1.10*B*). In addition, unlike what occurred to mutant B37 proteins, mutation at N^{1496} within B50 did not give aberrant electrophoretic mobility of $B50N^{158\text{-}1496}$ (data not shown). This result suggests that sequences between the carboxyl termini of B37 and B50 can overcome the instability of the proteins introduced by N^{1496}-to-Q substitution.

3.1.5. Conclusion

In conclusion, selective or combined site-specific mutagenesis at N-linked glycosylation sites within the N-terminal half of B100 confirmed the results obtained using tunicamycin treatment, namely, that inhibition of N-linked glycosylation results in significant impairment of up to 50% of the apolipoprotein B polypeptide secretion efficiency. Our results suggest the presence of N-linked oligosaccharides at all five sites (*i.e.* N^{158}, N^{956}, N^{1341}, N^{1350}, and N^{1496}) is required for efficient secretion of human B37 and B50 polypeptides, although a single N-linked oligosaccharide at N^{1496} may play a critical role in the secretion of B37. The lipid-binding sequences downstream of B17 cannot overcome the impairment of secretion efficiency of the B37 polypeptide introduced by N^{1496}-to-Q or $N^{158\text{-}1496}$–to-Q substitutions. However, the sequences downstream of B37, to a certain extent, stabilize the secretion efficiency of the B50 polypeptide, and thus, overcome the instability introduced by the N^{1496}-to-Q substitution.

FIG. 3.1.1. **Effect of tunicamycin on synthesis and secretion of apolipoprotein B from McA-RH7777 cells.** *A*, the line depicts position of the N-linked oligosaccharides within human apoB100. *Closed rectangles* represent utilized glycosylation sites in human LDL. The five most N-terminal sites are at N^{158}, N^{956}, N^{1341}, N^{1350}, and N^{1496}, respectively. *B*, McA-RH7777 cells stably transfected with human B17, B37, and B50 variants were pre-treated for 3 h (± 5 μg/ml tunicamycin), pulse-labeled with ^{35}S-amino acids (200 μCi/ml) for 1 h, and chased up to 2 h (± 5 μg/ml tunicamycin). The medium-associated ^{35}S-apoBs during chase were subjected to SDS–PAGE and visualized by fluorography *(left)*. Secretion efficiency of each apoB variant is presented as (medium apoB at 2 h chase) / (initial apoB at 60 min pulse) × 100 % *(right)*. *C*, medium-associated endogenous rat ^{35}S-apoB100 during chase. *D*, cell-associated ^{35}S-apoB at 0 h chase following tunicamycin treatment, presented as percent of control, *i.e.* untreated apoB. Data are presented as the mean ± S.D. from three independent experiments.

Fig. 3.1.1.

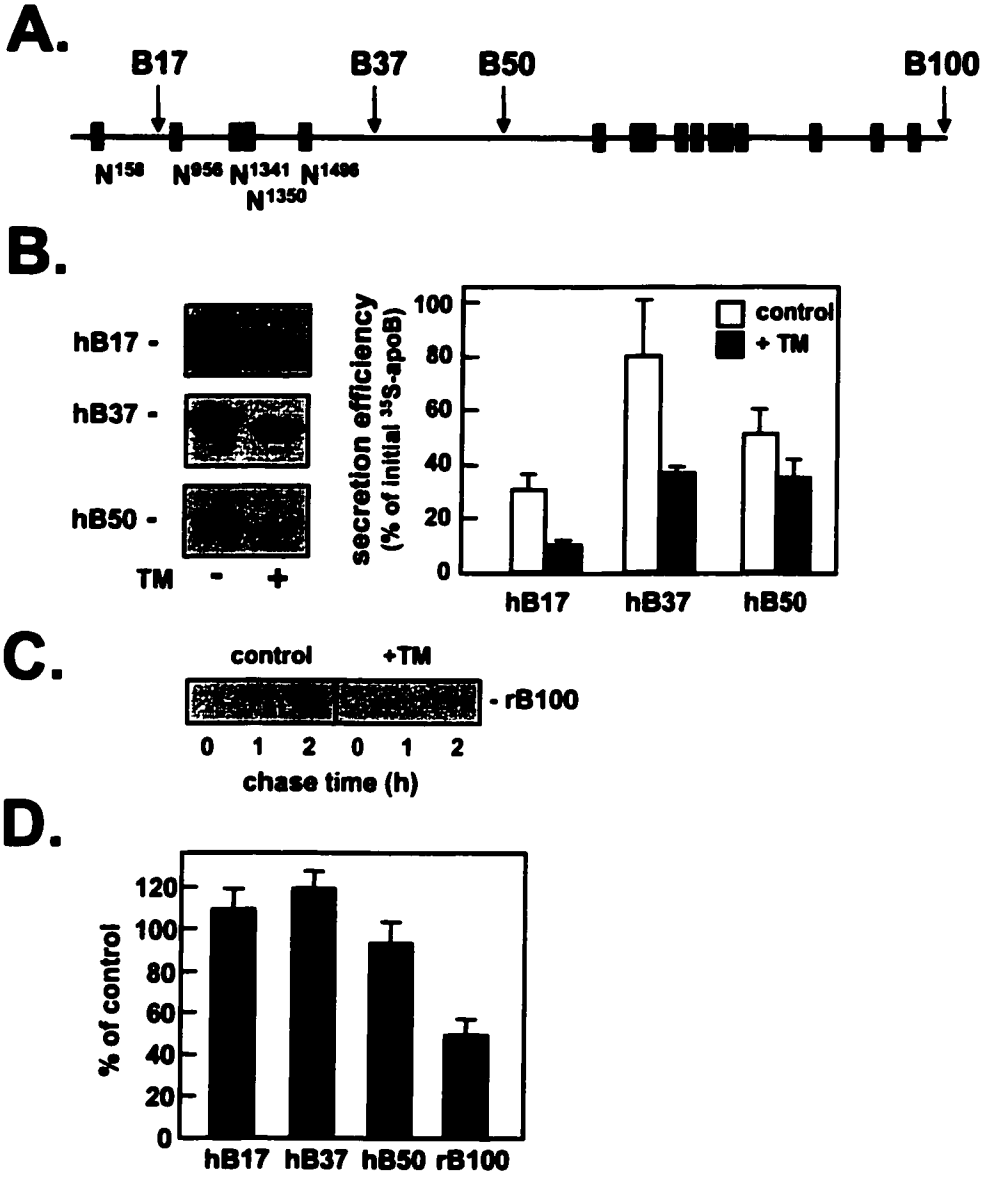
A.
B17
B37
B50
B100
N158
N956
N1341
N1350
N1496
B.
hB17 -
hB37 -
hB50 -
TM - +
secretion efficiency (% of initial 35S-apoB)
100
80
60
40
20
0
control
+ TM
hB17
hB37
hB50
C.
control
+TM
- rB100
0 1 2 0 1 2
chase time (h)
D.
% of control
120
100
80
60
40
20
0
hB17 hB37 hB50 rB100

FIG. 3.1.2. **Secretion time course of recombinant human apolipoprotein B17 containing N^{158}-to-Q substitution.** *A*, the top line depicts position of the N-linked oligosaccharide at N^{158} within apoB17. The human apoB17N^{158} variant containing N^{158}-to-Q substitution *(open oval)* was prepared using site-specific mutagenesis at N^{158} residue *(closed rectangle)* within human apoB17. *B*, McA-RH7777 cells stably transfected with human B17wt or B17N^{158} were incubated in DMEM (20% serum) for up to 16 h. Secretion of recombinant human apoBs at indicated time points was verified by immunoblotting of the conditioned media using monoclonal antibody 1D1. The experiment was performed once.

Fig. 3.1.2.

FIG. 3.1.3. **Lack of N-linked oligosaccharide at N^{158} impairs apolipoprotein B17 secretion.** Cells transiently transfected with human B17wt or $B17N^{158}$ were pre-treated for 3 h (± 5 μg/ml tunicamycin), pulse-labeled with ^{35}S-amino acids (200 μCi/ml) for 1 h, and chased up to 2 h (± 5 μg/ml tunicamycin). The medium *(A)* and cell-associated ^{35}S-apoB17 *(B)* during chase were subjected to SDS–PAGE and visualized by fluorography. The recovery of medium and cell-associated ^{35}S-apoB17 during chase was presented as "% of initial counts" that associated with cell B17 at the end of pulse. *Insets,* representative fluorograms. Data are presented as the mean ± S.D. from three independent experiments.

Fig. 3.1.3.

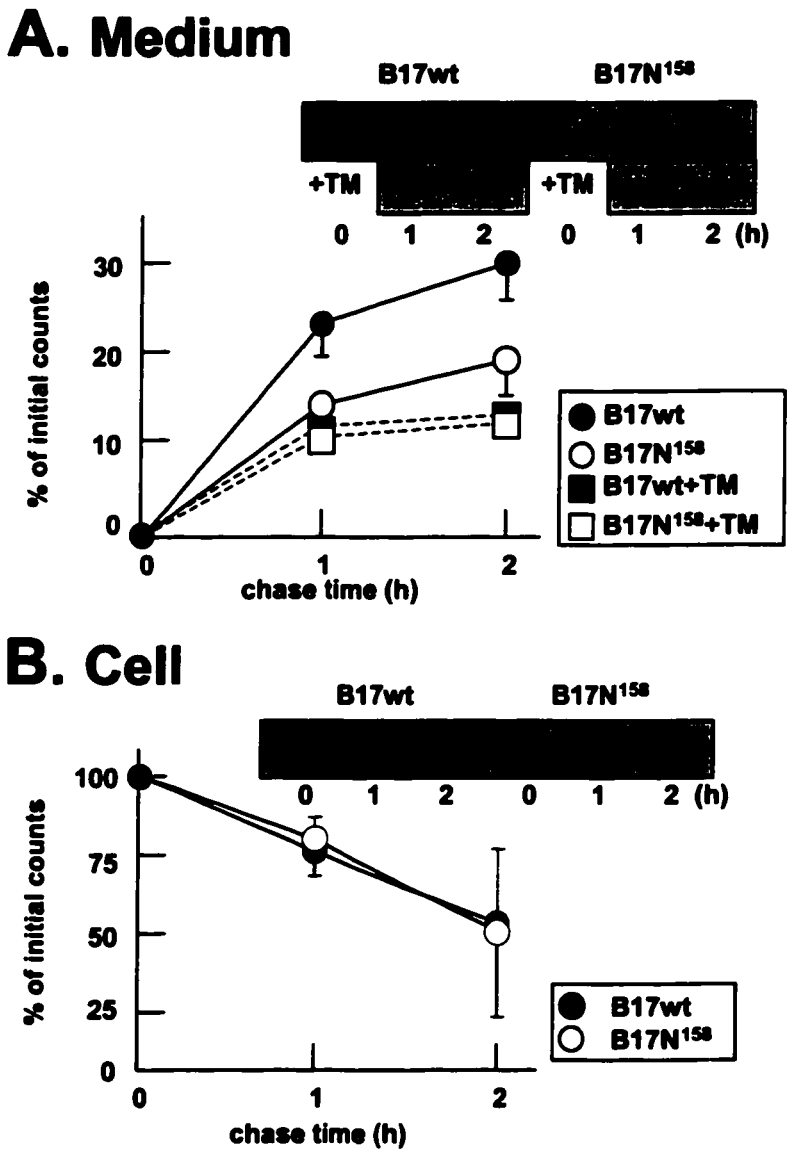
A. Medium
B17wt
B17N158
+TM
+TM
0 1 2 0 1 2 (h)
30
20
10
0
% of initial counts
0 1 2
chase time (h)
B17wt
B17N158
B17wt+TM
B17N158+TM
B. Cell
B17wt
B17N158
0 1 2 0 1 2 (h)
100
75
50
25
0
% of initial counts
0 1 2
chase time (h)
B17wt
B17N158

FIG. 3.1.4. **Effect of N^{158}-to-Q substitution on synthesis and degradation of apolipoprotein B17.** Cells stably transfected with expression plasmids encoding human B17wt or $B17N^{158}$ were continuously labeled with ^{35}S-amino acids (200 μCi/ml) in methionine-deficient DMEM (20% serum) for indicated times in the absence or presence of proteasomal inhibitors ALLN or MG132. *A*, representative fluorograms. *B*, quantification of radioactivity associated with ^{35}S-B17wt, –$B17N^{158}$, and -rB100. The labeling experiment without the inhibitors was performed twice with similar results, while the labeling in the presence of inhibitors was performed once.

Fig. 3.1.4.

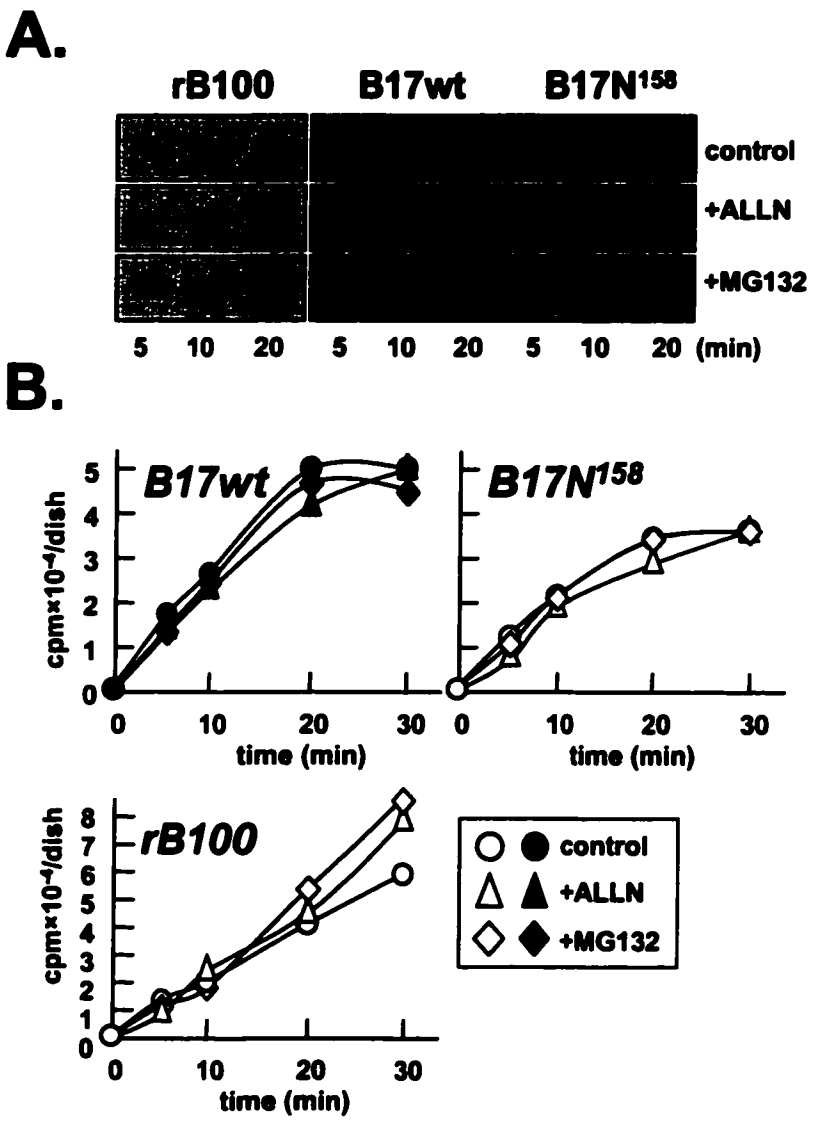
A.
rB100
B17wt
B17N158
control
+ALLN
+MG132
5 10 20 5 10 20 5 10 20 (min)
B.
B17wt
B17N158
rB100
cpm×10-4/dish
time (min)
control
+ALLN
+MG132

FIG. 3.1.5. **Effect of N^{158}-to-Q substitution on apolipoprotein B17 conformation.** *A,* the epitopes of monoclonal antibody 1D1 and MB19 within human apoB100. Cells stably transfected with plasmids encoding human B17wt or $B17N^{158}$ were homogenized. Aliquots of total cell extracts were subjected to *(B)* non-reducing or *(C)* reducing SDS–PAGE, transferred to nitrocellulose membranes, and immunoblotted with *(B)* MB19 antibody or *(C)* 1D1 antibody. The experiment was performed once.

Fig. 3.1.5.

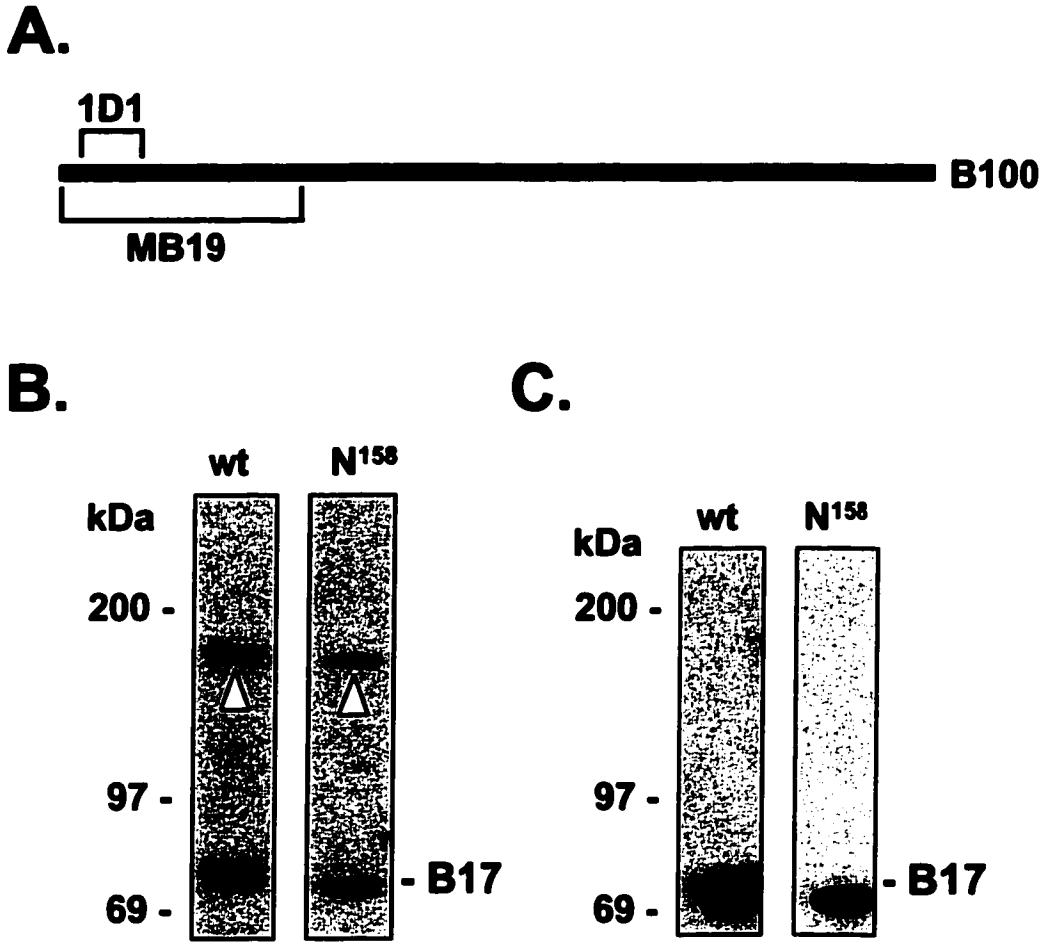
A.
1D1
B100
MB19
B.
wt
N158
kDa
200 -
97 -
69 -
- B17
C.
wt
N158
kDa
200 -
97 -
69 -
- B17

FIG. 3.1.6. **Effect of N^{158}-to-Q substitution on secretion of apolipoprotein B37 and apolipoprotein B48.** *A*, the top line depicts position of the N-linked oligosaccharides within human apoB100. *Closed rectangles* represent utilized glycosylation sites in human LDL. The bottom lines represent human B17, B37, and B48 variants containing the N^{158}-to-Q substitution *(open oval)*. *B*, cells stably transfected with wild-type or mutant B17, B37, or B48 were pre-treated for 3 h (± 5 μg/ml tunicamycin), pulse-labeled with ^{35}S-amino acids (200 μCi/ml) for 1 h, and chased up to 2 h (± 5 μg/ml tunicamycin). The medium-associated ^{35}S-apoBs at the end of 2 h chase were subjected to SDS-PAGE and visualized by fluorography *(top)*. Data are presented as the mean ± S.D. from three independent experiments.

Fig. 3.1.6.

A.

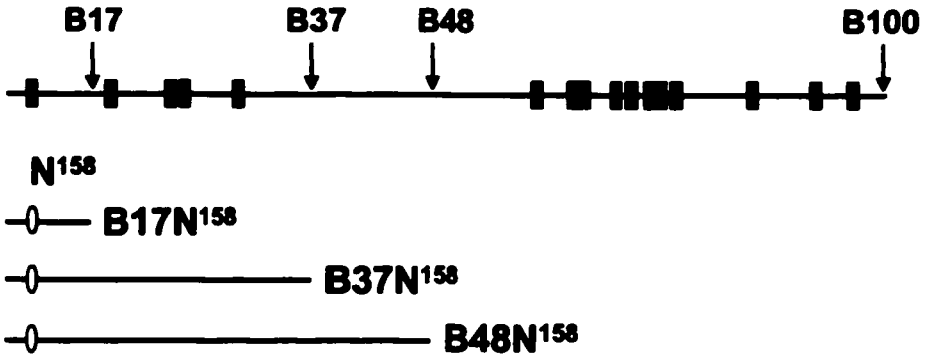
B17
B37
B48
B100
N158
B17N158
B37N158
B48N158

B.

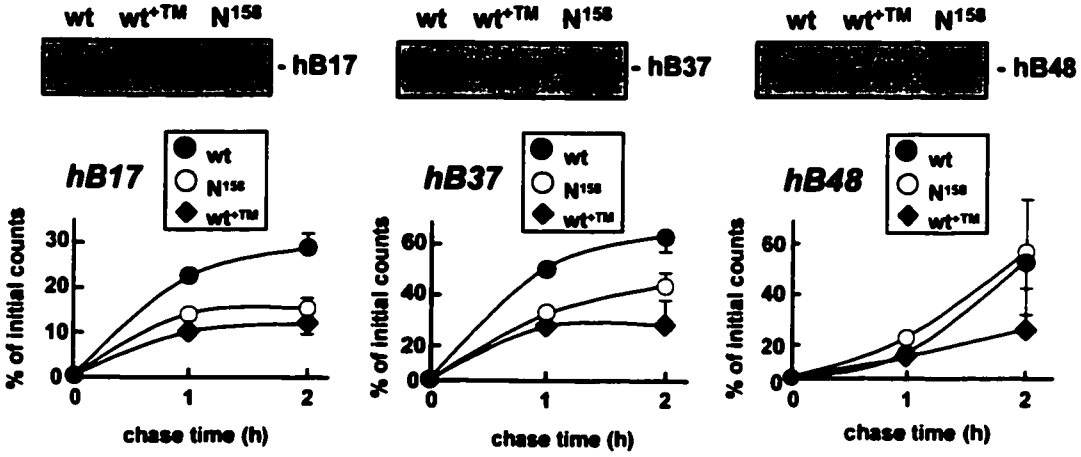
wt
wt+TM
N158
- hB17
- hB37
- hB48
hB17
hB37
hB48
% of initial counts
chase time (h)

FIG. 3.1.7. **Schematic diagram of apolipoprotein B37 variants containing N-to-Q substitution.** *Closed rectangles* represent potential glycosylation sites in human apoB37. The bottom lines depict mutant B37s that contain single or combined N-to-Q substitution at residues N^{158}, N^{956}, N^{1341}, N^{1350}, and N^{1496} *(open ovals)*.

Fig. 3.1.7.

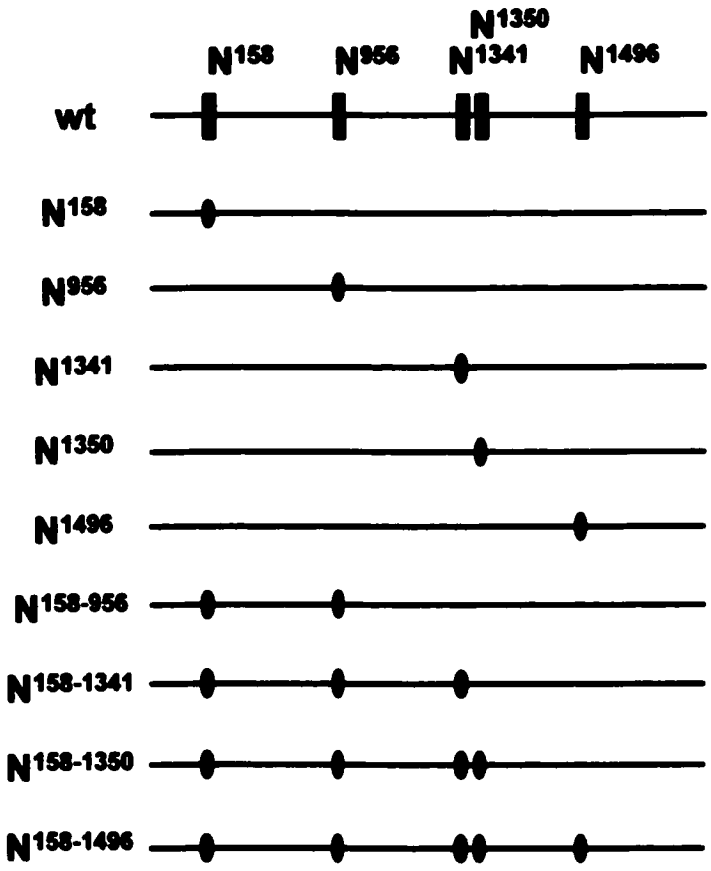
N1350
N158
N956
N1341
N1496
wt
N158
N956
N1341
N1350
N1496
N158-956
N158-1341
N158-1350
N158-1496

FIG. 3.1.8. **Effect of selective or combined N-to-Q substitution on apolipoprotein B37 synthesis and secretion.** Cells transiently transfected with wild type and nine mutant B37s containing various N-to-Q substitution were pulse-labeled with ^{35}S-amino acids (200 μCi/ml) for 1 h and chased for 2 h. Exogenous oleate (0.4 mM) was included in pulse and chase media. The cell- *(A)* and media-associated *(B)* ^{35}S-apoB37, ^{35}S-B100, and ^{35}S-A-I at the end of 2 h chase were subjected to SDS-PAGE and visualized by fluorography *(top)*. The recovery of ^{35}S-B37 and ^{35}S-A-I from mutant B37-transfected cells is presented as % B37 or A-I from B37wt-transfected cells. Data for B37 are the average of 2-3 independent transfection experiments. Secretion of A-I was determined once.

Fig. 3.1.8.

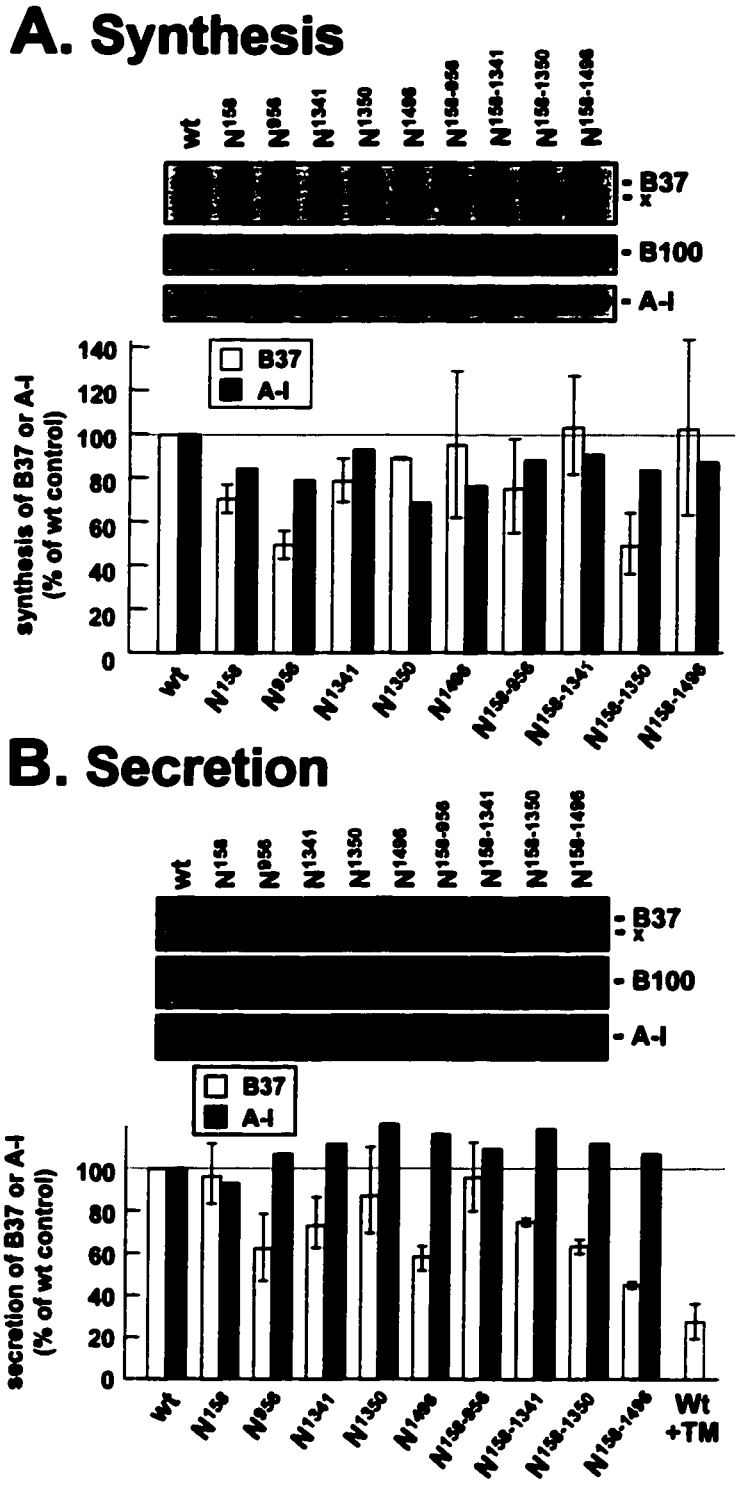
A. Synthesis
wt
N158
N956
N1341
N1350
N1496
N158-956
N158-1341
N158-1350
N158-1496
B37
B100
A-I
B37
A-I
synthesis of B37 or A-I (% of wt control)
0
20
40
60
80
100
120
140
B. Secretion
secretion of B37 or A-I (% of wt control)
Wt +TM

FIG. 3.1.9. **Lack of N-linked oligosaccharides impairs the secretion of apolipoprotein B37.** Cells stably transfected with human B37wt or B37N$^{158\text{-}1496}$ were pre-treated for 3 h (± 5 μg/ml tunicamycin), pulse-labeled with ^{35}S-amino acids (200 μCi/ml) for 1 h, and chased up to 2 h (± 5 μg/ml tunicamycin). The medium *(A)* and cell-associated ^{35}S-apoB37 *(B)* during chase were subjected to SDS–PAGE and visualized by fluorography. The recovery of medium and cell-associated ^{35}S-apoB17 during chase was presented as "% of initial counts" that associated with cell B37 at the end of pulse. *Insets*, representative fluorograms. Data are presented as the mean ± S.D. from three independent experiments.

Fig. 3.1.9.

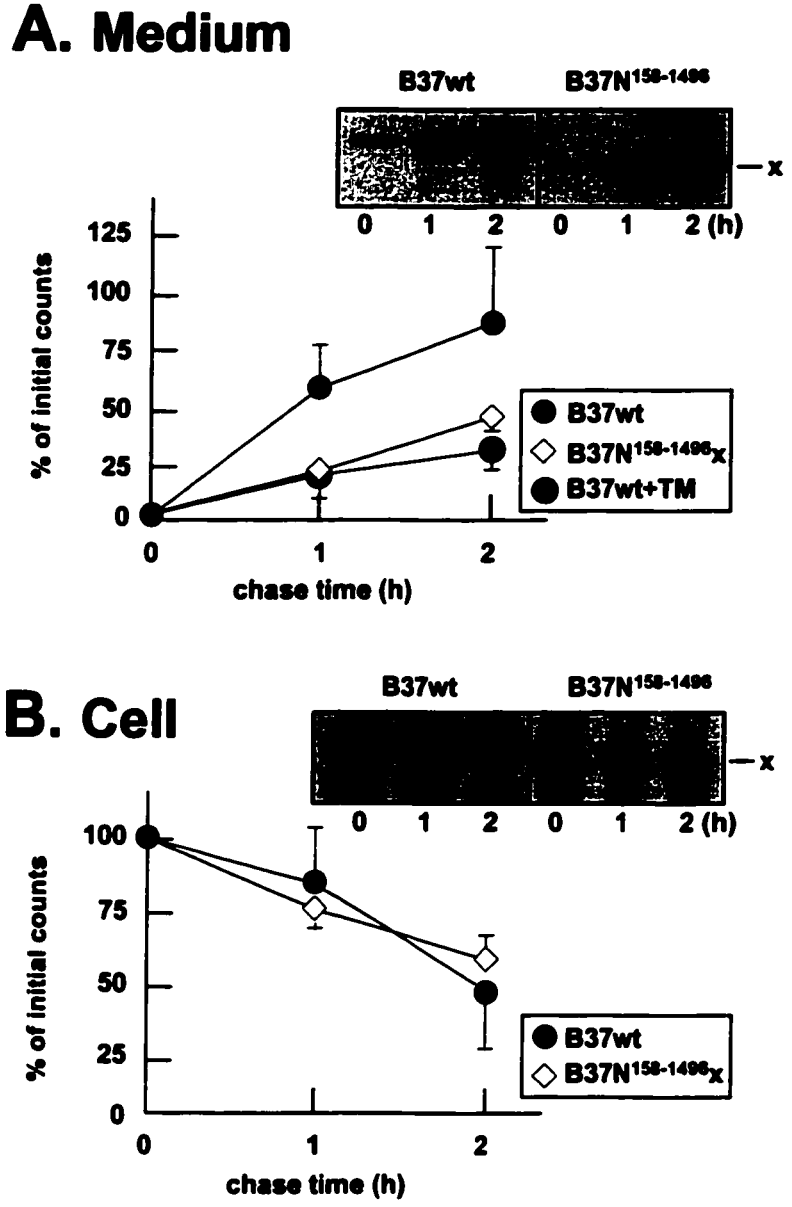
A. Medium
B37wt
B37N158-1496
x
0 1 2 0 1 2 (h)
125
100
75
50
25
0
% of initial counts
0 1 2
chase time (h)
B37wt
B37N158-1496x
B37wt+TM
B. Cell
B37wt
B37N158-1496
x
0 1 2 0 1 2 (h)
100
75
50
25
0
% of initial counts
0 1 2
chase time (h)
B37wt
B37N158-1496x

FIG. 3.1.10. **Lack of N-linked oligosaccharides impairs the secretion of apolipoprotein B50.** Cells stably transfected with human B50wt or B50N$^{158\text{-}1496}$ were pre-treated for 3 h (± 5 μg/ml tunicamycin), pulse-labeled with ^{35}S-amino acids (200 μCi/ml) for 1 h, and chased up to 3 h (± 5 μg/ml tunicamycin). *A*, cell-associated ^{35}S-apoB50 during chase was subjected to SDS- PAGE and visualized by fluorography. Cell-associated ^{35}S-apoB50 during chase was presented as "% of initial counts" that were associated with cell B50 at the end of pulse. *B*, medium-associated ^{35}S-apoB50 and ^{35}S-apoA-I during chase presented as "% of initial counts" that were associated with cell B50 and A-I at the end of pulse. Data are presented as the mean ± S.D. from three independent experiments using different stable clones, except for apoA-I data where experiments were performed twice.

Fig. 3.1.10.

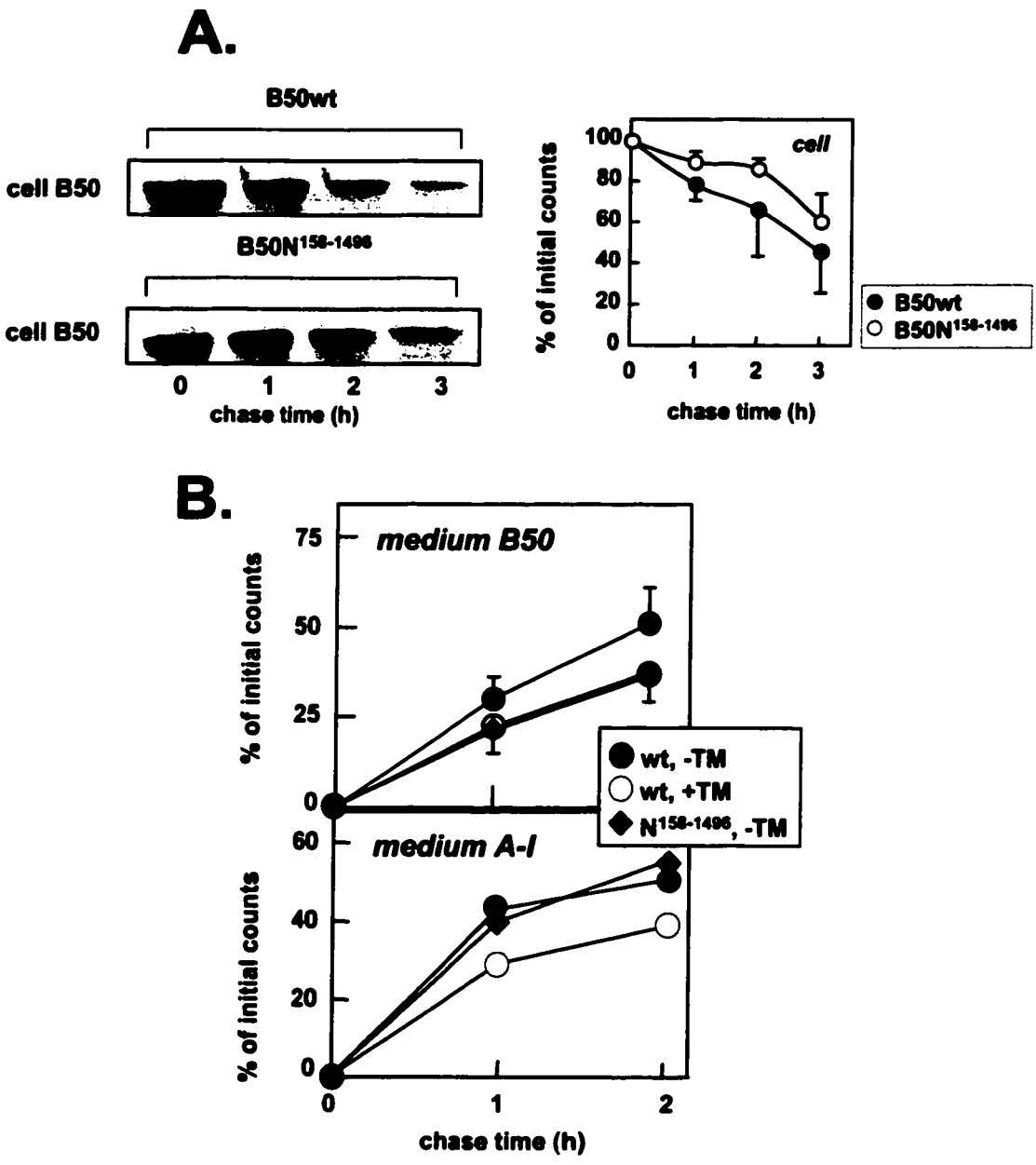
A.
B50wt
cell B50
B50N158-1496
cell B50
0
1
2
3
chase time (h)
% of initial counts
100
80
60
40
20
0
cell
0
1
2
3
chase time (h)
B50wt
B50N158-1496
B.
75
50
25
0
medium B50
% of initial counts
wt, -TM
wt, +TM
N158-1496, -TM
60
40
20
0
medium A-I
% of initial counts
0
1
2
chase time (h)

TABLE IV

The effect of the N^{158}-to-Q substitution on apolipoprotein B secretion efficiency decreases as the length of apolipoprotein B increases

McA-RH7777 cells stably transfected with human B17, B37, and B48 variants were pre-treated for 3 h (± 5 μg/ml tunicamycin), pulse-labeled with ^{35}S-amino acids (200 μCi/ml) for 1 h, and chased up to 2 h (± 5 μg/ml tunicamycin). The medium-associated ^{35}S-apoBs during chase was subjected to SDS–PAGE and fluorography. Secretion efficiency of each apoB variant is presented as (medium ^{35}S-apoB at 2 h chase) / (initial ^{35}S-apoB at 60 min pulse) × 100 %. Data are presented as the mean ± S.D. from three independent experiments.

	Secretion efficiency (%)		
Apolipoprotein	wild-type	mutant	wild-type $^{+TM}$
B17	29 ± 3	16 ± 1	12 ± 2
B37	62 ± 4	43 ± 3	27 ± 12
B48	53 ± 23	57 ± 20	25 ± 18

3.2. N-linked oligosaccharides are important for assembly and secretion of the apolipoprotein B-containing very low density lipoproteins

The early studies with rat and chicken hepatocytes suggested that inhibition of N-linked glycosylation of apoB with the chemical inhibitor tunicamycin had no major impact on VLDL secretion (213, 214). With recent evidence suggesting that tunicamycin treatment does impair the secretion of apoB (216, 217), the conflicting results on the effect of tunicamycin treatment highlighted limitations associated with the use of this inhibitor (*e.g.* the dose and duration of tunicamycin used for the treatment with different cells). We re-examined the role of N-linked oligosaccharides of apoB in the assembly and secretion of apoB-containing lipoproteins, using transfected McA-RH7777 cells expressing C-terminally truncated forms of human apoB100, namely B37 and B50, which contain N-to-Q substitutions at various N-linked glycosylation site(s).

Rat hepatoma McA-RH7777 cells secrete apoB100 in the form of apoB100-containing VLDL, while B48 is secreted in the form of lipid-poor particles (designated as apoB48-containing HDL) and apoB48-containing VLDL. The C-terminally truncated forms of apoB, namely apoB37 and apoB50, contain lipid-binding sequences and can also assemble VLDL (240). We addressed the following questions: (a) Does the inhibition of apoB N-linked glycosylation using site-specific mutagenesis (N-to-Q substitution) impair the secretion of apoB-containing lipoproteins? (b) If so, does the inhibition of apoB N-linked glycosylation using site-specific mutagenesis (N-to-Q substitution) impair the assembly of apoB-containing lipoproteins? We addressed these questions using transfected McA-RH7777 cells expressing mutant apoB variants

containing N-to-Q substitution at all five N-linked glycosylation sites, namely B37N$^{158-1496}$ and B50N$^{158-1496}$.

3.2.1. The N-to-Q substitution impairs the assembly and secretion of apolipoprotein B37-containing lipoproteins

The effect of N-to-Q substitution at all five N-linked glycosylation sites within B37 was determined using mixed cultures of stable transfectants. Following pulse-chase analysis (± 5 μg/ml tunicamycin), the medium was collected at the end of chase and fractionated by ultracentrifugation in a sucrose density gradient. The ^{35}S-B37 in each fraction was detected using SDS-PAGE and fluorography, and radioactivity associated with B37wt and B37N$^{158-1496}$ was quantified by scintillation counting. The decreased secretion of B37N$^{158-1496}$ was observed in both VLDL and HDL fractions (Fig 3.2.1*A*). The inhibitory effect of N$^{158-1496}$–to-Q substitution on secretion of B37-containing lipoproteins was similar to that observed with tunicamycin treatment (Fig. 3.2.1*A*, *bottom*).

Moreover, the lack of N-linked oligosaccharides resulted in a skewed distribution of B37N$^{158-1496}$ towards denser fractions in the microsomal lumen (Fig. 3.2.1*B*). Thus, the lack of N-linked glycosylation in B37 not only decreases its secretion as lipid-poor particles (*i.e.* the HDL-like species), but also impairs its ability to associate with neutral lipids in VLDL assembly.

3.2.2. The N-to-Q substitution impairs the assembly and secretion of apolipoprotein B50-containing lipoproteins

To test whether N-to-Q substitution impairs the secretion of apoB50-containing lipoproteins, we performed pulse-chase experiments using two stable cell lines that expressed similar level of B50wt or B50N$^{158\text{-}1496}$. Secretion of ^{35}S-B50N$^{158\text{-}1496}$ was decreased in both $d < 1.02$ and $d > 1.02$ g/ml fractions as compared to that of B50wt (Fig. 3.2.2.). Furthermore, examination of density distribution of the medium ^{35}S-B50N$^{158\text{-}1496}$ confirmed the above pulse-chase data, showing diminished secretion of ^{35}S-B50N$^{158\text{-}1496}$ in both VLDL and HDL fractions (Fig. 3.2.3). The decrease in secretion of B50N$^{158\text{-}1496}$ as VLDL was also observed by immunoblot analysis to measure B50N$^{158\text{-}1496}$ mass (data not shown).

Examination of the microsomal lumen contents showed reduced B50N$^{158\text{-}1496}$ in HDL-like fractions and absence of B50N$^{158\text{-}1496}$ in VLDL fractions as compared with B50wt (Fig. 3.2.4*A*). Thus, the diminished B50N$^{158\text{-}1496}$ secretion as VLDL was likely attributable to a defect in assembly of neutral lipid.

Pulse-chase experiments performed in two stable cell lines expressing B50wt or B50N$^{158\text{-}1496}$ were used to examine density distribution of the secreted endogenous ^{35}S-B100 (Fig. 3.2.4*B*). The expression of B50N$^{158\text{-}1496}$ resulted in 50% decrease in endogenous B100 secretion efficiency (Fig. 3.2.4*B*), although synthesis of endogenous B100 was not affected (data not shown). The inhibitory effect of B50N$^{158\text{-}1496}$ expression

on endogenous B100 secretion was reminiscent of previous observation where expression of B50 disulfide linkage mutants also inhibited endogenous B100 secretion (106).

The expression of B50wt resulted in increased secretion of [^{3}H]glycerol-labeled TG as compared with that of non-transfected McA-RH7777 cells, but expression of B50N$^{158\text{-}1496}$ had no effect on [^{3}H]TG secretion (Fig. 3.2.5*A*). The inability of B50N$^{158\text{-}1496}$ to assemble VLDL, however, was not attributable to limited synthesis in the transfected cells, as the synthesis of TG (Fig. 3.2.5*B*) and PC (Fig. 3.2.5*D*) in B50N$^{158\text{-}1496}$- and B50wt-transfected cells were comparable. Nor was the inability of B50N$^{158\text{-}1496}$ to assemble VLDL attributable to availability of lipids in the transfected cells, as the mass of TG in B50N$^{158\text{-}1496}$- and B50wt-transfected cells was similar (data not shown). These results suggest that the N-linked oligosaccharides play an important role during bulk TG incorporation in B50-VLDL assembly process.

3.2.3. Conclusion

In conclusion, abolishing apoB N-linked glycosylation by site-specific mutagenesis (N-to-Q substitution) impairs the secretion of B37 and B50-containing lipoproteins. The lack of N-linked oligosaccharides in B37 and B50 not only decreases their secretion as lipid-poor particles, but also impairs their ability to secrete as VLDL. Moreover, our results show that the diminished B50N$^{158\text{-}1496}$ secretion as VLDL is likely attributable to a defect in assembly of neutral lipid. Hence, the N-linked oligosaccharides play an important role during bulk TG incorporation in B50-VLDL assembly process.

FIG. 3.2.1. **Lack of N-linked oligosaccharides impairs secretion and formation of apolipoprotein B37-containing lipoproteins.** *A*, cells stably transfected with human B37wt or $B37N^{158-1496}$ were pre-treated for 3 h (± 5 μg/ml tunicamycin), pulse-labeled with ^{35}S-amino acids (200 μCi/ml) for 1 h, and chased for 2 h (± 5 μg/ml tunicamycin). The medium was collected at the end of chase and fractionated by ultracentrifugation in a sucrose density gradient. The ^{35}S-B37 in each fraction was detected using SDS-PAGE and fluorography *(top)*. The radioactivity associated with B37wt and $B37N^{158-1496}$ was quantified by scintillation counting *(bottom)*. Data are the representative of two experiments with similar results. *B*, the luminal content isolated from carbonate treated microsomes was fractionated by sucrose density gradient. The B37 proteins in each fraction were detected by 1D1 immunoblotting. The experiment was performed once.

Fig. 3.2.1.

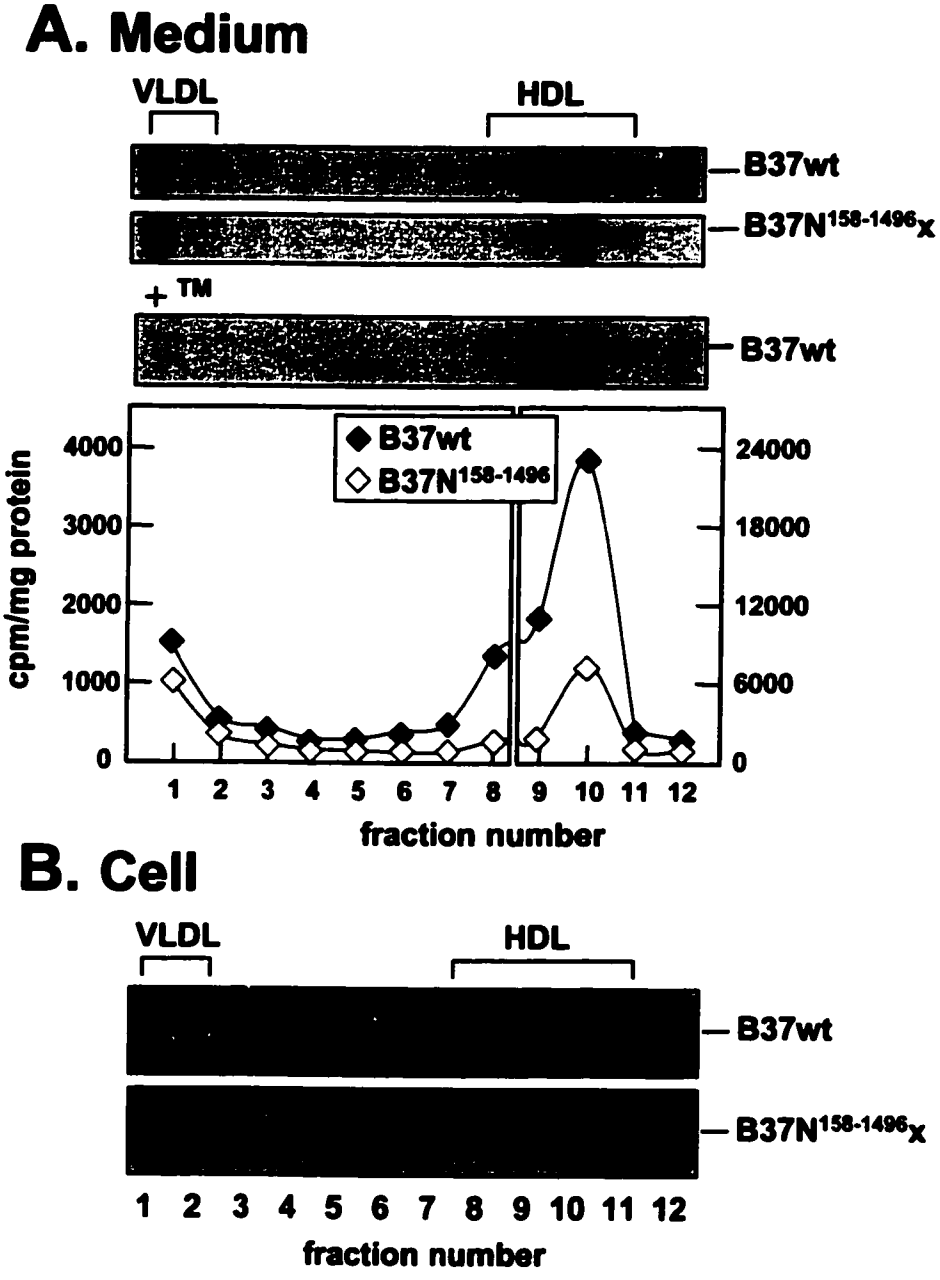
A. Medium
VLDL
HDL
B37wt
B37N158-1496X
+ TM
B37wt
B37wt
B37N158-1496
cpm/mg protein
4000
3000
2000
1000
0
24000
18000
12000
6000
0
1 2 3 4 5 6 7 8 9 10 11 12
fraction number
B. Cell
VLDL
HDL
B37wt
B37N158-1496X
1 2 3 4 5 6 7 8 9 10 11 12
fraction number

FIG. 3.2.2. **Lack of N-linked oligosaccharides impairs secretion of apolipoprotein B50-containing lipoproteins.** Cells stably transfected with human B50wt or $B50N^{158-1496}$ were pulse-labeled with ^{35}S-amino acids (200 μCi/ml) for 1 h and chased for up to 3 h. The chase media were separated into d <1.02 and d > 1.02 g/ml fractions using ultracentrifugation at fixed density. The radioactivity associated with ^{35}S-B50 in d <1.02 and d > 1.02 g/ml fractions was quantified by scintillation counting following SDS-PAGE and fluorography *(bottom)*. Data are an average of two independent experiments with similar results.

Fig. 3.2.2.

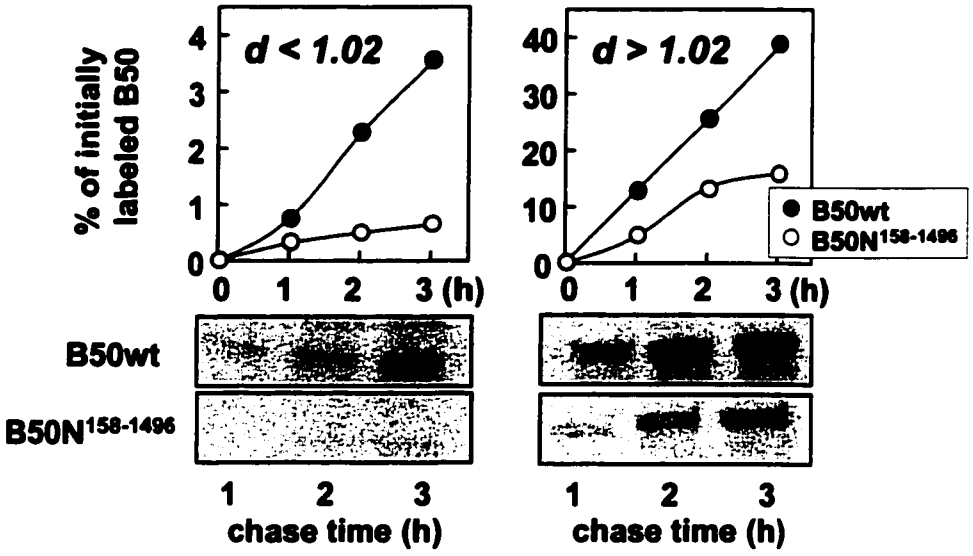
% of initially labeled B50
d < 1.02
d > 1.02
B50wt
B50N158-1496
0 1 2 3 (h)
chase time (h)

FIG. 3.2.3. **Lack of N-linked oligosaccharides impairs secretion of apolipoprotein B50-containing VLDL.** Cells stably transfected with plasmids encoding human B50wt and $B50N^{158-1496}$ were labeled with ^{35}S-amino acids (200 μCi/ml) for 1 h, and chased for up to 2 h. The medium collected at the end of chase was fractionated by ultracentrifugation in a sucrose density gradient. *Top,* the ^{35}S-B50 in each fraction analyzed by SDS-PAGE and fluorography. *Bottom,* the radioactivity associated with ^{35}S-B50wt and ^{35}S-$B50N^{158-1496}$ at 2 h chase was quantified by scintillation counting. The experiment was performed twice with similar results.

Fig. 3.2.3.

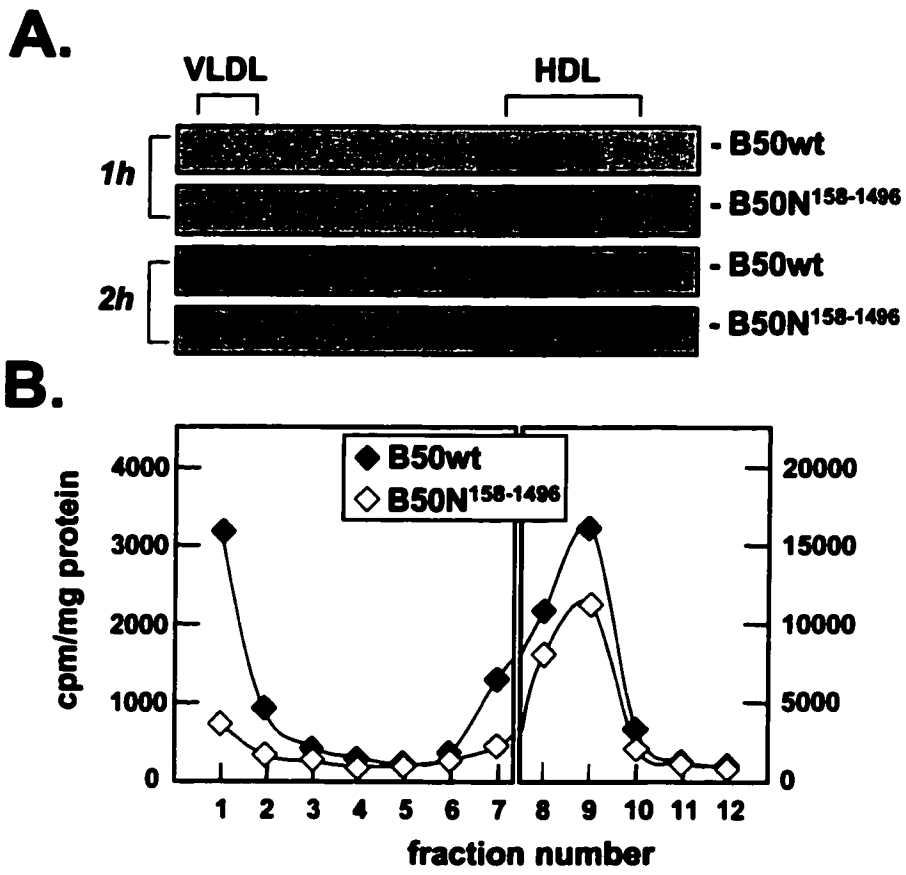
A.
VLDL
HDL
1h
2h
- B50wt
- B50N158-1496
- B50wt
- B50N158-1496
B.
B50wt
B50N158-1496
cpm/mg protein
4000
3000
2000
1000
0
20000
15000
10000
5000
0
1 2 3 4 5 6 7 8 9 10 11 12
fraction number

FIG. 3.2.4. **The N-to-Q substitution impairs assembly of apolipoprotein B50-containing VLDL and secretion of endogenous rat apolipoprotein B100.** Cells stably transfected with human B50wt or B50N$^{158\text{-}1496}$ were labeled with ^{35}S-amino acids (200 μCi/ml) for 1 h, and chased for up to 2 h. *A*, density distribution of ^{35}S-B50wt and ^{35}S-B50N$^{158\text{-}1496}$ in the microsomal lumen. Microsomes were prepared after labeling and the lumenal content was fractionated using cumulative rate flotation. The ^{35}S-B50 in each fraction was immunoprecipitated, and subjected to SDS-PAGE and fluorography. The experiment was performed once. *B*, rat ^{35}S-B100 following fractionation of medium after 1 h or 2 h chase by ultracentrifugation in a sucrose density gradient. The ^{35}S-B100 in each fraction was subjected to SDS-PAGE and visualized by fluorography. Data are representative of three experiments with similar results.

Fig. 3.2.4.

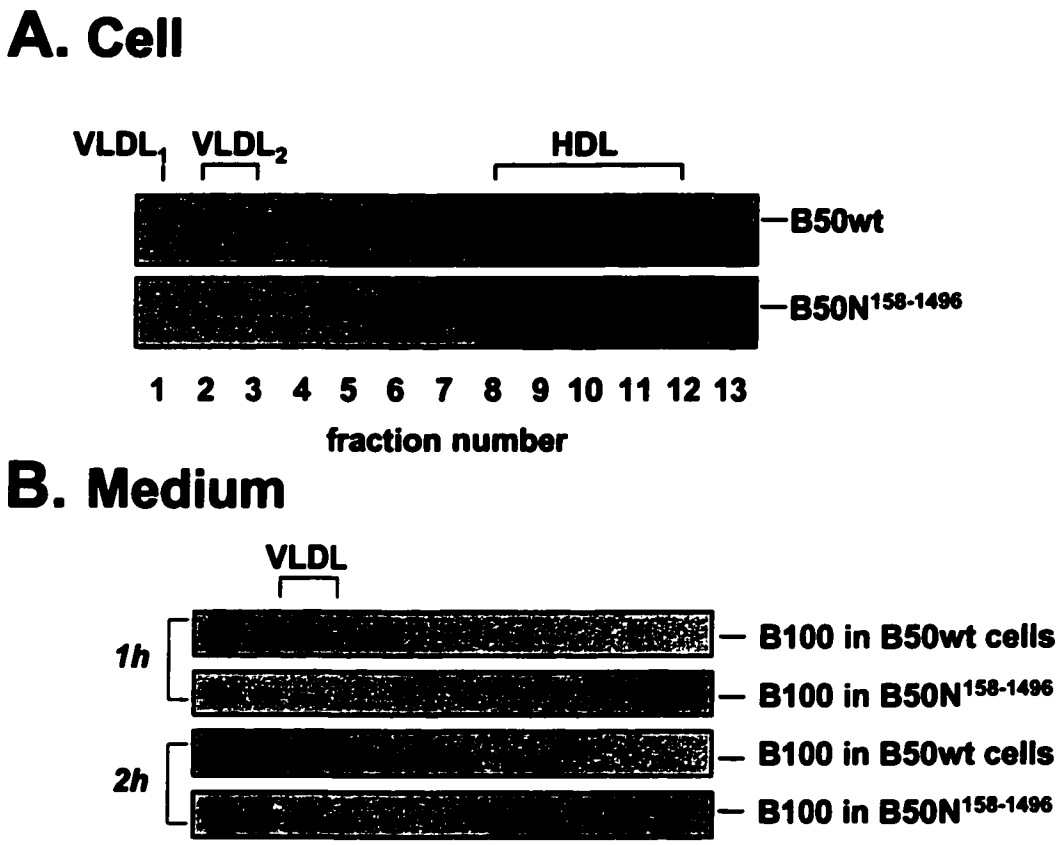
A. Cell
VLDL1
VLDL2
HDL
B50wt
B50N158-1496
1 2 3 4 5 6 7 8 9 10 11 12 13
fraction number
B. Medium
VLDL
1h
2h
B100 in B50wt cells
B100 in B50N158-1496
B100 in B50wt cells
B100 in B50N158-1496

FIG. 3.2.5. **Effect of N-to-Q substitution on lipid synthesis and secretion.** Cells (6-well plates) stably transfected with human B50wt or B50N$^{158\text{-}1496}$ were labeled with [^{3}H]glycerol (5 μCi/well) in DMEM (20% serum and 0.4 mM oleate) for indicated times. Lipids extracted from cells *(B)(D)* and medium *(A)(C)* were resolved by thin-layer chromatography. Radioactivity associated with TG and PC (mean ± S.D., n=3) was quantified by scintillation counting.

Fig. 3.2.5.

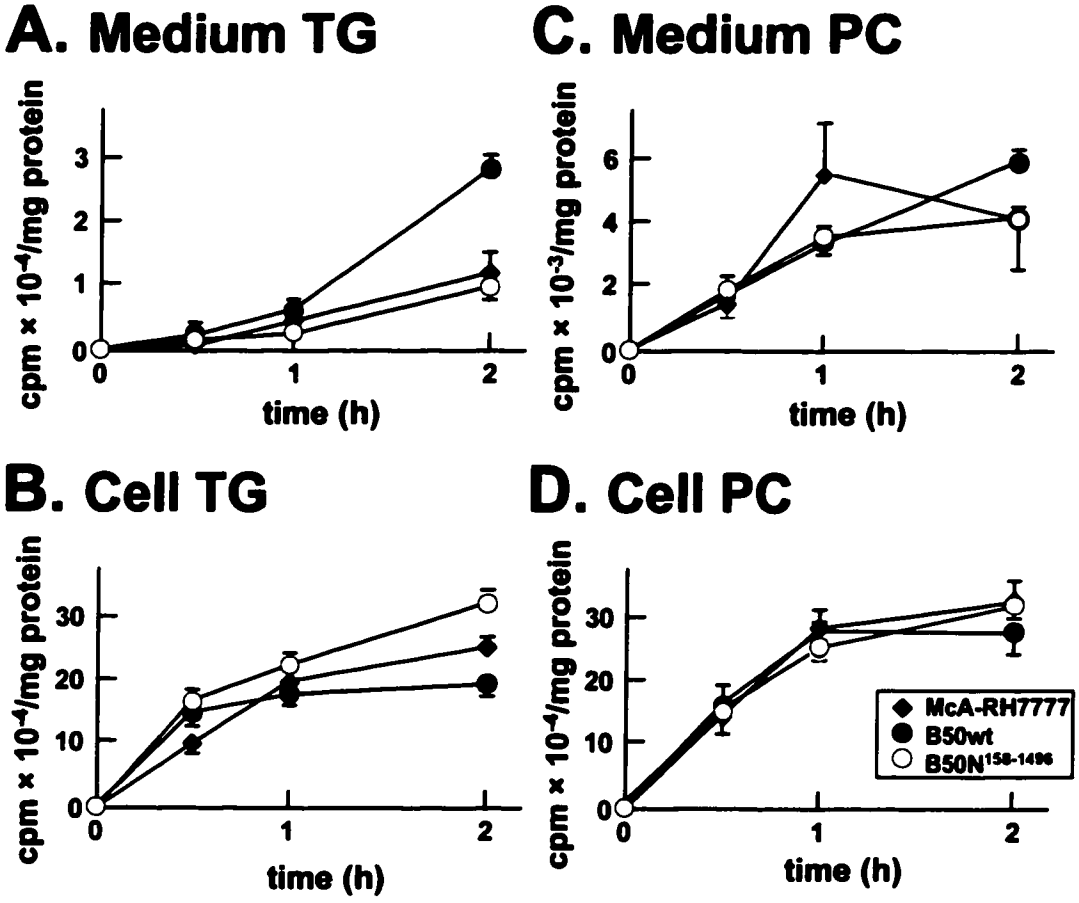
A. Medium TG
C. Medium PC
B. Cell TG
D. Cell PC
cpm x 10-4/mg protein
cpm x 10-3/mg protein
time (h)
McA-RH7777
B50wt
B50N158-1496

3.3. The role of N-linked oligosaccharides in the intracellular distribution of apolipoprotein B

Loss of N-linked oligosaccharides in proteins has been shown to associate with delayed ER exit (234). To gain insight into the mechanisms responsible for the impaired secretion of mutant apoB variants containing N-to-Q substitution, we raised two questions: (a) Is impaired secretion of mutant apoB variants containing N-to-Q substitution associated with impaired intracellular distribution or intracellular accumulation of apoB? (b) Is impaired secretion of mutant apoBs containing N-to-Q substitution associated with alterations in abundance or activity of ER molecular chaperones thought to interact with apoB, for instance BiP, calnexin, or MTP ? To address these questions we used transfected McA-RH7777 cells expressing human B17, B37, or B50, which contain N-to-Q substitution at various N-linked glycosylation site(s).

3.3.1. Intracellular distribution of mutant apolipoprotein B determined following subcellular fractionation using Nycodenz gradient ultracentrifugation

To determine if the N-linked oligosaccharides play a role in the intracellular distribution of apoB, we examined subcellular distribution of mutant apoB containing N-to-Q substitution by Nycodenz gradient ultracentrifugation. The post-nuclear supernatants from cells stably transfected with expression plasmid encoding human B17 were isolated and fractionated by ultracentrifugation using Nycodenz gradient. Calnexin and α-mannosidase II were used as ER and medial Golgi markers, respectively (Fig. 3.3.1*A*). Immunoblot analysis of apoB17 showed two discernible peaks that were localized closely with the respective ER and Golgi markers (Fig. 3.3.1*B*).

Analysis of subcellular distribution of human B17wt and B17N^{158} was performed at 15 (Fig. 3.3.2*A*) and 60 min (Fig. 3.3.2*B*) after metabolic labeling, as determined by subcellular fractionation, no discernible difference was observed in the relative distribution in ER or Golgi between B17wt and B17N^{158}. Interestingly, while the intracellular distribution of endogenous B100 was similar in cells expressing B17wt and B17N^{158} 15 min after metabolic labeling (Fig. 3.3.3*A*), intracellular accumulation of the endogenous B100 in the ER compartment was observed in cells expressing mutant B17N^{158} at 60 min after metabolic labeling (Fig. 3.3.3*B*). The observed intracellular accumulation of rB100 in cells expressing B17N^{158} suggests that expression of mutant B17 might exert a negative effect on the endogenous apoB100 secretion. This is in agreement with the previous evidence (Fig. 3.2.4*B*) showing that the expression of B50N$^{158\text{-}1486}$ resulted in impaired secretion of endogenous apoB100. Whether the expression of B37N$^{158\text{-}1496}$ and B50N$^{158\text{-}1496}$ results in retention of endogenous apoB100 in the ER remains to be determined.

The subcellular distribution of mutant B37 and B50 containing N-to-Q substitution was examined by Nycodenz gradient ultracentrifugation (Fig. 3.3.4). Immunoblot analysis showed that at steady state, there was no difference in the distribution in the ER or Golgi compartments between B37wt and B37N$^{158\text{-}1496}$ (Fig. 3.3.4*A*). The lack of an accumulation of B37N$^{158\text{-}1496}$ within cells agrees with the pulse-chase results (Fig. 3.1.9*B*). In the case of B50, even though the concentration of B50N$^{158\text{-}1496}$ at steady state was increased in the ER and Golgi compartment (Fig. 3.3.4*B*), the relative distribution of B50N$^{158\text{-}1496}$ was nearly identical to that of B50wt. The elevated amount of cell-

associated B50N$^{158\text{-}1496}$ agrees with the pulse-chase results showing prolonged retention of B50N$^{158\text{-}1496}$ in the cells after translation (Fig. 3.1.10*A*). The majority of both B50wt and B50N$^{158\text{-}1496}$ was localized within the fractions containing the ER marker calnexin. A proportion of B50N$^{158\text{-}1496}$ accumulated in a compartment that contained neither calnexin nor α-mannosidase II (Fig. 3.1.10*B*, fractions 3-5). These data suggest that the loss of N-linked oligosaccharides in B50 was probably not associated with delayed ER exit, however, it was likely associated with impaired secretion from distal compartments.

3.3.2. Intracellular localization of mutant apolipoprotein B determined using immunocytochemistry and confocal microscopy

To identify the cellular compartments corresponding to the distribution of B50wt and B50N$^{158\text{-}1496}$, we performed indirect double immunofluorescence co-localization studies. Confocal images showed that both B50wt and B50N$^{158\text{-}1496}$ appeared as punctate staining throughout the cell with high intensity near the perinuclear area (Fig. 3.3.5, *left* panels labeled with *1D1*). The overall intensity of B50N$^{158\text{-}1496}$ was relatively stronger than that of B50wt, which is in agreement with the observation of prolonged intracellular retention of B50N$^{158\text{-}1496}$ (Fig. 3.1.10*A*). Merge of fluorescence derived from apoB with that from calnexin or α-mannosidase II showed substantial co-localization of apoB with the ER or medial Golgi marker (Fig. 3.3.5). Besides the relatively stronger overall intensity of B50N$^{158\text{-}1496}$ compared with B50wt (in agreement with the Nycodenz gradient data shown in Fig. 3.3.4.), there was no apparent difference in the distribution of B50wt and B50N$^{158\text{-}1496}$. A proportion of B50wt and B50N$^{158\text{-}1496}$ was not entirely co-localized with either calnexin or α-mannosidase II (Fig. 3.3.5, right panels). The identity of the

compartment where this proportion of B50 proteins was localized remains to be determined. These results further suggest that the loss of N-linked oligosaccharides had little effect on intracellular distribution of B50N$^{158\text{-}1496}$.

The effect of the loss of N-glycan on intracellular distribution was more directly determined using GFP (green fluorescent protein) tagged apoB protein (*i.e.* B46). The B46wt-GFP and B46N$^{158\text{-}1496}$-GFP fusion proteins contained the amino-terminal 2099 amino acids of apoB plus GFP at their carboxyl termini. Including GFP at the carboxyl terminus of B46 did not affect its ability to form and secrete lipoproteins in transiently transfected McA-RH7777 cells. Live cell imaging of B46-wt-GFP and B46N$^{158\text{-}1496}$ using video microscopy did not detect difference in their intracellular distribution (data not shown). These data further corroborated evidence that the loss of N-glycans is not associated with gross alterations in the intracellular distribution of apoB.

3.3.3. Abundance of molecular chaperones and triglyceride transfer activity of the microsomal triglyceride transfer protein

We tested the intracellular abundance of molecular chaperones, including calnexin, BiP, GRP94, and MTP, in cells expressing mutant apoBs containing the N-to-Q substitution. The post-nuclear supernatants were isolated from cells expressing human B17wt or B17N^{158} and immunoblotting with anti-calnexin, anti-BiP, or anti-MTP antibody was performed (Fig. 3.3.6*A*). While no detectable changes were observed in signal for calnexin, GRP94, BiP, or PDI, there was a striking increase in the intracellular levels of MTP in cells expressing mutant B17N^{158} (Fig. 3.3.6*A*). Increase in the

intracellular levels of MTP was also observed in cells expressing mutant B37N$^{158\text{-}1496}$ (Fig. 3.3.6*B*) but not B50N$^{158\text{-}1496}$ (Fig. 3.3.6*C*). The reason for the increase in MTP levels remains unclear.

We tested the triglyceride (TG) transfer activity of MTP in cells expressing human wild-type B17 and B50 as well as mutant B17N^{158} and B50N$^{158\text{-}1496}$ (Fig. 3.3.7). The post-nuclear supernatants were isolated, and the TG transfer activity of MTP was measured and quantified. Increased MTP activity was observed in cells expressing B50N$^{158\text{-}1496}$ (Fig. 3.3.7*B*) but not in cells expressing B17N^{158} (Fig. 3.3.7*A*). The reason why the MTP immunoblotting data does not agree with the activity assay data is unclear. It is possible, however, that the MTP assay not only measures the TG transfer activity of MTP, but also of other intracellular transfer proteins.

3.3.4. Conclusion

We have shown that the loss of N-linked oligosaccharides in apolipoprotein B mutants containing N-to-Q substitution has little effect on their intracellular distribution. Accumulation of apoB50N$^{158\text{-}1496}$ within entire secretory compartments was probably associated with impaired secretion from the distal compartments. Furthermore, our results show changes in abundance and activity of one molecular chaperone, MTP, but not that of BiP, calnexin or grp94, once mutant apoBs containing N-to-Q substitution are expressed. The mechanism by which impaired secretion of mutant apoBs containing N-to-Q substitution directly or indirectly involves the function of MTP remains to be determined.

FIG. 3.3.1. **Subcellular fractionation using Nycodenz gradient ultracentrifugation.** *A*, cells (100-mm dish, 80% confluent) stably transfected with human B17 were washed with PBS and homogenized. The post-nuclear supernatants were isolated and fractionated by ultracentrifugation in a Nycodenz gradient. Aliquots were subjected to SDS-PAGE, transferred to nitrocellulose membranes, and probed with anti-calnexin or anti-α-mannosidase II (α-MII) antibody. The intensity of the bands was semi-quantified by scanning densitometry. Data are presented as "% maximum value" in which 100% corresponds to the highest value. *B*, the human apoB17 protein in each fraction was probed with monoclonal antibody 1D1. The intensity of the bands was semi-quantified by scanning densitometry. Data are representative of two experiments with similar results.

Fig. 3.3.1.

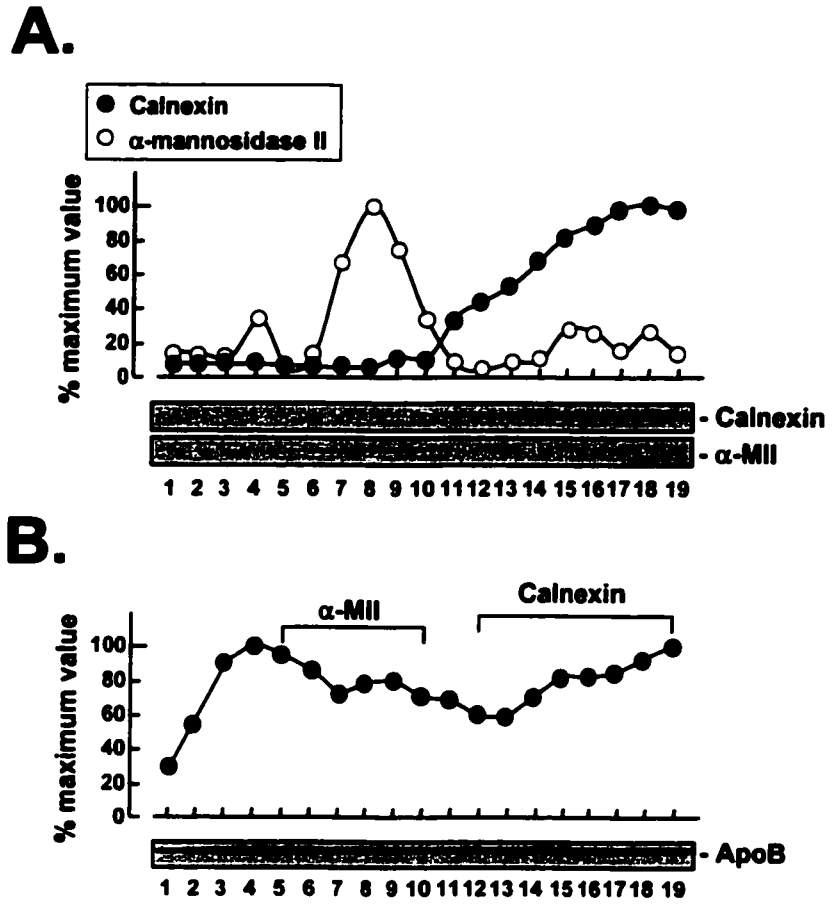
A.
Calnexin
α-mannosidase II
% maximum value
100
80
60
40
20
0
- Calnexin
- α-MII
1 2 3 4 5 6 7 8 9 10 11 12 13 14 15 16 17 18 19
B.
α-MII
Calnexin
% maximum value
100
80
60
40
20
0
- ApoB
1 2 3 4 5 6 7 8 9 10 11 12 13 14 15 16 17 18 19

FIG. 3.3.2. **Effect of N^{158}-to-Q substitution on intracellular distribution of apolipoprotein B17.** Cells (100-mm dish, 80% confluent) stably transfected with expression plasmid encoding human B17wt or $B17N^{158}$ were labeled with ^{35}S-amino acids (200 μCi/ml) for 15 min *(A)* or 60 min *(B)*. The post-nuclear supernatants were isolated and fractionated by ultracentrifugation in a Nycodenz gradient. Aliquots were subjected to SDS-PAGE, and fluorography. The intensity of apoB17 proteins on the fluorograms *(bottom)* was semi-quantified by scanning densitometry. Data are presented as "% maximum value" in which 100% corresponds to the highest value *(top)*. The experiment was performed once.

Fig. 3.3.2.

A. 15 min labeling

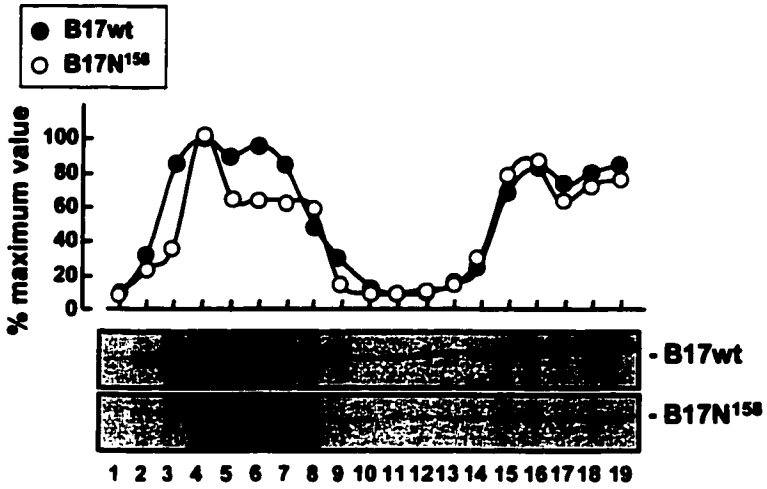

B. 60 min labeling

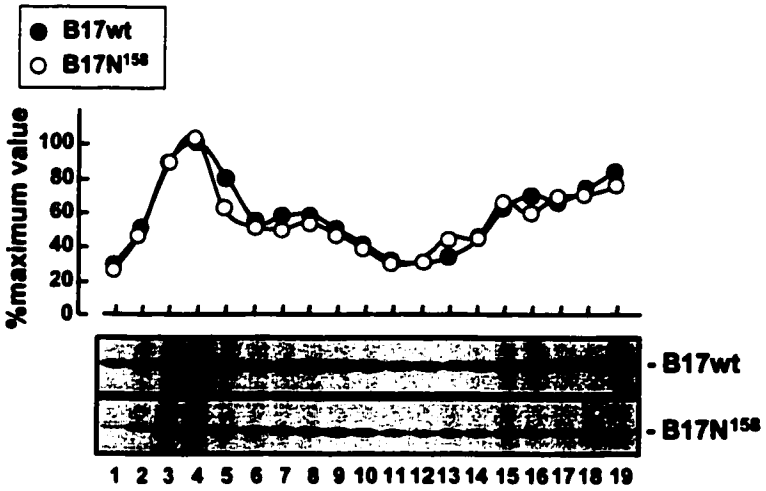

FIG. 3.3.3. **Impaired exit of endogenous apolipoprotein B100 from ER of cells transfected with apolipoprotein B17N^{158}.** Cells (100-mm dish, 80% confluent) stably transfected with human B17wt or B17N^{158} were labeled with ^{35}S-amino acids (200 μCi/ml) for 15 min *(A)* or 60 min *(B)*. The post-nuclear supernatants were isolated and fractionated by ultracentrifugation in a Nycodenz gradient. Aliquots were subjected to SDS-PAGE, and fluorography. The intensity of endogenous rat apoB100 on the fluorograms *(bottom)* was semi-quantified by scanning densitometry. Data are presented as "% maximum value" in which 100% corresponds to the highest value *(top)*. The experiment was performed once.

Fig. 3.3.3.

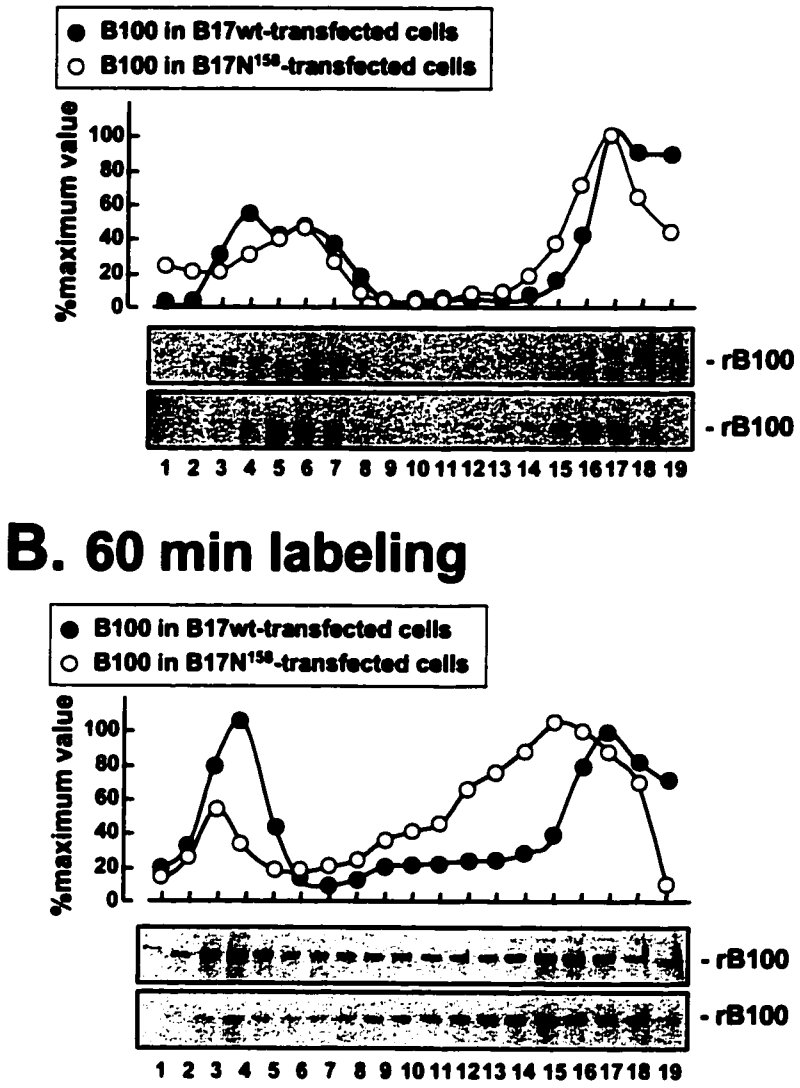
A. 15 min labeling
B100 in B17wt-transfected cells
B100 in B17N158-transfected cells
%maximum value
100
80
60
40
20
0
- rB100
- rB100
1 2 3 4 5 6 7 8 9 10 11 12 13 14 15 16 17 18 19
B. 60 min labeling
B100 in B17wt-transfected cells
B100 in B17N158-transfected cells
%maximum value
100
80
60
40
20
0
- rB100
- rB100
1 2 3 4 5 6 7 8 9 10 11 12 13 14 15 16 17 18 19

FIG. 3.3.4. **Lack of N-linked oligosaccharides did not affect intracellular distribution of apolipoprotein B37 and apolipoprotein B50.** The post-nuclear supernatants were isolated from cells (100-mm dish, 80% confluent) and fractionated by ultracentrifugation in a Nycodenz gradient. Aliquots were resolved by SDS-PAGE, transferred to nitrocellulose membranes, and subjected to immunoblotting. *A*, distribution of B37wt and $B37N^{158-1496}$ within Nycodenz gradient. Human apoB proteins were probed with monoclonal antibody 1D1 *(insets)*. The intensity of apoB on immunoblots was semi-quantified by scanning densitometry. *B*, distribution of B50wt and $B50N^{158-1496}$ within Nycodenz gradient. Repetition of the experiment yielded similar results.

Fig. 3.3.4.

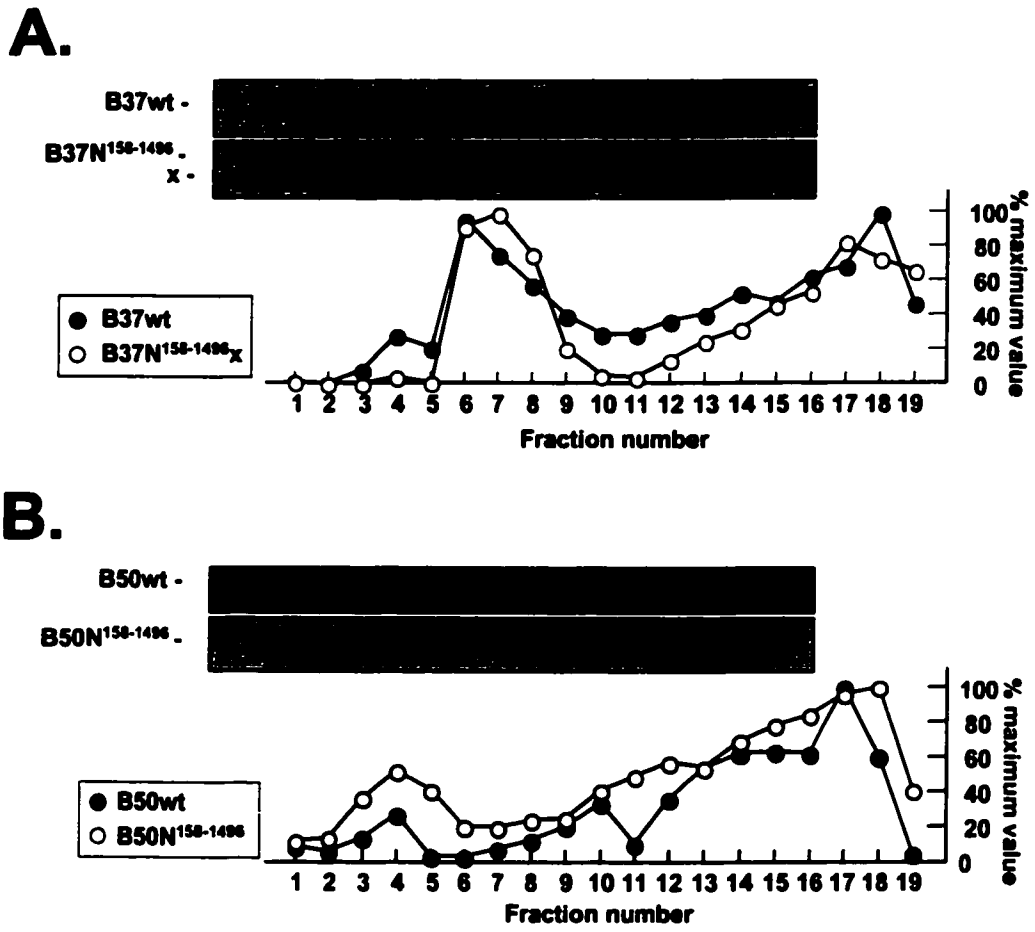
A.
B37wt -
B37N158-1496 -
X -
B37wt
B37N158-1496X
% maximum value
100
80
60
40
20
0
1 2 3 4 5 6 7 8 9 10 11 12 13 14 15 16 17 18 19
Fraction number
B.
B50wt -
B50N158-1496 -
B50wt
B50N158-1496
% maximum value
100
80
60
40
20
0
1 2 3 4 5 6 7 8 9 10 11 12 13 14 15 16 17 18 19
Fraction number

FIG. 3.3.5. **Lack of N-linked oligosaccharides did not affect intracellular localization of apolipoprotein B50.** Cells stably transfected with B50wt or B50N$^{158\text{-}1496}$ were plated on cover slips, fixed, and permeabilized. Monoclonal antibody 1D1 was used to probe the recombinant human apoB with goat anti-mouse IgG Alexa Fluro 488 conjugate as secondary antibody. The ER and Golgi were probed with anti-calnexin and anti-α-mannosidase II antibodies, respectively, with Alexa Fluro 594 conjugated anti-rabbit IgG as secondary antibody. The images were captured using the MRC-1024 laser scanning confocal imaging system. Data are representative of two experiments with similar results.

Fig. 3.3.5.

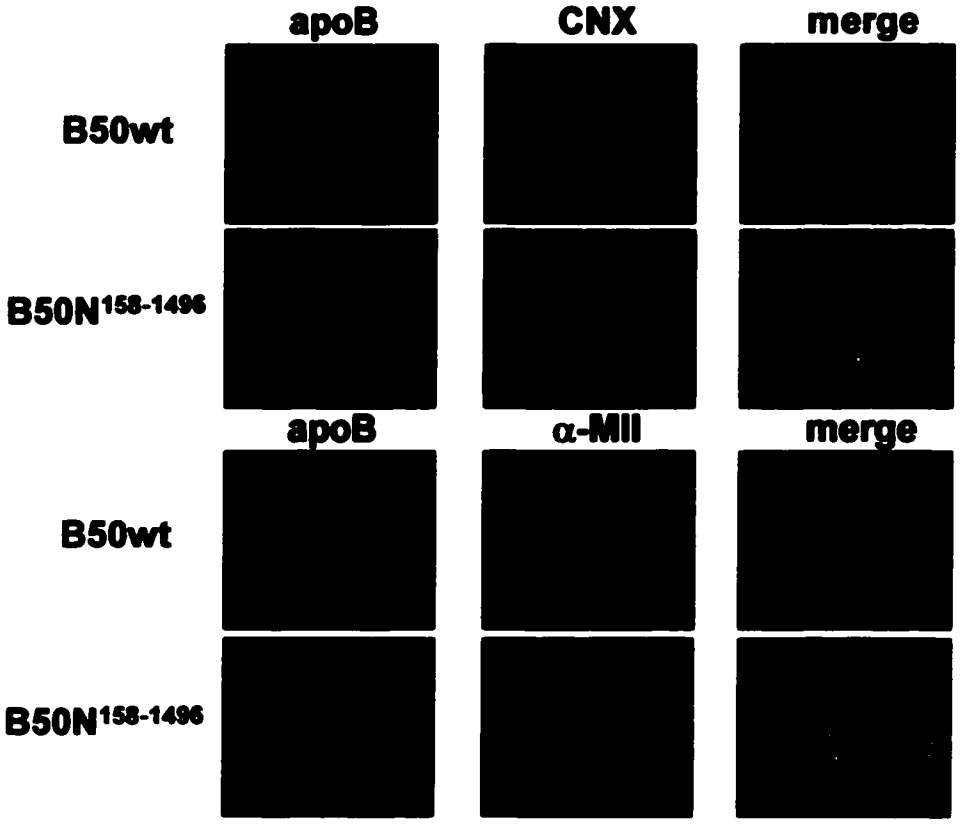
apoB
CNX
merge
B50wt
B50N158-1496
apoB
α-MII
merge
B50wt
B50N158-1496

FIG. 3.3.6. **Effect of N-to-Q substitution on intracellular abundance of chaperone proteins.** *A*, cells (100-mm dish, 80% confluent) stably transfected with human B17wt or $B17N^{158}$ were washed with PBS and homogenized. The post-nuclear supernatants were isolated. Aliquots in triplicate (lanes 1, 2, and 3) containing equal amount of total cell protein from each sample were subjected to SDS-PAGE, transferred to nitrocellulose membranes, and probed with anti-calnexin, anti-BiP, or anti-MTP antibody. *B*, immunoblots using anti-MTP antibody on isolated post-nuclear supernatants from cells stably transfected with human B37wt or $B37N^{158\text{-}1496}$. *C*, immunoblots using anti-MTP antibody on isolated post-nuclear supernatants from cells stably transfected with human B50wt or $B50N^{158\text{-}1496}$. Data are representative of three experiments with similar results.

Fig. 3.3.6.

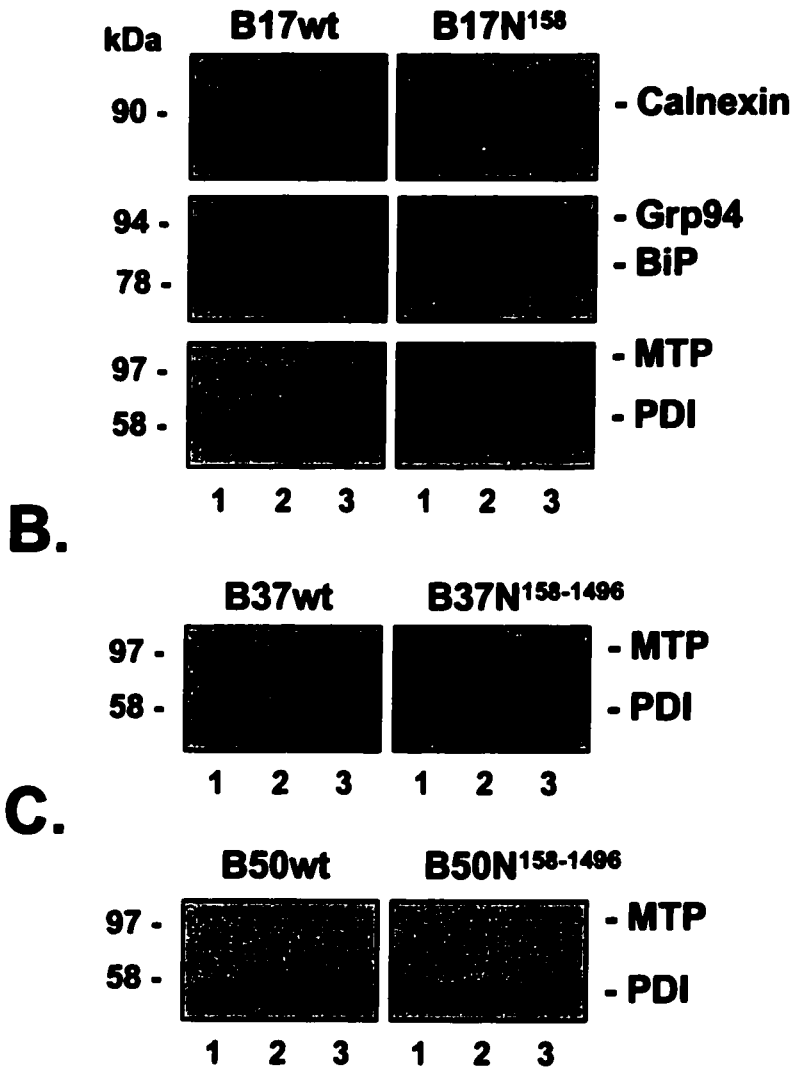
A.
kDa
B17wt
B17N158
90 -
- Calnexin
94 -
- Grp94
78 -
- BiP
97 -
- MTP
58 -
- PDI
1 2 3 1 2 3
B.
B37wt
B37N158-1496
97 -
- MTP
58 -
- PDI
1 2 3 1 2 3
C.
B50wt
B50N158-1496
97 -
- MTP
58 -
- PDI
1 2 3 1 2 3

FIG. 3.3.7. **Increased triglyceride transfer activity in cells overexpressing apolipoprotein B50N$^{158-1496}$.** Cells (100-mm dish, 80% confluent) stably transfected with human wild type and mutant B17 or B50 were washed with PBS and homogenized. The post-nuclear supernatants were isolated and protein concentration determined. The TG transfer activity of MTP was measured using [^{14}C]triolein as a substrate, as previously described (5). Data are an average of two independent experiments.

Fig. 3.3.7.

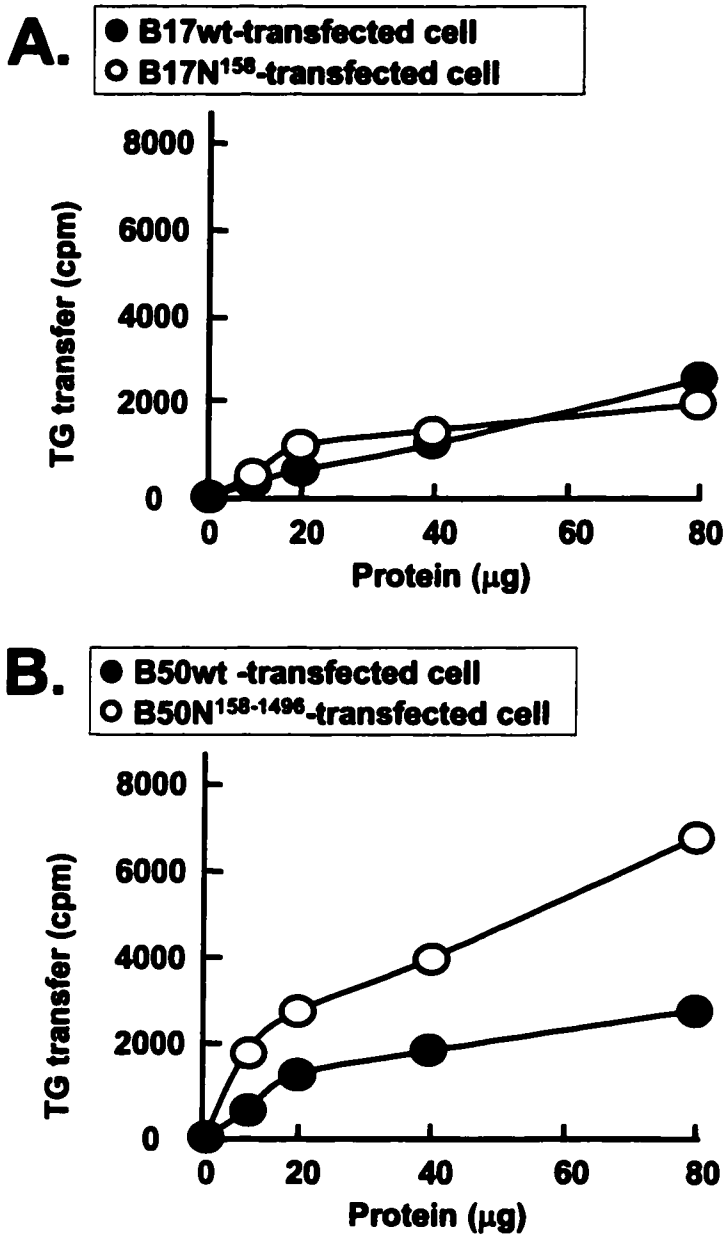
A.
● B17wt-transfected cell
○ B17N158-transfected cell
TG transfer (cpm)
8000
6000
4000
2000
0
0
20
40
60
80
Protein (μg)
B.
● B50wt -transfected cell
○ B50N158-1496-transfected cell
TG transfer (cpm)
8000
6000
4000
2000
0
0
20
40
60
80
Protein (μg)

3.4. Discussion

Although the obligatory role of apolipoprotein B in hepatic VLDL assembly is well known, neither the tertiary structure of apolipoprotein B nor modifications of the structural element(s) within apolipoprotein B have been well characterized. Since both apoB100 and the N-terminal 48% of full-length apoB100 have the ability to assemble VLDL, the indispensable structural elements(s) required for VLDL assembly and secretion are likely localized within apoB48. In this study, we have attempted to determine the requirement of N-linked glycosylation at the N-terminus of apoB during biogenesis of apolipoprotein B-containing VLDL in rat hepatoma McA-RH7777 cells. The approach that was used to study the requirement and possible role(s) of N-linked oligosaccharides of human apoB involved tunicamycin treatment and mutagenesis at consensus N-linked glycosylation site(s) within C-terminally truncated human apoB variants.

We observed close to 50% decrease in secretion efficiency of human apoB17 following N-to-Q substitution at a single glycosylation site (N^{158}) within B17 (Fig. 3.1.3*B*). The B17 represents the amino-terminal β-α1 domain of apoB100 (38) that is highly disulfide bonded and secreted as a lipid-poor form. (41). Although B17 itself is unable to assemble neutral lipids to form lipoproteins, it has strong binding affinity towards MTP (105, 241) and is essential for lipid recruitment mediated by downstream lipid-binding sequences (104). Studies *in vivo* of patients with hypobetalipoproteinemia (242) and cell culture studies with truncated forms of human apoB (40, 238) have suggested that the ability to assemble VLDL lies between ~30% and ~40% of the

apoB100 length, a region enriched with amphipathic β-strands (31). The observation that loss of a single N-glycan in B17 results in impaired secretion of mutant B17N^{158} (Fig. 3.1.3.) is striking, which indicates that the β-α1 domain structure not only requires appropriate disulfide bonding (102, 106) but also N-linked oligosaccharides. The residue N^{158} in apoB is conserved between apoB and MTP, and is immediately adjacent to a disulfide bridge (C^{159}-C^{185} in apoB) that is also conserved between the two proteins. On the basis of the known crystal structure of lamprey lipovitellin, this disulfide bridge (C^{159} -C^{185}) is believed to connect two β-strands within the amino-terminal β-barrel structure of the β-α1 domain in human apoB (37). Although the current data suggest a significant role of N^{158} –glycan in B17, previous mutagenesis studies showed that loss of the adjacent disulfide bond (C^{159} -C^{185}) had no impact on the secretion of B29 (102, 106). Insights into a functional role of the N^{158} –linked glycan in B17 folding and stability have to await structural information on the β-α1 domain.

Observations of differential sensitivity of recombinant apoB variants to tunicamycin treatment and of decreased effect of N^{158}-to-Q substitution on longer apoBs (B37 and B48) could be interpreted by two alternate possibilities: (a) Increased lipid-binding ability associated with increased length of recombinant apoB variants can offset the requirement for N-linked oligosaccharides. (b) Since additional N-linked glycosylation sites are found within N-terminal half of apoB, the differential sensitivity of the recombinant apoB variants to tunicamycin treatment may reflect the requirement of N-linked oligosaccharide at a particular site(s) within apoB. To distinguish between these two alternatives we performed N-to-Q substitution at the other four N-linked glycosylation

sites within B37, namely at N^{956}, N^{1341}, N^{1350}, and N^{1496}. We observed a decrease (by 50%) in the secretion efficiency of B37 (Fig. 3.1.9.), suggesting that the lipid-binding sequences downstream of B17 cannot offset the requirement of N-linked oligosaccharides for B37 secretion efficiency. Furthermore, we also observed a similar decrease in the secretion efficiency of B50, which contains additional hydrophobic sequences downstream of B37, when we performed N-to-Q substitution at all five glycosylation sites within B50 (Fig. 3.1.10.). Thus, neither the lipid-binding sequences downstream of B17 nor those downstream of B37 could offset the requirement of N-linked oligosaccharide conjugation onto apoB.

It is noteworthy that N-to-Q substitution at any single N-glycan site within B37 had marginal effect on its secretion, except for N^{1496}. The loss of N^{1496} in B37 not only resulted in decreased secretion (although not to the same extent as in $B37N^{158\text{-}1496}$) but also affected electrophoretic mobility of $B37N^{1496}$ and $B37N^{158\text{-}1496}$ (Fig. 3.1.8.). At the moment we are unable to conclude definitively that N^{1496} is of particular significance to B37 structure, since aberrant electrophoretic mobility was not evident for mutant $B50N^{158\text{-}1496}$. Induced proteolysis as a result of loss of N-glycans has been reported for the mutant of human transferrin receptor (239). The aberrant electrophoretic mobility of $B37N^{1496}$ and $B37N^{158\text{-}1496}$ is likely due to proteolysis. Since the low molecular weight species of $B37N^{158\text{-}1496}$ (designated $B37N^{158\text{-}1496}$ -x) was observed at the earliest time point of labeling within the ER, the proteolysis likely occurred in the ER. The mechanism for this loss of N-glycan induced proteolysis is currently unknown.

When N-to-Q substitution performed at a single N-glycan site was contrasted with that performed at multiple sites, it became clear that secretion of B37 was gradually impaired as the number of mutated N-glycan sites increased (Fig. 3.1.8*B*, *right five* bars marked *B37*). These data support the notion that cooperative action of multiple N-linked oligosaccharides takes place in the attainment of proper folding of the protein (185). Additionally, the difference in the effect of $N^{158\text{-}1496}$ mutation on electrophoretic mobility between B37 and B50 is intriguing. It suggests that whatever has happened to $B37N^{158\text{-}1496}$ could be offset in B50, apparently by acquisition of lipid-binding sequences downstream of B37. The nature of this compensation is unclear. However, it suggests strongly the existence of interplay between the lipid-binding sequences and N-linked oligosaccharides in achieving efficient biosynthesis of apoB.

Current studies indicated that the lack of N-glycans not only impairs the efficient secretion of the apoB polypeptide but also the assembly and secretion of the apoB-containing lipoproteins. We used metabolic labeling followed by ultracentrifugation methods to separate apoB-containing lipoproteins isolated from the microsomal lumen or the medium of McA-RH7777 cells stably transfected with wild-type or glycosylation mutants of B37 and B50. We observed that the lack of N-linked glycans not only decreased the secretion of the lipid-poor lipoproteins (*i.e.* the HDL-like species containing B37 or B50) but also compromised the association of B37 and B50 with neutral lipids in forming VLDL (Figs. 3.2.1. and 3.2.3.). Hence, conjugation of N-linked oligosaccharides to apoB represents an important pre-requisite for the assembly and secretion of apoB-containing VLDL.

Although the mechanism responsible for the impaired secretion of VLDL with mutants B37 or B50 is currently unclear, it is noted that the lack of N-glycans exerts different effects on the fate of these proteins. Pulse-chase experiments showed that while the impaired secretion of mutant $B37N^{158\text{-}1496}$ ($B17N^{158}$ as well) was not accompanied with intracellular accumulation (Figs. 3.3.4*A* and 3.3.2.), there was a prolonged intracellular retention of nascent $B50N^{158\text{-}1496}$ (Figs. 3.1.10*A*, 3.3.4*B*, and 3.3.5.). The lack of an accumulation of $B17N^{158}$ or $B37N^{158\text{-}1496}$ during chase is indicative of intracellular degradation of these mutant proteins. The degradation of $B17N^{158}$ and $B37N^{158\text{-}1496}$ is unlikely mediated by proteasomes that have been implicated in co-translational degradation of apoB100. Thus, including proteasomal inhibitors during continuous labeling renders no increase in the incorporation of ^{35}S-amino acids into $B17N^{158}$, even though the inhibitor treatment does prevent co-translational degradation of endogenous apoB100 in transfected cells (Fig. 3.1.4.).

However, that no $B17N^{158}$ or $B37N^{158\text{-}1496}$ was accumulated in the ER suggests that degradation, probably occurring in this compartment, preceded ER exit. In contrast, the effect of loss of N-glycan on intracellular B50 was different from that on B17 or B37. Under no circumstances have we observed rapid degradation of $B50N^{158\text{-}1496}$ during the chase. The prolonged retention of B50 within the secretory pathway suggests that amino acid sequences between the carboxyl termini of B37 and B50 make the protein less susceptible to degradation, even though these sequences cannot compensate for the requirement of N-glycans for efficient lipid recruitment. However, although the use of site-specific mutagenesis has allowed examination of the role of N-linked glycosylation

of apoB more directly than the use of the chemical inhibitor tunicamycin, it remains to be determined if the N-to-Q substitutions has caused gross structural changes that affects apoB function independent of N-glycans.

The mechanisms responsible for rapid degradation of mutant B17, B37 and for the ultimate degradation of mutant B50 that is retained within the cells need to be defined further. Recently, the existence of a dual mechanism for ER associated degradation of misfolded proteins has been reported. Thus, while misfolded membrane proteins are retained in the ER, misfolded soluble proteins are trafficked to the Golgi and then retrieved back to the ER for degradation (193). In the case of apoB, a secreted membrane protein, multiple degradation mechanisms have been postulated (79, 238). It will be of interest to determine if apoB N-glycan mutants undergo ER exit and then retrograde retrieval prior to the ER degradation. It will also be of interest to examine if the loss of N-glycans in apoB affects apoB translocation and retrograde translocation across the ER membrane.

MTP has been postulated to play a dual role of a chaperone that can facilitate apoB folding and also a role in lipid recruitment by apoB (243). The reported thresholds in the sensitivity of various truncated forms of apoB to MTP and in their requirement for MTP (241) can potentially explain our conflicting results suggesting that loss of N-linked glycosylation of apoB may be associated with changes in either the MTP mass or activity. We observed increased mass of MTP in cells overexpressing the $B17N^{158}$ and $B37N^{158\text{-}1496}$ mutants, but not in cells overexpressing $B50N^{158\text{-}1496}$ (Fig. 3.3.6.). On the

contrary, repeated MTP activity assays suggested increased triglyceride transfer activity in cells overexpressing B50N$^{158\text{-}1496}$ but not B17N^{158} (Fig. 3.3.7.). We postulate that the short apoB variants, *e.*g. B17, that do not have significant lipid-binding ability, require MTP to act predominantly as a chaperone, and in turn, the effect of mutagenizing N^{158} within B17 may lead to an up-regulation of MTP mass. On the other hand, for variants such as apoB50, the lipid-loading function of MTP may be more important than the role of MTP as chaperone. Hence, the effect of mutagenizing N-linked glycosylation sites within B50 may lead to, rather than changes in MTP mass, changes in the MTP activity, as reflected by the increased triglyceride transfer. Further experiments are required to determine whether this is the case and also, to determine whether loss of N-linked oligosaccharides of apoB leads to modification of interaction between apoB and MTP.

Chapter 4 The Role of Palmitoylation of Apolipoprotein B

4.1. Requirement of palmitoylation for the secretion of apolipoprotein B-containing very low density lipoproteins

Earlier studies have demonstrated that apoB undergoes palmitoylation, a post-translational modification whereby palmitate moiety is attached onto a free cysteine residue of the polypeptide (20-23). ApoB100 contains nine free cysteine residues available for palmitoylation. The role of palmitoylation of apoB was studied using site-specific mutagenesis of a single free cysteine at C^{1085} within human C-terminally truncated form of apoB, apoB29 (164). Studies using McA-RH7777 cells expressing either wild type B29 or palmitoylation mutant of B29 suggested a role for palmitoylation in lipoprotein assembly, since lack of palmitoylation at C^{1085} induced secretion of smaller and denser B29-containing lipoproteins. In addition, these studies suggested a positional role for palmitoylation in apoB trafficking, whereby lack of palmitoylation at C^{1085} resulted in accumulation of mutant B29 in the Golgi compartments (164).

The C-terminally truncated B29 does not contain significant lipid-binding sequences, and assembles into small, dense lipoprotein particles of HDL-like density. Inability of apoB29 to form VLDL precluded the determination of the role of apoB palmitoylation in VLDL assembly and secretion. We decided to examine the requirement of apoB palmitoylation in the assembly and secretion of the apoB-containing VLDL using an apoB variant that assembles VLDL, namely human apoB48. We raised the following questions: (a) Does inhibition of B48 palmitoylation impair the secretion of the apoB polypeptide? (b) How does the inhibition of B48 palmitoylation affect the assembly

and secretion of B48-containing lipoproteins? (c) Does lack of palmitoylation alter the intracellular distribution and localization of apoB48?

To address these questions, we treated McA-RH7777 cells stably expressing human apoB48 with 2-bromopalmitate, an agent that has been shown to inhibit palmitoylation by as yet unidentified mechanism (244). Following treatment with 2-bromopalmitate, the apoB48-containing lipoprotein secretion profile was determined using immunoblotting with 1D1 (Fig. 4.1.1.). We found that the treatment with 2-bromopalmitate completely abolished the secretion of apoB48-containing VLDL (Fig. 4.1.1 *bottom*).

4.1.1. Palmitoylation is not required for secretion of human apolipoprotein B48-containing very low density lipoproteins

To test the role of palmitoylation on secretion of the apoB-containing lipoproteins more specifically, we used transfected McA-RH7777 cells expressing variants of human apoB48 that contain C-to-S substitution at potential palmitoylation sites. We performed progressive C-to-S substitution at four potential palmitoylation sites at cysteine residues C^{1085}, C^{1395}, C^{1479}, and C^{1635}, respectively, within human B48 (Fig. 4.1.2*A*). Media was collected from McA-RH7777 cells stably transfected with wild type (B48wt) and mutant B48s containing the C-to-S substitution (designated $B48C^{1085}$, $B48C^{1085\text{-}1395}$, $B48C^{1085\text{-}1479}$, and $B48C^{1085\text{-}1635}$), and the apoB signal was detected semi-quantitatively using monoclonal antibody 1D1 specific for human apoB. The secretion of mutant B48s containing C-to-S substitution in this experiment suggested that C-to-S substitution does not impair secretion of the apoB polypeptide (Fig. 4.1.2*B*). The absence of palmitoylation

in mutant apoB48 containing $C^{1085-1635}$-to-S substitution was confirmed using metabolic labeling with [^{125}I]palmitate (Fig. 4.1.2*C*).

To test whether C-to-S substitution impairs secretion of the apoB48-containing lipoproteins, experiments were performed in stable cell lines expressing B48wt or mutant B48 containing C-to-S substitution. The medium was collected from the cells and fractionated by ultracentrifugation in a sucrose density gradient. The B48 in each fraction was detected using immunoblotting with monoclonal antibody 1D1 (Fig. 4.1.3.). No decrease of B48-containing lipoproteins in either VLDL or HDL fractions was observed in cells expressing mutant B48 containing either C-to-S substitution at a single ($B48C^{1085}$) or at multiple sites ($B48C^{1085-1395}$, $B48C^{1085-1479}$, and $B48C^{1085-1635}$).

The effect of C-to-S substitution at all four palmitoylation sites within B48 was confirmed using pulse-chase analysis (± 0.4mM oleate) and fractionation by ultracentrifugation in a sucrose density gradient (Fig. 4.1.4*A*). The ^{35}S-B48 in each fraction was detected using SDS-PAGE and fluorography. No inhibitory effect of $C^{1085-1635}$–to-S substitution on secretion of B48-containing VLDL lipoproteins was observed in cells that were treated with oleate (Fig. 4.1.4*A*). Similarly, immunoblotting of human B48-containing lipoproteins following fractionation using ultracentrifugation in a KBr gradient suggested no inhibitory effect of $C^{1085-1635}$–to-S substitution on secretion of B48-containing VLDL lipoproteins (Fig. 4.1.4*B*). However, treatment with 2-bromopalmitate almost completely abolished the secretion of apo$B48C^{1085-1635}$-containing VLDL (Fig. 4.1.4*C*). Whether the inhibition of apoB48-containing VLDL secretion is associated with

the inhibition of apoB palmitoylation or with an altogether different intracellular action elicited by using 2-bromopalmitate remains to be elucidated.

4.1.2. Palmitoylation is not required for intracellular transport of human apolipoprotein B48

In light of evidence suggesting palmitoylation at C^{1085} might play a role in regulation of apoB29 intracellular trafficking (164), we examined whether palmitoylation plays a role in the intracellular distribution of apoB48. We determined the subcellular distribution of mutant apoB containing C-to-S substitution using Nycodenz gradient ultracentrifugation. The post-nuclear supernatant from cells stably transfected with expression plasmid encoding human B48wt and $B48C^{1085\text{-}1635}$ were isolated and fractionated by ultracentrifugation using Nycodenz gradient (Fig. 4.1.5.). After SDS-PAGE and transfer onto nitrocellulose membranes, the samples were immunoblotted with anti-calnexin or anti-α-mannosidase II (α-MII) antibody to detect ER and Golgi markers, respectively (Fig. 4.1.5*A*), and with 1D1 to detect B48 (Fig. 4.1.5*B*). The reason for the predominant localization of the B48 signal in the Golgi compartment, unlike that observed for B100, B50, B37, or B17, which were mainly located in the ER, may be due to high expression level of apoB in the apoB48-transfected cells. The intracellular distribution of $B48C^{1085\text{-}1635}$ between ER and Golgi compartments was almost identical to that of B48wt (Fig. 4.1.6).

To identify the cellular compartments corresponding to the distribution of B48wt and $B48C^{1085\text{-}1635}$, we performed indirect double immunofluorescence co-localization

studies. Confocal images showed that both B48wt and B48C$^{1085-1635}$ appeared as punctate staining throughout the cell with high intensity near the perinuclear area (Fig. 4.1.6, *left* panels labeled with *1D1*). Merge of fluorescence derived from apoB with that from calnexin or α-mannosidase II showed substantial co-localization of apoB with the ER or medial Golgi marker (Fig. 4.1.6). Thus, similar to results obtained using Nycodenz gradient fractionation, the data from this experiment suggest that the loss of palmitoylation of B48 was probably not associated with impaired intracellular distribution of B48C$^{1085-1635}$.

4.1.3. Conclusion

In conclusion, the results from this preliminary study show no evidence for a deleterious effect on the secretion of apoB48-containing VLDL or on the intracellular distribution of apoB48 in the absence of palmitoylation following C-to-S substitution at four potential palmitoylation sites within human apoB48. Hence, contrary to the proposed role(s) of palmitoylation in apoB29-containing lipoprotein assembly and trafficking, our studies demonstrate that palmitoylation may not be required for the assembly and secretion of apoB48-containing VLDL or intracellular apoB48 distribution.

FIG. 4.1.1. **Effect of 2-bromopalmitate treatment on secretion of apolipoprotein B48-containing VLDL from McA-RH7777 cells.** Cells stably transfected with human B48wt were pre-treated for 16 h (± 100 μM 2-bromopalmitate), and further incubated in media supplemented with 0.4 mM exogenous oleate (± 100 μM 2-bromopalmitate) for 4 h. The medium was collected and fractionated by ultracentrifugation in a sucrose density gradient. The B48 protein in each fraction was detected by 1D1 immunoblotting. The experiment was performed once.

Fig. 4.1.1.

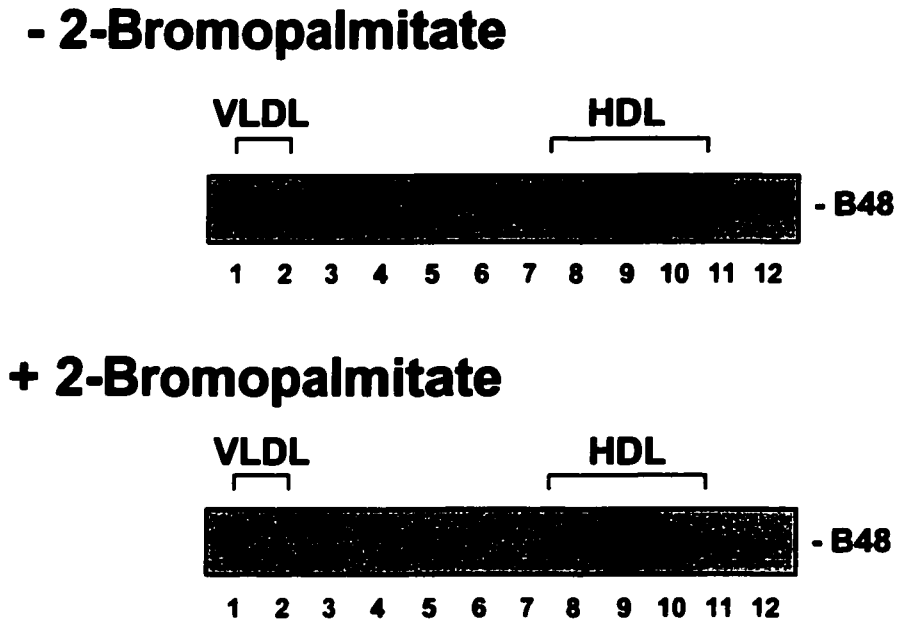
- 2-Bromopalmitate
VLDL
HDL
- B48
1 2 3 4 5 6 7 8 9 10 11 12
+ 2-Bromopalmitate
VLDL
HDL
- B48
1 2 3 4 5 6 7 8 9 10 11 12

FIG. 4.1.2. **Schematic diagram, expression, and palmitoylation of apolipoprotein B48 variants containing C-to-S substitution.** *A,* the top line depicts the location of free and disulfide bonded cysteine residues within human apoB100. The bottom lines depict mutant B48 that contain C-to-S substitution at cysteine residues C^{1085}, C^{1395}, C^{1479}, and C^{1635}, respectively. *B,* cells were stably transfected with human B48wt or mutant B48 containing C-to-S substitution. Expression of recombinant human apoBs was verified by immunoblotting of the conditioned media using monoclonal antibody 1D1. *C,* non-transfected McA-RH7777 cells *(control)*, and cells stably transfected with expression plasmids encoding human B48wt or $B48C^{1085\text{-}1635}$ were labeled with [^{125}I]palmitate as described previously (164). *Top,* conditioned media was immunoprecipitated for apoB proteins, resolved by SDS-PAGE, and subjected to fluorography. *Bottom,* expression of apoBs was verified by immunoblotting of the conditioned media using 1D1. The experiment was performed once.

Fig. 4.1.2.

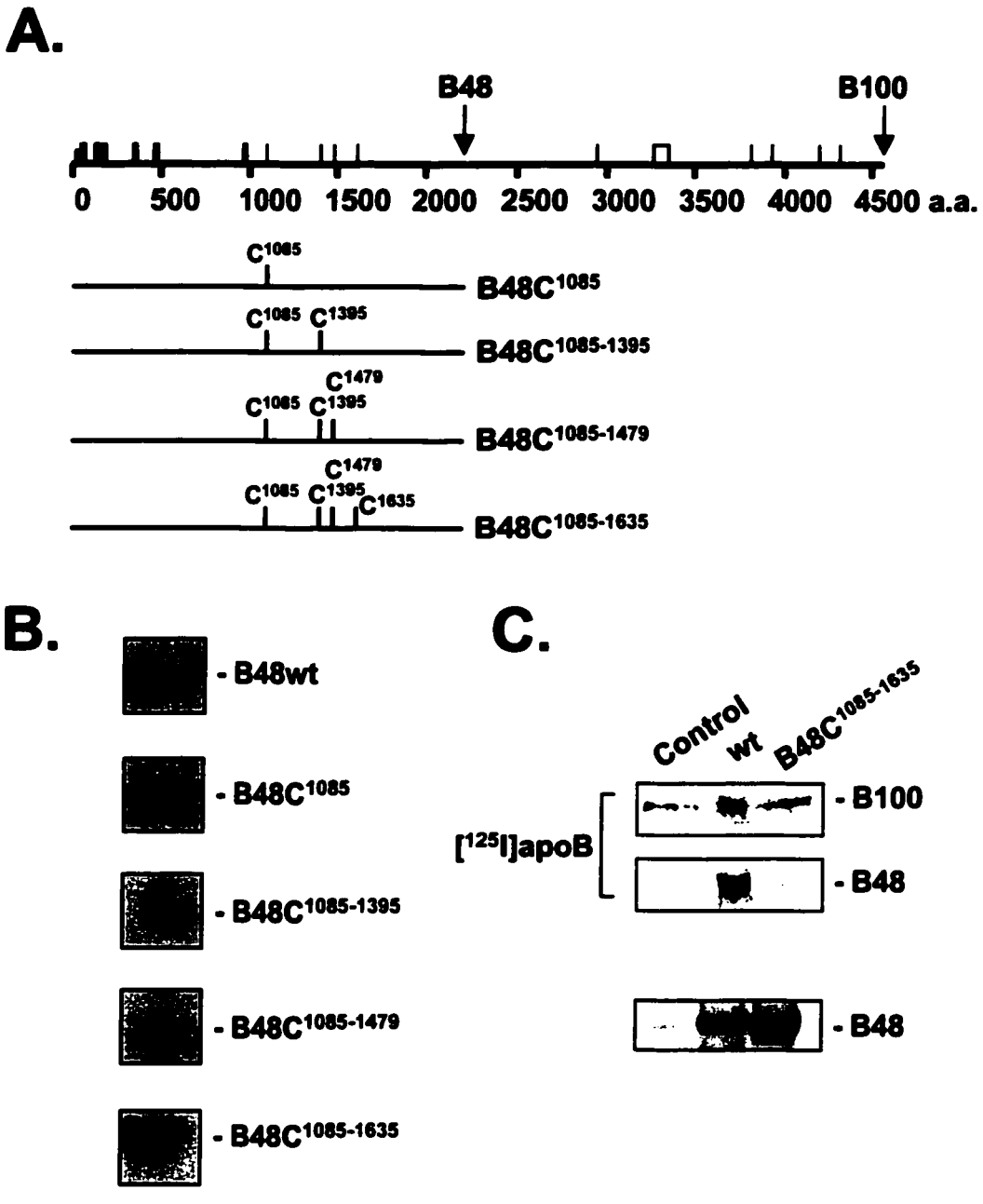
A.
B48
B100
0 500 1000 1500 2000 2500 3000 3500 4000 4500 a.a.
C1085
B48C1085
C1085 C1395
B48C1085-1395
C1479
C1085 C1395
B48C1085-1479
C1479
C1085 C1395 C1635
B48C1085-1635
B.
- B48wt
- B48C1085
- B48C1085-1395
- B48C1085-1479
- B48C1085-1635
C.
Control
wt
B48C1085-1635
[125I]apoB
- B100
- B48
- B48

FIG. 4.1.3. **Lack of palmitoylation did not impair secretion of apolipoprotein B48-containing VLDL.** Cells stably transfected with human B48wt or mutant B48 containing C-to-S substitution were incubated for 4 h in DMEM media (20% serum) supplemented with 0.4mM exogenous oleate. The medium was collected and fractionated by ultracentrifugation in a sucrose density gradient. The B48 proteins in each fraction were detected by 1D1 immunoblotting. Data are representative of five independent experiments using stable clones expressing different levels of apoB48.

Fig. 4.1.3.

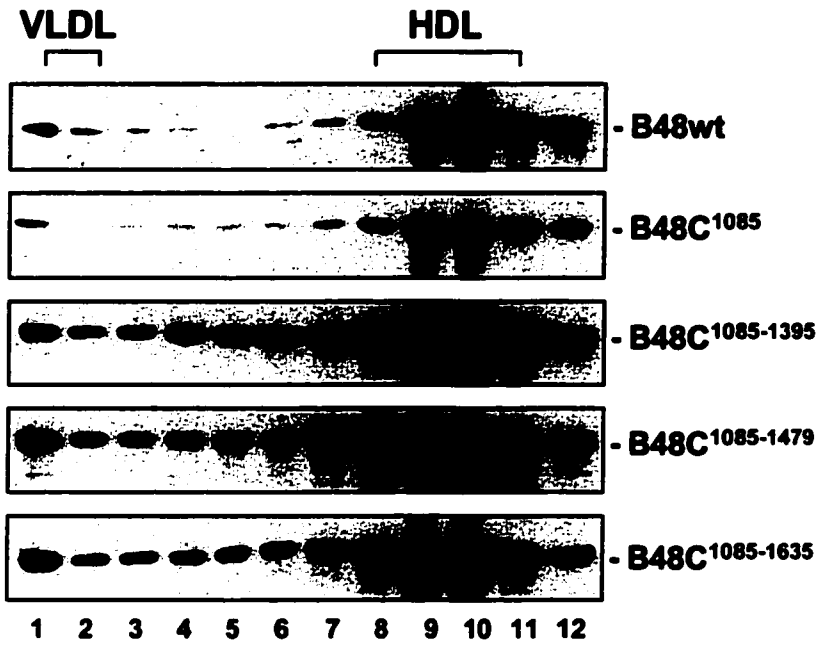
VLDL
HDL
- B48wt
- B48C1085
- B48C1085-1395
- B48C1085-1479
- B48C1085-1635
1 2 3 4 5 6 7 8 9 10 11 12

FIG. 4.1.4. **Apolipoprotein B48-containing lipoprotein secretion profile.** *A,* cells stably transfected with human B48wt or B48C$^{1085\text{-}1635}$ were pulse-labeled with ^{35}S-amino acids (200 μCi/ml) for 1 h, and chased for 2 h in the presence of 0.4 mM oleate. The medium was collected at the end of chase and fractionated by ultracentrifugation in a sucrose density gradient. The ^{35}S-B48 in each fraction was detected using SDS-PAGE and fluorography. *B,* conditioned medium was collected from cells stably transfected with human B48wt or B48C$^{1085\text{-}1635}$ and fractionated by ultracentrifugation using KBr gradient. The B48 protein in each fraction was detected by 1D1 immunoblotting. *C,* cells stably transfected with human B48C$^{1085\text{-}1635}$ were pre-treated for 16 h (± 100 μM 2-bromopalmitate), and further incubated in media supplemented with 0.4 mM exogenous oleate (± 100 μM 2-bromopalmitate) for 4 h. The medium was collected and fractionated by ultracentrifugation in a sucrose density gradient. The B48 protein in each fraction was detected by 1D1 immunoblotting. The experiments were performed once.

Fig. 4.1.4.

A. Labeling

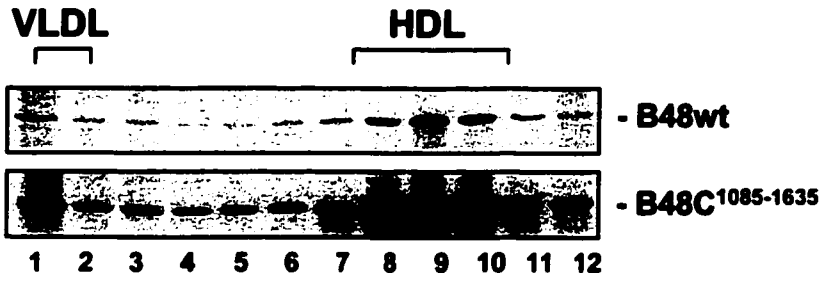

B. Potassium bromide gradient

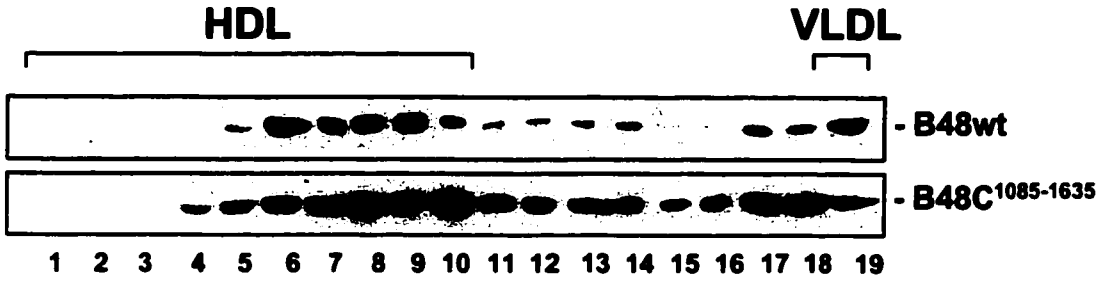

C. Treatment with 2-bromopalmitate

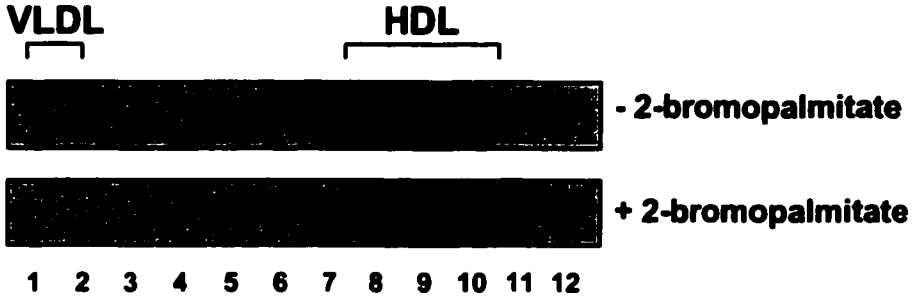

FIG. 4.1.5. **Lack of palmitoylation did not affect intracellular distribution of apolipoprotein B48.** Cells (100-mm dish, 80% confluent) stably transfected with human B48 or $B48C^{1085-1635}$ were washed with PBS and homogenized. The post-nuclear supernatants were isolated and fractionated by ultracentrifugation in a Nycodenz gradient. Aliquots were resolved by SDS-PAGE, transferred to nitrocellulose membranes, and subjected to immunoblotting. *A,* immunoblotting using anti-calnexin or anti-α-mannosidase II (α-MII) antibody. *B,* immunoblotting with monoclonal antibody 1D1 specific for human apoBs *(insets)*. The intensity of apoB on immunoblots was semi-quantified by scanning densitometry. Data are presented as "% maximum value" in which 100% corresponds to the highest value. The experiment was performed once.

Fig. 4.1.5.

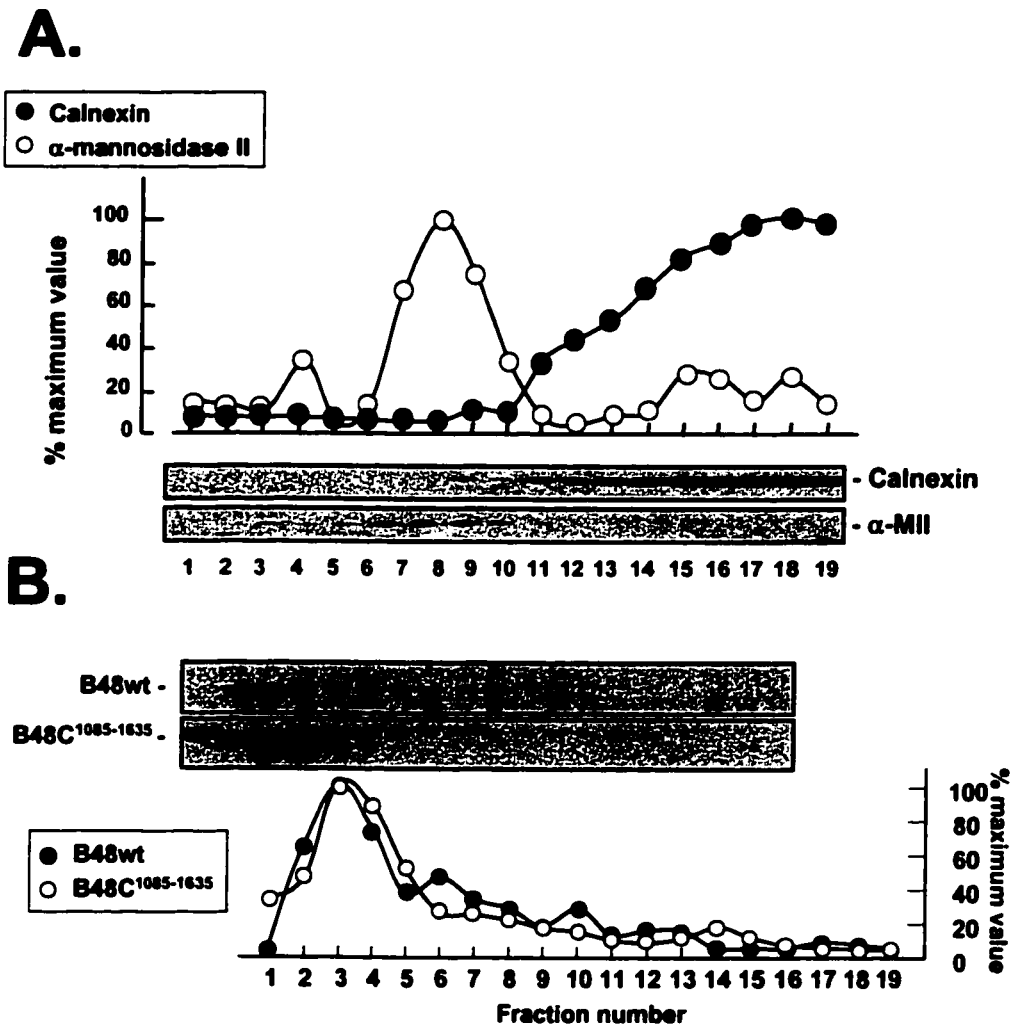
A.
Calnexin
α-mannosidase II
% maximum value
100
80
60
40
20
0
- Calnexin
- α-MII
1 2 3 4 5 6 7 8 9 10 11 12 13 14 15 16 17 18 19
B.
B48wt -
B48C1085-1635 -
B48wt
B48C1085-1635
100
80
60
40
20
0
% maximum value
1 2 3 4 5 6 7 8 9 10 11 12 13 14 15 16 17 18 19
Fraction number

FIG. 4.1.6. **Lack of palmitoylation did not affect intracellular localization of apolipoprotein B48.** Cells stably transfected with human B48wt or B48C$^{1085\text{-}1635}$ were plated on cover slips, fixed, and permeabilized. Monoclonal antibody 1D1 was used to probe the recombinant human apoB with goat anti-mouse IgG Alexa Fluro 488 conjugate as secondary antibody. The ER and Golgi were probed with anti-calnexin and anti-α-mannosidase II antibodies, respectively, with Alexa Fluro 594 conjugated anti-rabbit IgG as secondary antibody. The images were captured using the MRC-1024 laser scanning confocal imaging system. Data are representative of two independent experiments with similar results.

Fig. 4.1.6.

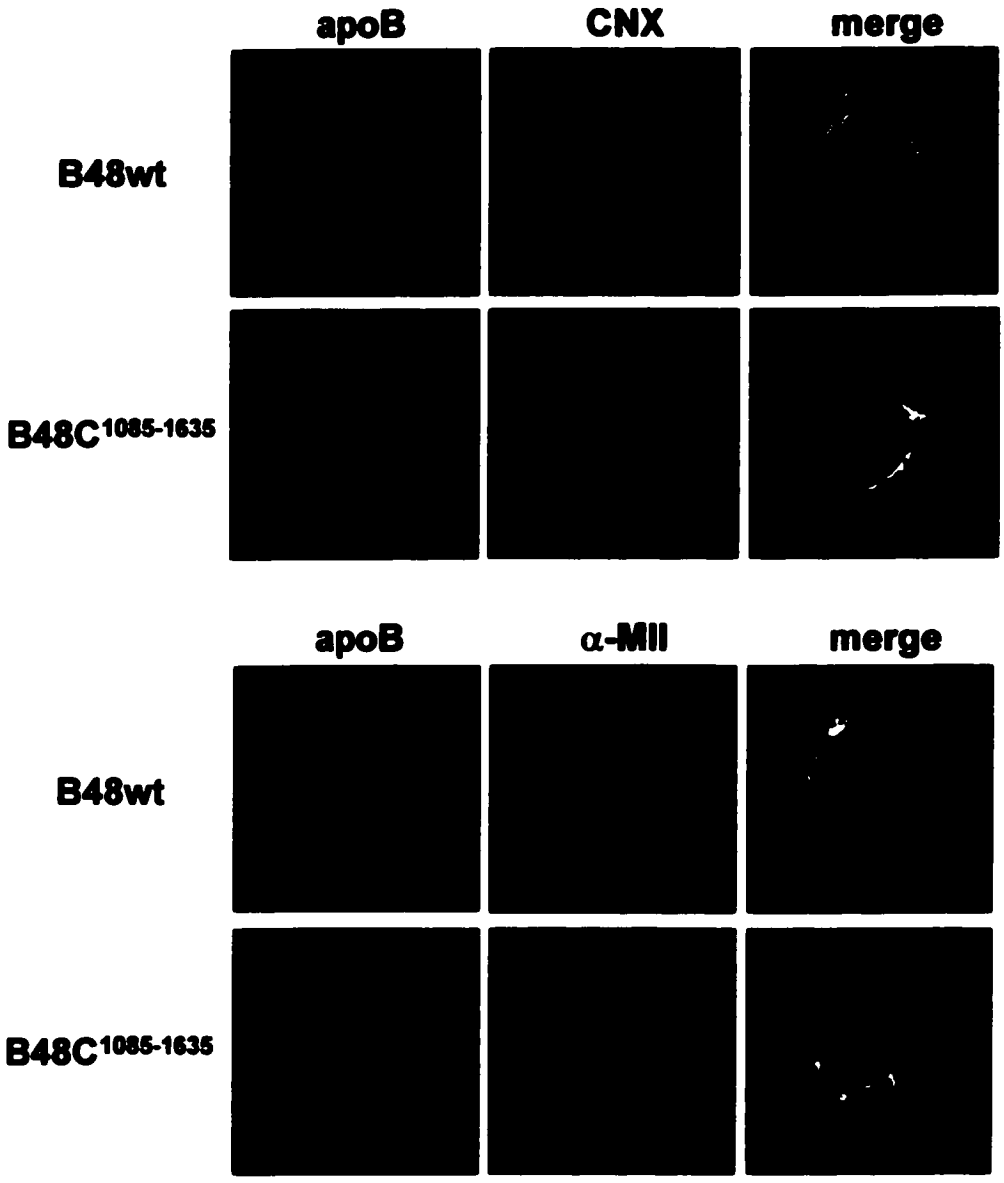
apoB
CNX
merge
B48wt
B48C1085-1635
apoB
α-MII
merge
B48wt
B48C1085-1635

4.2. Discussion

While the role of palmitoylation has been studied extensively in proteins with signal-transducing function, its involvement in the structure or function of apolipoprotein B has not been well characterized. To date, only one study has been performed addressing the role of palmitoylation in apoB biogenesis by using site-directed mutation of a single palmitoylated cysteine (Cys^{1085}) within the C-terminally truncated human apoB29 to prevent palmitoylation (164). The results of this study suggested a dual function of palmitoylation in regulating proper lipid recruitment and assembly into dense apoB29-containing lipoproteins but also in regulating the intracellular positioning of apoB29 (164). Thus, it was shown experimentally that the non-palmitoylated apoB29 accumulated in the Golgi and that the apoB29-containing lipoproteins that were secreted were smaller and denser than those of the wild-type palmitoylated apoB29.

Since apoB29 can only assemble dense lipoproteins of HDL buoyancy, it could not offer the opportunity to study the role of palmitoylation in the assembly and secretion of the apoB-containing VLDL. We hypothesized that if palmitoylation plays a role in assembly and secretion of apoB-containing VLDL, apoB forms that have the ability to recruit bulk TG would be more suitable than B29. It has been well documented that the naturally occurring truncated form of apoB, namely B48, has the ability to form VLDL in the rat liver. Thus, we used a rat hepatoma cell line that has been stably transfected with human apoB48 in the current study to address the requirement of palmitoylation in VLDL assembly and secretion.

Treatment of stably transfected McA-RH7777 cells expressing human apoB48 with 2-bromopalmitate, a palmitic acid analogue shown to irreversibly block palmitoylation of proteins (244), was used initially to address the requirement of palmitoylation of apoB in VLDL assembly and secretion. Impaired secretion of human apoB48-containing VLDL from stably transfected McA-RH7777 cells as a result of 2-bromopalmitate treatment (Fig. 4.1.1.) prompted us to further verify and study the requirement of palmitoylation in VLDL using site-directed mutagenesis of potentially palmitoylated cysteines within apoB48. Contrary to results obtained following treatment with 2-bromopalmitate, we observed no impairment in the secretion of apoB48-containing VLDL from McA-RH7777 cells expressing apoB48 forms containing C-to-S substitution (Fig. 4.1.3). Additional studies using 2-bromopalmitate treatment of McA-RH7777 cells expressing $B48C^{1085\text{-}1635}$ resulting in impaired secretion of $apoB48C^{1085\text{-}1635}$-containing VLDL (Fig. 4.1.4*C*.) suggested that treatment with 2-bromopalmitate may elicit unknown intracellular effects that are unrelated to the loss of palmitoylation and that lead to impaired assembly and secretion of VLDL. Supplementation of McA-RH7777 cells with palmitate has been shown to decrease VLDL production (personal communication). Thus, the effect observed following treatment with an analogue of palmitate, 2-bromopalmitate, may be similar to that observed following supplementation of McA-RH7777 cells with palmitic acid.

Site-directed mutagenesis was performed at four potentially palmitoylated cysteines within human apoB48 (Cys^{1085}, Cys^{1395}, Cys^{1479}, and Cys^{1635}), using cysteine-to-serine substitution at individual or multiple sites. While apoB29 contains a single palmitoylated

cysteine (Cys^{1085}), apoB48 contains additional three cysteines that are likely available for palmitoylation (164). Of note, the surrounding amino acid residues for three of these cysteines are very similar ($LCS^{1085}D$, $LSC^{1395}D$, and $LSC^{1479}Q$), suggesting the presence of a potential recognition motif. We did not determine whether each one of the four free cysteines is palmitoylated. However, the absence of palmitoylation was verified using metabolic labeling with the [^{125}I]palmitate analogue in McA-RH7777 cells stably transfected with the palmitoylation mutant of apoB containing C-to-S substitution at all four cysteine residues, $B48C^{1085-1635}$ (Fig. 4.1.2*C*). That loss of palmitate(s) of apoB is not associated with impaired secretion of apoB48-containing buoyant VLDL from cells expressing each of the generated palmitoylation mutants was confirmed (Fig. 4.1.2.) and further verified by results from other experiments (Fig. 4.1.4). That the lack of palmitoylation does not lead to an up-regulation rather than an impairment of VLDL secretion was assessed using pulse-chase analysis showing similar secretion efficiency of the nonpalmitoylated apoB48 compared to that of B48wt (data not shown).

Using Nycodenz gradient ultracentrifugation to fractionate apoB in ER and Golgi compartments, we observed no change in the distribution of nonpalmitoylated apoB48 compared with B48wt (Fig. 4.1.5.). This was confirmed using immunofluorescence studies with stably transfected McA-RH7777 expressing similar levels of B48wt or nonpalmitoylated mutant. Both B48wt and $B48C^{1085-1635}$ were found co-localized with the specific markers of the ER and Golgi (Fig. 4.1.6.) and no abnormal accumulation either in the ER or Golgi was observed for the $apoB48C^{1085-1635}$ mutant. Hence, contrary to the

previous study, our results suggest that palmitoylation of apoB has no effect on intracellular distribution of apoB.

What role does palmitoylation of apoB play? An important yet unsolved issue in the field of VLDL assembly and secretion is how the membrane-associated lipoprotein precursor particles recruit lipid and eventually "fall-off" the membrane as mature, soluble, lipid-loaded lipoprotein particles that are secretion competent. The fatty acids conjugated onto apoB may be the link that regulates the association/dissociation of the apoB-containing lipoproteins with the membrane. Furthermore, it is not clear whether apoB has a signaling function(s) or whether it interacts with other signaling proteins. It may be possible that palmitoylation of apoB plays a role in the distal intracellular compartment(s), *i.e.* at the vicinity of the plasma membrane, mediating the association of apoB-containing lipoproteins with signaling proteins.

Chapter 5 Concluding Remarks and Future Considerations

The major findings in this study are: (a) The presence of conjugated N-linked oligosaccharides at the N-terminus of human apoB is required for efficient secretion of the apoB polypeptide. The N-linked oligosaccharides conjugated to apoB are of greater importance in the regulation of efficient apoB secretion than are the lipid-binding sequence(s) present within apoB. (b) Cooperative action of N-linked oligosaccharides at multiple N-linked glycosylation sites within apoB is required for efficient secretion of apoB. However, the altered electrophoretic mobility of $B37N^{1496}$ and $B37N^{158\text{-}1496}$, and decreased secretion efficiency of $B37N^{1496}$ (although not to the same extent as in $B37N^{158\text{-}1496}$), suggest that the presence of N-linked oligosaccharide at N^{1496} may be of particular significance to B37 structure and function. (c) Conjugation of N-linked oligosaccharides to apoB is required for efficient assembly and secretion of the apoB-containing VLDL particles. (d) The N-linked oligosaccharides may play a role in regulation of the apoB conformational stability, since the absence of N-linked oligosaccharides leads to likely targeting of apoB for rapid, in case of the apoB17 and apoB37, or slow, in the case of apoB50 variant, degradation. (e) Palmitoylation of the human apoB48 is not required for assembly and secretion of the apoB-containing VLDL.

In conclusion, our studies on the role(s) of two post-translational modifications of human apolipoprotein B, namely N-linked glycosylation and palmitoylation, demonstrated the requirement of conjugated N-linked oligosaccharides to apoB but not of the other post-translational modification, the apoB palmitoylation, for proper assembly and secretion of VLDL. The hepatic VLDL assembly and secretion is a complex process,

which seems to involve multiple factors besides apoB and lipids. The absence of N-linked glycosylation, as shown in the current study, results in a decrease of up to 50% in secretion efficiency of the apoB polypeptide. Furthermore, a greater than 50% decrease in the secretion of apoB50-containing VLDL is observed from McA-RH7777 cells whose secretion of buoyant apoB50-containing VLDL particles under oleate-stimulated conditions represents 10-20% of the total secreted lipoprotein pool. If the presence of N-linked oligosaccharide conjugation to apoB is required for efficient assembly of VLDL, why the loss of the N-linked glycans did not completely impair VLDL assembly and secretion? Taking into account the multifactorial nature of the VLDL assembly process (Table I), the focus of our study has been on the functional requirement of a single factor, namely the N-linked oligosaccharides of apoB, of the many, both known and unknown, factors involved in VLDL assembly. Hence, the contribution of these other factor(s) is likely involved in regulating the half-normal secretion efficiency of the non-glycosylated apoB polypeptides and also the assembly and secretion of the small percentage of the non-glycosylated apoB-containing VLDL particles.

What role(s) does conjugation of N-linked oligosaccharides to apoB play? The underlying mechanism involved may be complex and may involve changes of apoB folding and/or structure in the absence of N-linked glycans, with little available strategy for further dissecting the molecular basis for perturbed lipoprotein assembly. Some evidence was provided that non-glycosylated apoB may be a likely target of rapid (or slow) degradation. Limited evidence also pointed at a possible change in the association of the non-glycosylated apoB with its suggested chaperone and facilitating factor in lipid

recruitment, MTP, with observations of altered intracellular activity or abundance of MTP in cell expressing the non-glycosylated apoB. The presence of N-linked oligosaccaharides on the surface of many proteins has been suggested necessary for regulation of the interaction between the newly synthesized proteins and the ER quality control chaperones (*i.e.* calnexin and calreticulin), and in turn, for the facilitation of correct folding of newly synthesized glycoproteins. The determination of the possibly similar function of N-linked oligosaccharides present on the surface of apoB has been impeded by the lack of tools that could be used to monitor apoB folding. However, it has been shown recently that the interaction of newly synthesized apoB with calnexin requires glucose trimming (182) and that multiple chaperones, including BiP, calreticulin, and GRP94 interact with apoB during its maturation (181). Moreover, molecular chaperones were identified in the VLDL-containing fractions within the lumen of the microsome (107), all suggesting that the postulated role(s) of N-linked oligosaccharides conjugated to proteins may extend to N-linked oligosaccharides of apoB. We postulate that the N-linked oligosaccharides of apoB are required for the regulation of the biogenesis of the apoB-containing lipoproteins by the intracellular quality control mechanisms, and we envisage that the loss of N-linked glycans of apoB may activate the following: (1) misfolding of apoB. (2) altering of the interaction between apoB and molecular chaperones such as MTP, calreticulin, and BiP. (3) transient intracellular retention of apoB. (4) impaired secretion of apoB due to targeting of non-glycosylated apoB for degradation.

Some of the unanswered questions from the current study include: How are the folding and/or structure of apoB affected in the absence of N-linked glycosylation? How does the presence of the N-linked oligosaccharides to apoB influence the conformational stability of apoB? What is the mechanism by which N-linked oligosaccharides of apoB play a role in the intracellular quality control mechanisms? Does lack of N-linked glycosylation trigger interaction of the non-glycosylated apoB with molecular chaperones, and if so, what are the consequences of this interaction? How does the absence of N-linked oligosaccharide lead to impaired VLDL assembly and secretion? Once useful tools are readily available to monitor the apoB folding as well as the interaction between apoB and molecular chaperones, the McA-RH7777 cells expressing various glycosylation mutants of apoB generated in the current studies can serve as a useful system to address these questions.

While our studies demonstrated a requirement for modification of apoB with N-linked oligosaccharides for VLDL assembly and secretion, no requirement in this process was observed for the modification of apoB with palmitate. At this point, it is unclear whether all of the post-translational modifications found associated with the apoB biosynthesis must have a function. Is it possible that apoB is palmitoylated for no reason? On the other hand, is it possible that palmitoylation of apoB plays a yet unidentified role?

If palmitoylation of apoB is not required for assembly and secretion of VLDL, what role(s) (if any) does it play? The proposed role of palmitoylation in regulation of the affinity of signaling molecules for membranes and targeting of many signaling molecules

to the signaling depots at the plasma membrane, suggests that palmitoylation may be an important post-translational modification for intracellular event(s) occurring at the vicinity of the plasma membrane. The intracellular event(s) preceding the secretion of the assembled apoB-containing lipoproteins from cells have not been well characterized. Is secretion of the assembled apoB-containing lipoproteins regulated? If so, what is the trigger for release of apoB-containing lipoproteins from cells? How do the apoB-containing lipoproteins traffic from the distal Golgi compartment of the cell to reach the outside of the cell? In light of evidence that apoB is phosphorylated, another important unanswered question is whether apoB is a signaling molecule? If so, what proteins (if any) interact with apoB at the vicinity of distal Golgi and plasma membrane? Considering that no answers are yet available to these questions, we envisage that palmitoylation of apoB may play a role in the intracellular events occurring in the distal intracellular compartments. Hence, the McA-RH7777 cells expressing various palmitoylation mutants of apoB could possibly be used in the future studies to address these questions.

The contributions of the current studies represent an increase in the understanding of the complicated metabolic process of VLDL biogenesis. Innovative approaches will be necessary in the future studies in order to delineate the complete mechanism responsible for VLDL assembly. Understanding the mechanism responsible for the biogenesis of apoB-containing VLDL should lead to important new insights in biochemistry and also, to significant medical implications.

Chapter 6 Appendix

6.1. Structure-function studies of the LDL receptor-related protein

Human LDL receptor-related protein (LRP) is a type I membrane protein consisting of 4522 amino acids. The extracellular domain of LRP is comprised primarily of three structural modules: (i) the class A ligand-binding repeats clustered in four domains, (ii) the EGF-like precursor repeats, and (iii) YWTD β-propellers (Fig. 6.1*A*) (245). LRP is synthesized as a 600-kDa proreceptor that undergoes post-translational processing yielding a non-covalently associated α (515 kDa) and β (85 kDa) dimer (246). LRP has been implicated as a receptor for chylomicron remnants. Other studies have suggested that LRP also binds to multiple ligands including apoE-enriched β-VLDL, protease/protease inhibitor complexes, lipases, lactoferrin, β-amyloid precursor protein, and a 39-kDa protein termed receptor associated protein (RAP) (247). Sequence elements within LRP that are responsible for the multifunctionality of LRP have not been delineated, mainly because antibodies that can specifically block ligand binding to LRP are unavailable. We wanted to delineate those functional sequence elements within the human and chicken LRP using blocking antibodies.

6.2. Materials and methods

Materials – A synthetic scFv library #1 was provided by Dr. G. Winter (MRC Center for Protein Engineering, Cambridge). Subcutaneous adipose tissue was obtained from human subjects undergoing reduction mammoplasty surgery at Ottawa Civic Hospital. Dulbecco's modified Eagle's medium (DMEM), fetal calf serum (FCS), and antibiotics were obtained from Invitrogen. Pre-tested polyethylene glycol (PEG), hypoxanthine, aminopterine, thymidine (HAT) powder, and myeloma cells (SP2/O) were obtained from the American Type Culture Collection (ATCC). Reagents for polyacrylamide gel electrophoresis (PAGE), and nitrocellulose membrane were obtained from Bio-Rad. Octyl-glucopyranoside was obtained from Sigma/Aldrich. ProMix™ (a mixture of [^{35}S]methionine and [^{35}S]cysteine, 1000 Ci/mmol), Sepharose CL-4B and glutathione-sepharose beads, peroxidase-conjugated anti-mouse and anti-rabbit immunoglobulin G antibody, reagents for enzyme-linked immunosorbent assay (ELISA), and Amplify were obtained from Amersham/Pharmacia. Leupeptin, enhanced chemiluminescence (ECL) immunoblot detection system, and tunicamycin were obtained from Roche. Freund's complete and incomplete adjuvant, and a double hub emulsification needle were obtained from Cedarlane Laboratories Limited. The polyclonal anti-LDL receptor-related protein antiserum was a gift of G. Bu (Washington University School of Medicine, St. Louis).

Expression and Purification of Recombinant GST-RAP Expression Plasmid from E.coli – The fusion protein of glutathione-S-transferase and receptor-associated protein (GST-RAP) was expressed in bacteria and purified using a previously published method (247).

Purification of LDL-receptor Related Protein from Adipose Tissue – Human or chicken adipose tissue (100 g) was homogenized in homogenization buffer (TBS, (50 mM Tris-Cl pH 7.4, 150 mM NaCl), 1% octyl-glucopyranoside, 2 mM $CaCl_2$, 5 μM leupeptin) for 60 seconds in a blender. The homogenate was subjected to centrifugation at 7, 000 rpm (4 °C, 20 min). The homogenate supernatant, extracted from the buoyant fat pellet using a 60cc syringe, was passed over a gel filtration column of Sepharose CL-4B (total volume 100 ml). The flow-through was incubated for 16 h at 4 °C with approximately 16 mg purified GST-RAP immobilized to glutathione-sepharose. LRP was purified from the homogenate supernatant using recombinant GST-RAP as a ligand for affinity chromatography on glutathione-sepharose and additional gel filtration column (Sepharose CL-4B) in order to minimize co-elution of GST-RAP with LRP. The column was washed with approximately 100 ml of the homogenization buffer), and LRP was eluted using 40 ml of the elution buffer (TBS, 20 mM EDTA, 1 % octyl-glucopyranoside, pH 3.58). Purification of LRP was verified by subjecting aliquots of each elution fraction to 3-8 % SDS-PAGE followed by coomassie staining or immunoblotting with polyclonal anti-human LRP antibody. Pooled elution fractions were dialyzed in 2 mM ammonium bicarbonate, and purified LRP was concentrated to approximately 0.1 mg /ml.

Generation of ScFv Fragments Specific for LDL Receptor-related Protein – A synthetic phage display library (repertoire ~10^8) was screened for anti-LRP specific scFv fragments, using a previously published method (248).

Generation of Polyclonal Anti-human LDL Receptor-related Protein Antibody – The rabbit anti-human LRP polyclonal antiserum was obtained using standard immunization protocols. Prior to immunization, pre-immune serum was obtained from two healthy rabbits, designated as Emily and Theodore. Primary immunization involved intramuscular injection of a total of 0.25 ml purified LRP mixed with 0.25 ml Freund's complete adjuvant into three sites followed by booster injection two months after of antigen in Freund's incomplete adjuvant. Samples of the serum were collected using an ear vein test bleed two weeks after the injection to check for the production of anti-LRP specific antibodies by ELISA. After a second booster injection the titer of the antibodies was tested using ELISA. The rabbits were exsanguinated by coronary artery catheterization, and serum was stored in aliquots containing 0.1% azide at –80 °C.

Analysis of LDL Receptor-related Proteins- The LRP immunoprecipitated using polyclonal anti-human LRP antibody was recovered using protein A-Sepharose CL-4B. LRP proteins were eluted from the beads, and subjected to electrophoresis on 3-8% (w/v) gradient polyacrylamide gels with 0.1% (w/v) SDS. For radiolabeled LRP proteins, the gels were treated with Amplify for 30 min, dried, and LRP was detected by fluorography. For non-radiolabeled LRP, total protein from post-nuclear supernatant of HepG2 cell extracts was subjected to electrophoresis. After electrophoresis, LRP proteins were transferred onto nitrocellulose membranes at 125V for 6 h with a transfer buffer (190 mM glycine, 25 mM Tris base, 20% methanol) at –10 °C, and detected by immunoblotting with polyclonal anti-LRP antibody.

Protein Metabolic Labeling – HepG2 cells were pretreated in the presence or absence of 5 μg/ml tunicamycin for 3 h, labeled with [^{35}S]methionine/cysteine (200 μCi/ml) for an hour, and chased for up to 6 h in the presence or absence of tunicamycin treatment. At different time points of the chase, cell-associated LRP was immunoprecipitated using polyclonal anti-LRP antibody, analyzed by SDS-PAGE and fluorography.

Generation of Monoclonal Anti-LDL Receptor-related Protein Antibodies – Purified human and chicken LRP were used as antigens for immunization of mice by intraperitoneal injection of 100 μg LRP in 100 μl of PBS emulsified in 100 μl complete Freund's adjuvant. At intervals greater than a month, mice were given two intraperitoneal booster injections with LRP emulsified in incomplete Freund's adjuvant. Three days before fusion, mice were injected intravenously with 10 μg of LRP in 100 μl PBS. Splenocytes isolated from an immunized mouse were fused with myeloma cells (SP2/O) using PEG, according to standard procedure. Generated hybridomas were screened for their reactivity against purified LRP using ELISA. Monoclonality of antibodies was ensured following three rounds of subcloning of hybridomas tested positive against human LRP. Multiple clones of anti-chicken LRP specific monoclonal antibodies were frozen in aliquots at –120 °C.

6.3.1. Novel method for purification of the human and chicken LDL receptor-related protein

Standard protocols for LRP purification take advantage of rat liver or human placenta as a source of LRP. Availability of significant amount of pure LRP from these tissues has been hampered by the relatively poor yield of LRP following purification using affinity chromatography with ligands, such as α2-M or RAP, and also by the co-purification of RAP with LRP.

We developed a novel method to purify LRP from human and chicken adipose tissue using recombinant GST-RAP affinity chromatography. Using human or chicken adipose tissue extracts, purification was achieved through binding of LRP to a recombinant GST-RAP fusion that is immobilized to glutathione-sepharose. LRP was eluted from the affinity column using 20 mM EDTA at pH 3.6 (Fig. 6.1*B*). The purity of the human LRP (mainly the 515-kDa α chain) was demonstrated by coomassie blue staining of the receptor resolved by SDS-PAGE (Fig. 6.1*B*). Even though RAP co-eluted with LRP, the peaks of elution of LRP and GST-RAP were resolved using a simple Sepharose 4B cushion. The Sepharose 4B cushion acting as gel filtration column separated the peaks of elution of the larger LRP proteins with that of smaller GST-RAP. Using approximately 100 g of adipose tissue, this method of purification yielded regularly between 300–800 μg of purified LRP. Thus, this method represents a good purification procedure for obtaining high amounts of relatively pure LRP.

6.3.2. Generation of human and chicken anti-LDL receptor-related protein specific antibodies using phage display, polyclonal, and monoclonal techniques

We wanted to generate blocking antibodies using purified LRP as an antigen or a "bait" and taking advantage of multiple available technologies, such as those of phage display, rabbit immunization for generation of polyclonal antibodies, as well as mouse immunization for generation of monoclonal antibodies. Screening for anti-human LRP antibodies using phage display technique was conducted, however, the obtained antibody fragments were of moderate binding affinity towards LRP (data not shown).

Purified human LRP was used as antigen for rabbit immunization. Antibody titers were determined following immunoassays by ELISA (Fig. 6.2.). The reactivity of the antiserum was tested in uncoated plates or plates coated with 5 μg/ml bovine serum albumin, GST-RAP, or purified LRP. The results of ELISA suggested the presence of a titer of antibodies, in sera of both immunized rabbits, that are not specific for bovine serum albumin, but have strong reactivity against both LRP (EC_{50} of 1/32,000) and RAP (EC_{50} of 1/8,000) (Fig. 6.2.). The reactivity of the antiserum against RAP can be explained by the likely presence of co-purified RAP in the preparations of LRP used for injections.

The generated polyclonal anti-human LRP antiserum from both rabbits was used to detect purified LRP by immunoblotting following reducing SDS-PAGE (Fig. 6.3*A*). Newly generated polyclonal anti-human LRP antiserum was as good of a tool as previously available anti-human LRP antibody in detecting small amounts of LRP

present in elution fraction aliquots during subsequent purifications (Fig. 6.3*B*). Using immunoblotting weak reactivity of the polyclonal anti-human LRP antiserum was observed towards the non-covalently associated 85 kDa subunit of LRP (data not shown).

That the newly generated anti-LRP antibody is a good experimental tool was shown further following metabolic labeling conducted using human HepG2 cells to determine the effect of tunicamycin on post-translational stability of LRP. The newly generated antibody reacted with glycosylated and non-glycosylated LRP, as demonstrated by immunoprecipitation of pulse-labeled LRP from total cell lysate during chase (Fig. 6.3*C*). The results of this experiment suggested longer half-life of tunicamycin-treated, i.e. of the non-glycosylated LRP ($t½$ of more than 6 h) compared with that of wild type, tunicamycin-untreated LRP ($t½$ of 4 h). Thus, using tunicamycin treatment to inhibit N-linked glycosylation possibly induced intracellular retention with targeting of LRP degradation. Furthermore, the obtained antibody has been a useful tool for structure/function studies of LRP in which the kinetics of intracellular trafficking of wild type and mutant LRP were determined (data not shown).

Our novel purification procedure was used to purify LRP also from chicken adipose tissue. Both the purified human and chicken LRP were used as antigens for immunization of mice. Samples of serum were obtained from mice immunized with either human LRP (Fig. 6.4*A*) or chicken LRP (Fig. 6.4*B*) and immunoassays were performed using ELISA. Reactivity of the serum was tested against against bovine serum albumin, GST-RAP, or purified LRP. The mouse showing highest titer of LRP-specific antibodies was sacrificed,

and the spleen was used for fusion and generation of hybridomas that were subsequently tested for reactivity against LRP. At least two hybridoma clones, designated 3E4 and 9B1, were found to react with LRP isolated from HepG2 cell extract using immunoblotting (Fig. 6.4*C*). More than 90 frozen hybridomas showing specificity against LRP using ELISA immunoassays remain to be tested for secretion of potential monoclonal antibodies specific for chicken LRP.

6.4. Concluding remarks

We have developed an improved method for purification of the LDL-receptor related protein from human or chicken adipose tissue. Purified LDL receptor-related protein (LRP) was used as antigen for generation of antibodies using phage display, polyclonal and monoclonal techniques. While phage display did not yield scFv fragments of adequate affinity towards human LRP, the generated polyclonal antibody was shown to be a useful tool in studies of LRP structure and function. In addition, multiple clones of monoclonal antibodies against human or chicken LRP have been generated, and characterization of their specificities awaits determination.

LRP is a multifunctional receptor that binds multiple ligands. To date, ligand-binding sites on LRP have not been well defined. The generated antibodies specified above may serve as useful tools in the future studies to help delineate ligand-binding sites on LRP. Furthermore, these antibodies can be used in a facet of studies regarding different aspects of LRP biogenesis, including analysis of the LRP structure, function(s), and intracellular metabolism.

FIG. 6.1. **Novel method for purification of LDL receptor-related protein from adipose tissue.** *A*, schematic diagram depicts the modular structure of LRP. *B*, LRP was purified from human adipose tissue using GST-RAP affinity chromatography. The purification of the human LRP, mainly the 515-kDa α chain, was resolved by coomassie blue staining of the receptor following SDS-PAGE *(enclosed box)*. Data are representative of five purification experiments with similar results.

Fig. 6.1.

A. Structure

▮	class A module	▫	transmembrane domain
⬟	EGF module	△	NPXY motif
⬢	YWTD module	▬	cytoplasmic tail
✿	β-propeller domain	▲	proteolytic processing site

B. Purification

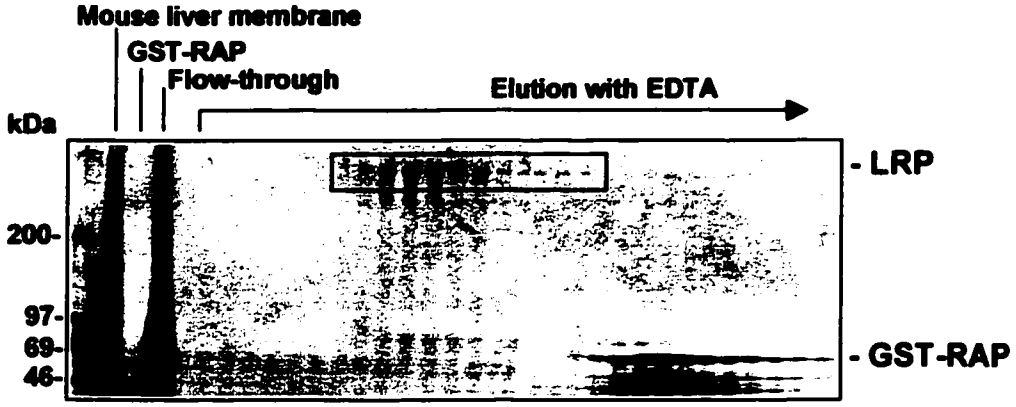

FIG. 6.2. **The specificity of the polyclonal anti-human LDL receptor-related protein antibody.** Immunoassays were performed using sera isolated from two immunized rabbits, Emily and Theodore, by ELISA. Plates (96-well) were coated for 16 h with 5 μg/ml bovine serum albumin, GST-RAP, or purified LRP. The plates were incubated for 90 min at 37 °C in 8 doubling dilutions of the newly generated antiserum in dilution buffer, starting at a dilution of 1/250. Anti-rabbit HRP-conjugated IgG was used as secondary antibody for 90 min at 37 °C, followed by incubation with 1 x ABTS solution. After 30 min, the ABTS-HRP reaction was read using microtiter plate reader set at 415 nm. The experiment was performed twice with similar results.

Fig. 6.2.

A. Emily

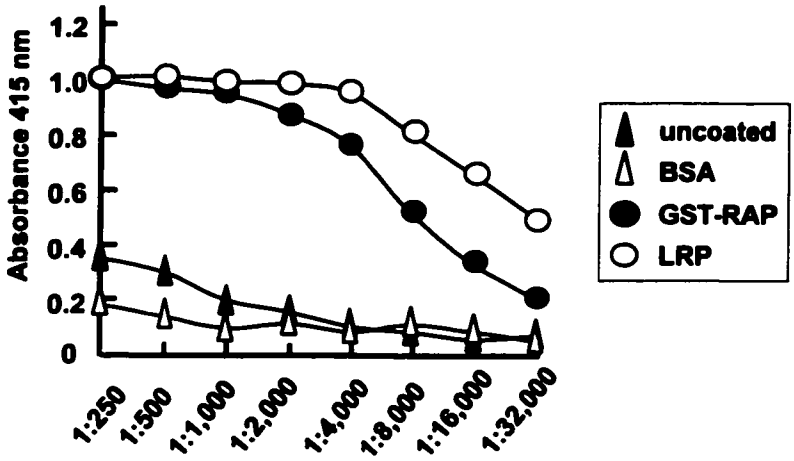

B. Theodore

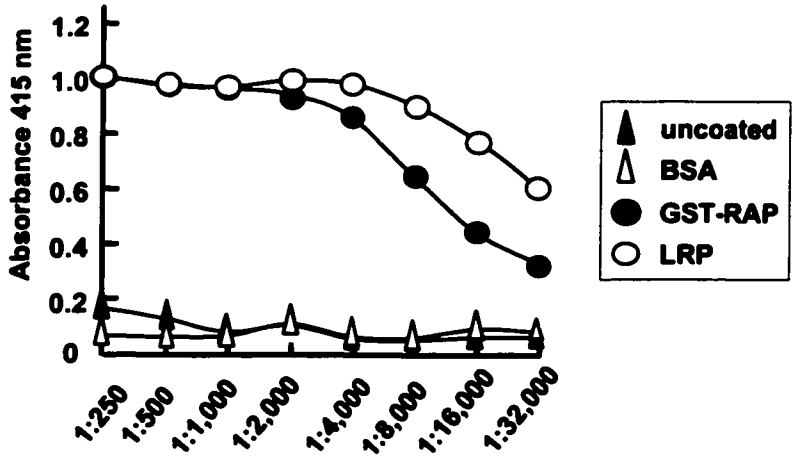

FIG. 6.3. **Reactivity of the polyclonal anti-human LDL receptor-related protein antibody.** *A,* aliquots of purified human LRP were subjected to SDS-PAGE, transferred to nitrocellulose membranes, and probed using 1/2000 dilution of the antiserum obtained from two immunized rabbits, Emily or Theodore. *B,* LRP was purified from human adipose tissue. Aliquots of elution fractions were subjected to SDS-PAGE, transferred to nitrocellulose membranes, and probed using previously available polyclonal anti-LRP antibody *(top)* or newly generated polyclonal anti-human LRP serum *(bottom). C,* HepG2 cells were pre-treated for 3 h (± 5 μg/ml tunicamycin), pulse-labeled with ^{35}S-amino acids (200 μCi/ml) for 1 h, and chased for up to 6 h (± 5 μg/ml tunicamycin). Cell-associated ^{35}S-LRP during chase was immunoprecipitated using polyclonal anti-human LRP antibody, resolved by SDS-PAGE, and visualized by fluorography *(insets).* The recovery of cell-associated ^{35}S-LRP during chase was presented as "% of initial counts" that associated with cell LRP at the end of pulse. The experiment was performed once.

Fig. 6.3.

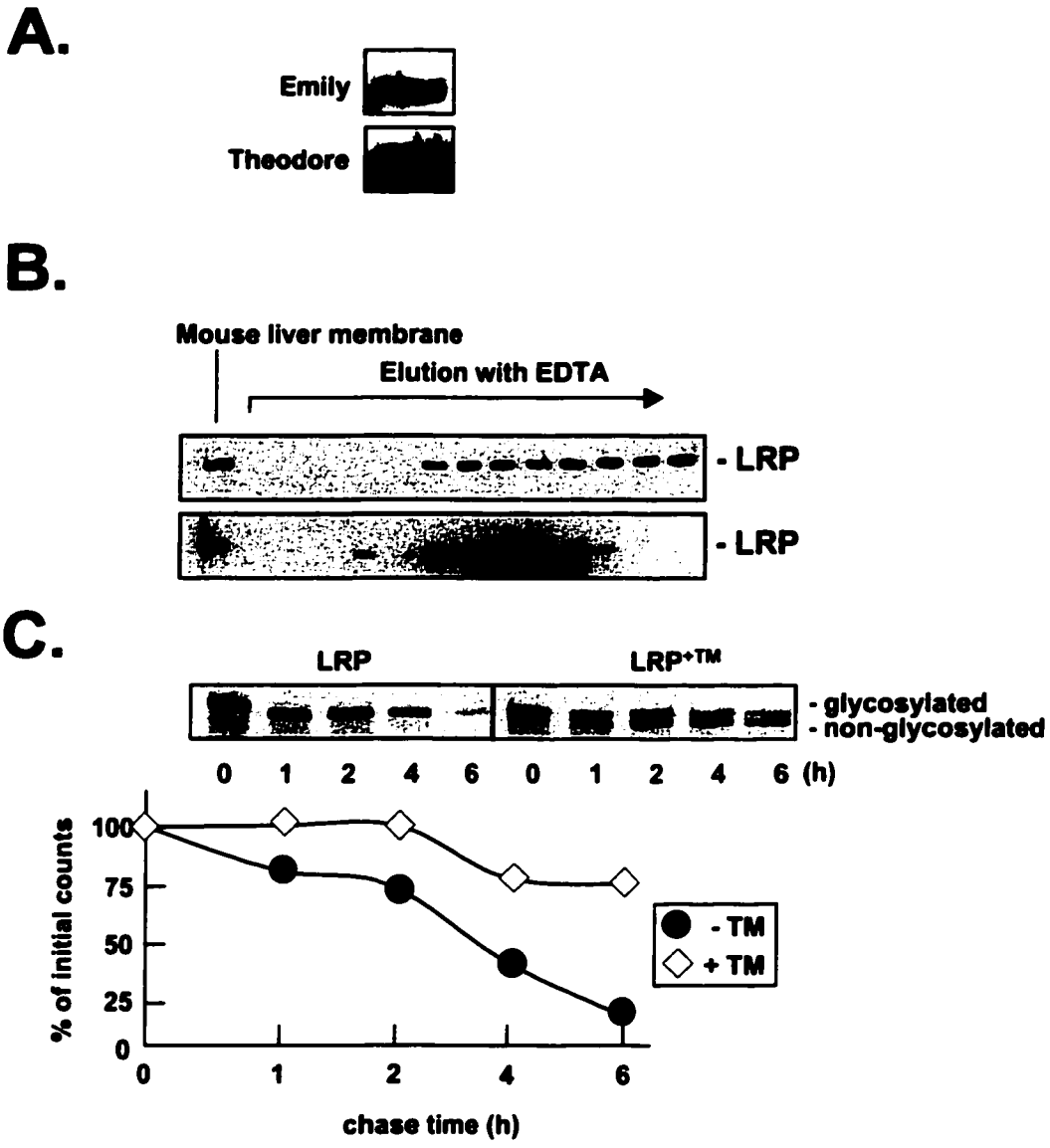
A.
Emily
Theodore
B.
Mouse liver membrane
Elution with EDTA
- LRP
- LRP
C.
LRP
LRP+TM
- glycosylated
- non-glycosylated
0 1 2 4 6 0 1 2 4 6 (h)
% of initial counts
100
75
50
25
0
0 1 2 4 6
chase time (h)
- TM
+ TM

FIG. 6.4. **Reactivity of the monoclonal anti-LDL receptor-related protein antibody.** *A,* immunoreactivity of monoclonal anti-human LRP sera obtained from three immunized mice; mouse #1 *(open ovals)*, mouse #2 *(red ovals)*, and mouse #3 *(closed ovals)*. Immunoassays were performed using ELISA. Plates (96-well) were coated for 16 h with purified LRP and incubated in 8 doubling dilutions of the antiserum buffer, starting at a dilution of 1/40. Plates (96-well) were also coated for 16 h with 5 μg/ml bovine serum albumin or GST-RAP, and incubated in 8 doubling dilutions of the antiserum buffer (mouse #2) starting at a dilution of 1/40. Anti-mouse HRP-conjugated IgG was used as secondary antibody. The ABTS-HRP reaction was read using microtiter plate reader set at 415 nm. The experiment was performed twice with similar results. *B,* immunoreactivity of monoclonal anti-chicken LRP serum obtained from three immunized mice. The experiment was performed twice with similar results. *C,* HepG2 cells (100-mm dish, 80% confluent) were washed with PBS and homogenized. The post-nuclear supernatants were isolated. Aliquots in triplicate were subjected to SDS-PAGE, transferred to nitrocellulose membranes, and probed using anti-human LRP monoclonal antibodies, 3E4 and 9B1. Data are representative immunoblots from three experiments with similar results.

Fig. 6.4.

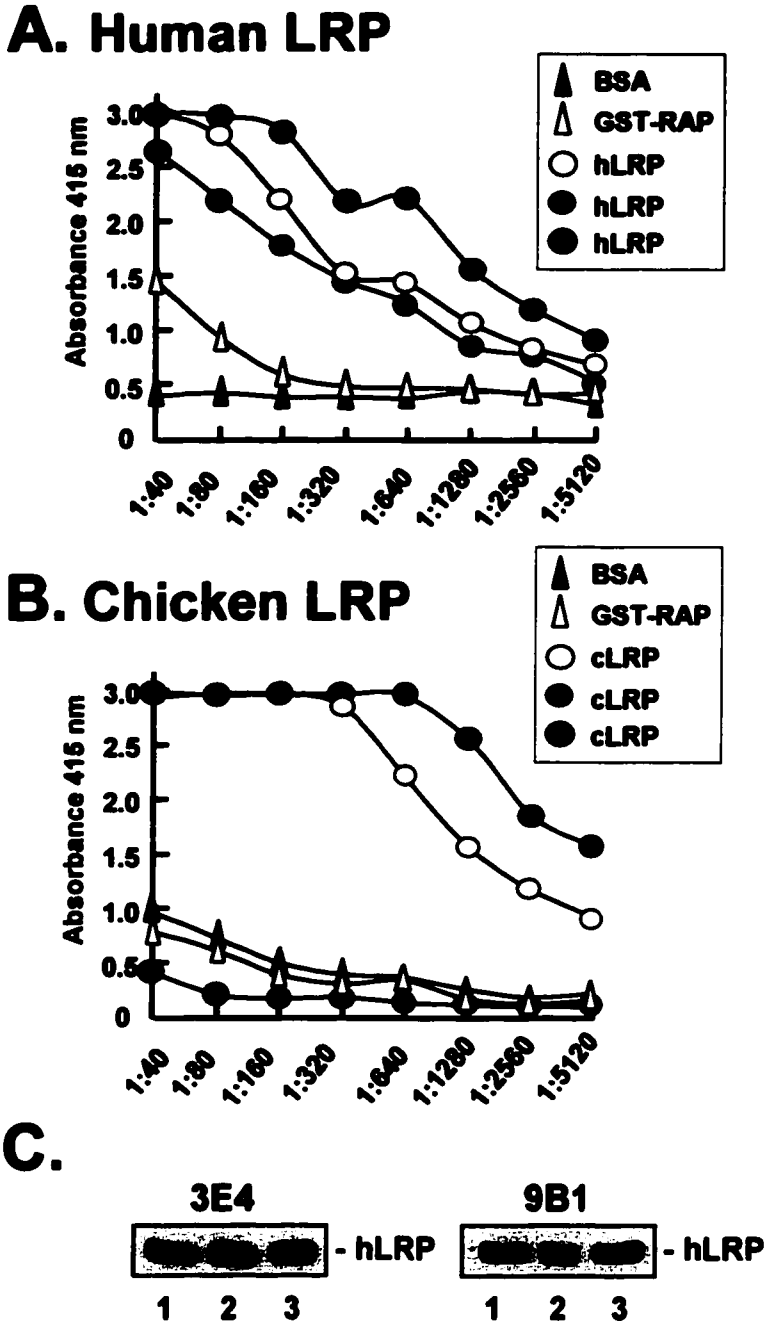
A. Human LRP
BSA
GST-RAP
hLRP
hLRP
hLRP
Absorbance 415 nm
3.0
2.5
2.0
1.5
1.0
0.5
0
1:40
1:80
1:160
1:320
1:640
1:1280
1:2560
1:5120
B. Chicken LRP
BSA
GST-RAP
cLRP
cLRP
cLRP
Absorbance 415 nm
3.0
2.5
2.0
1.5
1.0
0.5
0
1:40
1:80
1:160
1:320
1:640
1:1280
1:2560
1:5120
C.
3E4
9B1
- hLRP
- hLRP
1 2 3
1 2 3

References

1. Davis, R. A. 1996. Structure, assembly and secretion of plasma lipoproteins. In *Biochemistry of lipids, lipoproteins and membranes.* 3 ed. Edited by D.E. Vance, and J.E. Vance. Elsevier Science B.V.. pp.473-393.

2. Brown, M. S. and J. L. Goldstein. 1986. A receptor-mediated pathway for cholesterol homeostasis. *Science.* **232**: 34-47.

3. Farese, R. V., Jr., S. L. Ruland, L. M. Flynn, R. P. Stokowski, and S. G. Young. 1995. Knockout of the mouse apolipoprotein B gene results in embryonic lethality in homozygotes and protection against diet-induced hypercholesterolemia in heterozygotes. *Proc. Natl. Acad. Sci. U. S. A.* **92**: 1774-1778.

4. Kim, E. and S. G. Young. 1998. Genetically modified mice for the study of apolipoprotein B. *J. Lipid Res.* **39**: 703-723.

5. Wetterau, J. R., L. P. Aggerbeck, M. E. Bouma, C. Eisenberg, A. Munck, M. Hermier, J. Schmitz, G. Gay, D. J. Rader, and R. E. Gregg. 1992. Absence of microsomal triglyceride transfer protein in individuals with abetalipoproteinemia. *Science.* **258**: 999-1001.

6. Chen, S. H., G. Habib, C. Y. Yang, Z. W. Gu, B. R. Lee, S. A. Weng, S. R. Silberman, S. J. Cai, J. P. Deslypere, M. Rosseneu, and . 1987. Apolipoprotein B-48 is the product of a messenger RNA with an organ-specific in-frame stop codon. *Science.* **238**: 363-366.

7. Powell, L. M., S. C. Wallis, R. J. Pease, Y. H. Edwards, T. J. Knott, and J. Scott. 1987. A novel form of tissue-specific RNA processing produces apolipoprotein-B48 in intestine. *Cell.* **50**: 831-840.

8. Greeve, J., I. Altkemper, J. H. Dieterich, H. Greten, and E. Windler. 1993. Apolipoprotein B mRNA editing in 12 different mammalian species: hepatic expression is reflected in low concentrations of apoB-containing plasma lipoproteins. *J. Lipid Res.* **34**: 1367-1383.

9. Elovson, J., J. E. Chatterton, G. T. Bell, V. N. Schumaker, M. A. Reuben, D. L. Puppione, J. R. Reeve, Jr., and N. L. Young. 1988. Plasma very low density lipoproteins contain a single molecule of apolipoprotein B. *J. Lipid Res.* **29**: 1461-1473.

10. Carlsson, P., S. O. Olofsson, G. Bondjers, C. Darnfors, O. Wiklund, and G. Bjursell. 1985. Molecular cloning of human apolipoprotein B cDNA. *Nucleic Acids Res.* **13**: 8813-8826.

11. Law, S. W., K. J. Lackner, A. V. Hospattankar, J. M. Anchors, A. Y. Sakaguchi, S. L. Naylor, and H. B. Brewer, Jr. 1985. Human apolipoprotein B-100: cloning, analysis of liver mRNA, and assignment of the gene to chromosome 2. *Proc. Natl. Acad. Sci. U. S. A.* **82**: 8340-8344.

12. Lusis, A. J., R. West, M. Mehrabian, M. A. Reuben, R. C. LeBoeuf, J. S. Kaptein, D. F. Johnson, V. N. Schumaker, M. P. Yuhasz, M. C. Schotz, and . 1985. Cloning and expression of apolipoprotein B, the major protein of low and very low density lipoproteins. *Proc. Natl. Acad. Sci. U. S. A.* **82**: 4597-4601.

13. Mehrabian, M., V. N. Schumaker, G. C. Fareed, R. West, D. F. Johnson, T. Kirchgessner, H. C. Lin, X. B. Wang, Y. H. Ma, E. Mendiaz, and . 1985. Human apolipoprotein B: identification of cDNA clones and characterization of mRNA. *Nucleic Acids Res.* **13**: 6937-6953.

14. Knott, T. J., S. C. Wallis, L. M. Powell, R. J. Pease, A. J. Lusis, B. Blackhart, B. J. McCarthy, R. W. Mahley, B. Levy-Wilson, and J. Scott. 1986. Complete cDNA and derived protein sequence of human apolipoprotein B-100. *Nucleic Acids Res.* **14**: 7501-7503.

15. Cladaras, C., M. Hadzopoulou-Cladaras, R. T. Nolte, D. Atkinson, and V. I. Zannis. 1986. The complete sequence and structural analysis of human apolipoprotein B-100: relationship between apoB-100 and apoB-48 forms. *EMBO J.* **5**: 3495-3507.

16. Law, S. W., S. M. Grant, K. Higuchi, A. Hospattankar, K. Lackner, N. Lee, and H. B. Brewer, Jr. 1986. Human liver apolipoprotein B-100 cDNA: complete nucleic acid and derived amino acid sequence. *Proc. Natl. Acad. Sci. U. S. A.* **83**: 8142-8146.

17. Yang, C. Y., S. H. Chen, S. H. Gianturco, W. A. Bradley, J. T. Sparrow, M. Tanimura, W. H. Li, D. A. Sparrow, H. DeLoof, M. Rosseneu, and . 1986. Sequence, structure, receptor-binding domains and internal repeats of human apolipoprotein B-100. *Nature.* **323**: 738-742.

18. Yang, C. Y., Z. W. Gu, S. A. Weng, T. W. Kim, S. H. Chen, H. J. Pownall, P. M. Sharp, S. W. Liu, W. H. Li, A. M. Gotto, Jr., and . 1989. Structure of apolipoprotein B-100 of human low density lipoproteins. *Arteriosclerosis.* **9**: 96-108.

19. Yang, C. Y., T. W. Kim, S. A. Weng, B. R. Lee, M. L. Yang, and A. M. Gotto, Jr. 1990. Isolation and characterization of sulfhydryl and disulfide peptides of human apolipoprotein B-100. *Proc. Natl. Acad. Sci. U. S. A.* **87**: 5523-5527.

20. Hoeg, J. M., M. S. Meng, R. Ronan, S. J. Demosky, Jr., T. Fairwell, and H. B. Brewer, Jr. 1988. Apolipoprotein B synthesized by Hep G2 cells undergoes fatty acid acylation. *J. Lipid Res.* **29**: 1215-1220.

21. Huang, G., D. M. Lee, and S. Singh. 1988. Identification of the thiol ester linked lipids in apolipoprotein B. *Biochemistry*. **27**: 1395-1400.

22. Kamanna, V. S. and D. M. Lee. 1989. Presence of covalently attached fatty acids in rat apolipoprotein B via thiolester linkages. *Biochem. Biophys. Res. Commun.* **162**: 1508-1514.

23. Lee, D. M. and S. Singh. 1990. Intramolecular thiolester linkages in apolipoprotein B. *SAAS. Bull. Biochem. Biotechnol.* **3**: 74-79.

24. Davis, R. A., G. M. Clinton, R. A. Borchardt, M. Malone-McNeal, T. Tan, and G. R. Lattier. 1984. Intrahepatic assembly of very low density lipoproteins. Phosphorylation of small molecular weight apolipoprotein B. *J. Biol. Chem.* **259**: 3383-3386.

25. Milne, R., R. Theolis, Jr., R. Maurice, R. J. Pease, P. K. Weech, E. Rassart, J. C. Fruchart, J. Scott, and Y. L. Marcel. 1989. The use of monoclonal antibodies to localize the low density lipoprotein receptor-binding domain of apolipoprotein B. *J. Biol. Chem.* **264**: 19754-19760.

26. Knott, T. J., R. J. Pease, L. M. Powell, S. C. Wallis, S. C. Rall, Jr., T. L. Innerarity, B. Blackhart, W. H. Taylor, Y. Marcel, R. Milne, and . 1986. Complete protein sequence and identification of structural domains of human apolipoprotein B. *Nature*. **323**: 734-738.

27. Boren, J., I. Lee, W. Zhu, K. Arnold, S. Taylor, and T. L. Innerarity. 1998. Identification of the low density lipoprotein receptor-binding site in apolipoprotein B100 and the modulation of its binding activity by the carboxyl terminus in familial defective apo-B100. *J. Clin. Invest.* **101**: 1084-1093.

28. Chatterton, J. E., M. L. Phillips, L. K. Curtiss, R. Milne, J. C. Fruchart, and V. N. Schumaker. 1995. Immunoelectron microscopy of low density lipoproteins yields a ribbon and bow model for the conformation of apolipoprotein B on the lipoprotein surface. *J. Lipid Res.* **36**: 2027-2037.

29. Gantz, D. L., M. T. Walsh, and D. M. Small. 2000. Morphology of sodium deoxycholate-solubilized apolipoprotein B-100 using negative stain and vitreous ice electron microscopy. *J. Lipid Res.* **41**: 1464-1472.

30. Chan, L. 1992. Apolipoprotein B, the major protein component of triglyceride-rich and low density lipoproteins. *J. Biol. Chem.* **267**: 25621-25624.

31. Segrest, J. P., M. K. Jones, V. K. Mishra, G. M. Anantharamaiah, and D. W. Garber. 1994. apoB-100 has a pentapartite structure composed of three amphipathic alpha-helical domains alternating with two amphipathic beta-strand domains. Detection by the computer program LOCATE. *Arterioscler. Thromb.* **14**: 1674-1685.

32. Segrest, J. P., M. K. Jones, and N. Dashti. 1999. N-terminal domain of apolipoprotein B has structural homology to lipovitellin and microsomal triglyceride transfer protein: a "lipid pocket" model for self-assembly of apoB-containing lipoprotein particles. *J. Lipid Res.* **40**: 1401-1416.

33. Segrest, J. P., M. K. Jones, V. K. Mishra, V. Pierotti, S. H. Young, J. Boren, T. L. Innerarity, and N. Dashti. 1998. Apolipoprotein B-100: conservation of lipid-associating amphipathic secondary structural motifs in nine species of vertebrates. *J. Lipid Res.* **39**: 85-102.

34. Baker, M. E. 1988. Is vitellogenin an ancestor of apolipoprotein B-100 of human low-density lipoprotein and human lipoprotein lipase? *Biochem. J.* **255**: 1057-1060.

35. Shoulders, C. C., T. M. Narcisi, J. Read, A. Chester, D. J. Brett, J. Scott, T. A. Anderson, D. G. Levitt, and L. J. Banaszak. 1994. The abetalipoproteinemia gene is a member of the vitellogenin family and encodes an alpha-helical domain. *Nat. Struct. Biol.* **1**: 285-286.

36. Anderson, T. A., D. G. Levitt, and L. J. Banaszak. 1998. The structural basis of lipid interactions in lipovitellin, a soluble lipoprotein. *Structure.* **6**: 895-909.

37. Mann, C. J., T. A. Anderson, J. Read, S. A. Chester, G. B. Harrison, S. Kochl, P. J. Ritchie, P. Bradbury, F. S. Hussain, J. Amey, B. Vanloo, M. Rosseneu, R. Infante, J. M. Hancock, D. G. Levitt, L. J. Banaszak, J. Scott, and C. C. Shoulders. 1999. The structure of vitellogenin provides a molecular model for the assembly and secretion of atherogenic lipoproteins. *J. Mol. Biol.* **285**: 391-408.

38. Segrest, J. P., M. K. Jones, H. De Loof, and N. Dashti. 2001. Structure of apolipoprotein B-100 in low density lipoproteins. *J. Lipid Res.* **42**: 1346-1367.

39. McLeod, R. S., Y. Zhao, S. L. Selby, J. Westerlund, and Z. Yao. 1994. Carboxyl-terminal truncation impairs lipid recruitment by apolipoprotein B100 but does not affect secretion of the truncated apolipoprotein B-containing lipoproteins. *J. Biol. Chem.* **269**: 2852-2862.

40. McLeod, R. S., Y. Wang, S. Wang, A. Rusinol, P. Links, and Z. Yao. 1996. Apolipoprotein B sequence requirements for hepatic very low density lipoprotein assembly. Evidence that hydrophobic sequences within apolipoprotein B48 mediate lipid recruitment. *J. Biol. Chem.* **271**: 18445-18455.

41. Yao, Z. M., B. D. Blackhart, M. F. Linton, S. M. Taylor, S. G. Young, and B. J. McCarthy. 1991. Expression of carboxyl-terminally truncated forms of human apolipoprotein B in rat hepatoma cells. Evidence that the length of apolipoprotein B has a major effect on the buoyant density of the secreted lipoproteins. *J. Biol. Chem.* **266**: 3300-3308.

42. Benoist, F. and T. Grand-Perret. 1997. Co-translational degradation of apolipoprotein B100 by the proteasome is prevented by microsomal triglyceride transfer protein. Synchronized translation studies on HepG2 cells treated with an inhibitor of microsomal triglyceride transfer protein. *J. Biol. Chem.* **272**: 20435-20442.

43. Bostrom, K., J. Boren, M. Wettesten, A. Sjoberg, G. Bondjers, O. Wiklund, P. Carlsson, and S. O. Olofsson. 1988. Studies on the assembly of apo B-100-containing lipoproteins in HepG2 cells. *J. Biol. Chem.* **263**: 4434-4442.

44. Dashti, N., D. L. Williams, and P. Alaupovic. 1989. Effects of oleate and insulin on the production rates and cellular mRNA concentrations of apolipoproteins in HepG2 cells. *J. Lipid Res.* **30**: 1365-1373.

45. Pullinger, C. R., J. D. North, B. B. Teng, V. A. Rifici, A. E. Ronhild de Brito, and J. Scott. 1989. The apolipoprotein B gene is constitutively expressed in HepG2 cells: regulation of secretion by oleic acid, albumin, and insulin, and measurement of the mRNA half-life. *J. Lipid Res.* **30**: 1065-1077.

46. Chuck, S. L. and V. R. Lingappa. 1992. Pause transfer: a topogenic sequence in apolipoprotein B mediates stopping and restarting of translocation. *Cell.* **68**: 9-21.

47. Chuck, S. L. and V. R. Lingappa. 1993. Analysis of a pause transfer sequence from apolipoprotein B. *J. Biol. Chem.* **268**: 22794-22801.

48. Davidson, N. O. and G. S. Shelness. 2000. APOLIPOPROTEIN B: mRNA editing, lipoprotein assembly, and presecretory degradation. *Annu. Rev. Nutr.* **20**: 169-193.

49. Teng, B., C. F. Burant, and N. O. Davidson. 1993. Molecular cloning of an apolipoprotein B messenger RNA editing protein. *Science.* **260**: 1816-1819.

50. Yamanaka, S., M. E. Balestra, L. D. Ferrell, J. Fan, K. S. Arnold, S. Taylor, J. M. Taylor, and T. L. Innerarity. 1995. Apolipoprotein B mRNA-editing protein induces hepatocellular carcinoma and dysplasia in transgenic animals. *Proc. Natl. Acad. Sci. U. S. A.* **92**: 8483-8487.

51. Gorlich, D., S. Prehn, E. Hartmann, K. U. Kalies, and T. A. Rapoport. 1992. A mammalian homolog of SEC61p and SECYp is associated with ribosomes and nascent polypeptides during translocation. *Cell.* **71**: 489-503.

52. Gorlich, D. and T. A. Rapoport. 1993. Protein translocation into proteoliposomes reconstituted from purified components of the endoplasmic reticulum membrane. *Cell.* **75**: 615-630.

53. Hamman, B. D., L. M. Hendershot, and A. E. Johnson. 1998. BiP maintains the permeability barrier of the ER membrane by sealing the lumenal end of the translocon pore before and early in translocation. *Cell.* **92**: 747-758.

54. Bamberger, M. J. and M. D. Lane. 1990. Possible role of the Golgi apparatus in the assembly of very low density lipoprotein. *Proc. Natl. Acad. Sci. U. S. A.* **87**: 2390-2394.

55. Boren, J., M. Wettesten, A. Sjoberg, T. Thorlin, G. Bondjers, O. Wiklund, and S. O. Olofsson. 1990. The assembly and secretion of apoB 100 containing lipoproteins in Hep G2 cells. Evidence for different sites for protein synthesis and lipoprotein assembly. *J. Biol. Chem.* **265**: 10556-10564.

56. Bostrom, K., M. Wettesten, J. Boren, G. Bondjers, O. Wiklund, and S. O. Olofsson. 1986. Pulse-chase studies of the synthesis and intracellular transport of apolipoprotein B-100 in Hep G2 cells. *J. Biol. Chem.* **261**: 13800-13806.

57. Davis, R. A., R. N. Thrift, C. C. Wu, and K. E. Howell. 1990. Apolipoprotein B is both integrated into and translocated across the endoplasmic reticulum membrane. Evidence for two functionally distinct pools. *J. Biol. Chem.* **265**: 10005-10011.

58. Davis, R. A., A. B. Prewett, D. C. Chan, J. J. Thompson, R. A. Borchardt, and W. R. Gallaher. 1989. Intrahepatic assembly of very low density lipoproteins: immunologic characterization of apolipoprotein B in lipoproteins and hepatic membrane fractions and its intracellular distribution. *J. Lipid Res.* **30**: 1185-1196.

59. Dixon, J. L., R. Chattapadhyay, T. Huima, C. M. Redman, and D. Banerjee. 1992. Biosynthesis of lipoprotein: location of nascent apoAI and apoB in the rough endoplasmic reticulum of chicken hepatocytes. *J. Cell Biol.* **117**: 1161-1169.

60. Leiper, J. M., G. B. Harrison, J. Bayliss, J. D. Scott, and R. J. Pease. 1996. Systematic expression of the complete coding sequence of apoB-100 does not reveal transmembrane determinants. *J. Lipid Res.* **37**: 2215-2231.

61. Pease, R. J., G. B. Harrison, and J. Scott. 1991. Cotranslocational insertion of apolipoprotein B into the inner leaflet of the endoplasmic reticulum. *Nature.* **353**: 448-450.

62. Pease, R. J., J. M. Leiper, G. B. Harrison, and J. Scott. 1995. Studies on the translocation of the amino terminus of apolipoprotein B into the endoplasmic reticulum. *J. Biol. Chem.* **270**: 7261-7271.

63. Davis, R. A. 1993. The endoplasmic reticulum is the site of lipoprotein assembly and regulation of secretion. *Subcell. Biochem.* **21**: 169-187.

64. Sass, H. J., G. Buldt, E. Beckmann, F. Zemlin, M. van Heel, E. Zeitler, J. P. Rosenbusch, D. L. Dorset, and A. Massalski. 1989. Densely packed beta-structure at the protein-lipid interface of porin is revealed by high-resolution cryo-electron microscopy. *J. Mol. Biol.* **209**: 171-175.

65. Liang, J., X. Wu, H. Jiang, M. Zhou, H. Yang, P. Angkeow, L. S. Huang, S. L. Sturley, and H. Ginsberg. 1998. Translocation efficiency, susceptibility to

proteasomal degradation, and lipid responsiveness of apolipoprotein B are determined by the presence of beta sheet domains. *J. Biol. Chem.* **273**: 35216-35221.

66. Hegde, R. S. and V. R. Lingappa. 1996. Sequence-specific alteration of the ribosome-membrane junction exposes nascent secretory proteins to the cytosol. *Cell.* **85**: 217-228.

67. Hegde, R. S., S. Voigt, and V. R. Lingappa. 1998. Regulation of protein topology by trans-acting factors at the endoplasmic reticulum. *Mol. Cell.* **2**: 85-91.

68. Zhou, M., X. Wu, L. S. Huang, and H. N. Ginsberg. 1995. Apoprotein B100, an inefficiently translocated secretory protein, is bound to the cytosolic chaperone, heat shock protein 70. *J. Biol. Chem.* **270**: 25220-25224.

69. Borchardt, R. A. and R. A. Davis. 1987. Intrahepatic assembly of very low density lipoproteins. Rate of transport out of the endoplasmic reticulum determines rate of secretion. *J. Biol. Chem.* **262**: 16394-16402.

70. Dixon, J. L., S. Furukawa, and H. N. Ginsberg. 1991. Oleate stimulates secretion of apolipoprotein B-containing lipoproteins from Hep G2 cells by inhibiting early intracellular degradation of apolipoprotein B. *J. Biol. Chem.* **266**: 5080-5086.

71. White, A. L., D. L. Graham, J. LeGros, R. J. Pease, and J. Scott. 1992. Oleate-mediated stimulation of apolipoprotein B secretion from rat hepatoma cells. A function of the ability of apolipoprotein B to direct lipoprotein assembly and escape presecretory degradation. *J. Biol. Chem.* **267**: 15657-15664.

72. Moberly, J. B., T. G. Cole, D. H. Alpers, and G. Schonfeld. 1990. Oleic acid stimulation of apolipoprotein B secretion from HepG2 and Caco-2 cells occurs post-transcriptionally. *Biochim. Biophys. Acta.* **1042**: 70-80.

73. Furukawa, S., N. Sakata, H. N. Ginsberg, and J. L. Dixon. 1992. Studies of the sites of intracellular degradation of apolipoprotein B in Hep G2 cells. *J. Biol. Chem.* **267**: 22630-22638.

74. Bonnardel, J. A. and R. A. Davis. 1995. In HepG2 cells, translocation, not degradation, determines the fate of the de novo synthesized apolipoprotein B. *J. Biol. Chem.* **270**: 28892-28896.

75. Mitchell, D. M., M. Zhou, R. Pariyarath, H. Wang, J. D. Aitchison, H. N. Ginsberg, and E. A. Fisher. 1998. Apoprotein B100 has a prolonged interaction with the translocon during which its lipidation and translocation change from dependence on the microsomal triglyceride transfer protein to independence. *Proc. Natl. Acad. Sci. U. S. A.* **95**: 14733-14738.

76. Zhou, M., E. A. Fisher, and H. N. Ginsberg. 1998. Regulated Co-translational ubiquitination of apolipoprotein B100. A new paradigm for proteasomal degradation of a secretory protein. *J. Biol. Chem.* **273**: 24649-24653.

77. Yeung, S. J., S. H. Chen, and L. Chan. 1996. Ubiquitin-proteasome pathway mediates intracellular degradation of apolipoprotein B. *Biochemistry.* **35**: 13843-13848.

78. Cavallo, D., D. Rudy, A. Mohammadi, J. Macri, and K. Adeli. 1999. Studies on degradative mechanisms mediating post-translational fragmentation of apolipoprotein B and the generation of the 70-kDa fragment. *J. Biol. Chem.* **274**: 23135-23143.

79. Fisher, E. A., M. Pan, X. Chen, X. Wu, H. Wang, H. Jamil, J. D. Sparks, and K. J. Williams. 2001. The triple threat to nascent apolipoprotein B. Evidence for multiple, distinct degradative pathways. *J. Biol. Chem.* **276**: 27855-27863.

80. Wang, C. N., T. C. Hobman, and D. N. Brindley. 1995. Degradation of apolipoprotein B in cultured rat hepatocytes occurs in a post-endoplasmic reticulum compartment. *J. Biol. Chem.* **270**: 24924-24931.

81. Wu, X., N. Sakata, K. M. Lele, M. Zhou, H. Jiang, and H. N. Ginsberg. 1997. A two-site model for ApoB degradation in HepG2 cells. *J. Biol. Chem.* **272**: 11575-11580.

82. Omura, S., T. Fujimoto, K. Otoguro, K. Matsuzaki, R. Moriguchi, H. Tanaka, and Y. Sasaki. 1991. Lactacystin, a novel microbial metabolite, induces neuritogenesis of neuroblastoma cells. *J. Antibiot. (Tokyo).* **44**: 113-116.

83. Rock, K. L., C. Gramm, L. Rothstein, K. Clark, R. Stein, L. Dick, D. Hwang, and A. L. Goldberg. 1994. Inhibitors of the proteasome block the degradation of most cell proteins and the generation of peptides presented on MHC class I molecules. *Cell.* **78**: 761-771.

84. Liang, S., X. Wu, E. A. Fisher, and H. N. Ginsberg. 2000. The amino-terminal domain of apolipoprotein B does not undergo retrograde translocation from the endoplasmic reticulum to the cytosol. Proteasomal degradation of nascent apolipoprotein B begins at the carboxyl terminus of the protein, while apolipoprotein B is still in its original translocon. *J. Biol. Chem.* **275**: 32003-32010.

85. Adeli, K., J. Macri, A. Mohammadi, M. Kito, R. Urade, and D. Cavallo. 1997. Apolipoprotein B is intracellularly associated with an ER-60 protease homologue in HepG2 cells. *J. Biol. Chem.* **272**: 22489-22494.

86. Otsu, M., R. Urade, M. Kito, F. Omura, and M. Kikuchi. 1995. A possible role of ER-60 protease in the degradation of misfolded proteins in the endoplasmic reticulum. *J. Biol. Chem.* **270**: 14958-14961.

87. Urade, R., Y. Takenaka, and M. Kito. 1993. Protein degradation by ERp72 from rat and mouse liver endoplasmic reticulum. *J. Biol. Chem.* **268**: 22004-22009.

88. Cartwright, I. J. and J. A. Higgins. 1995. The role of intracellular proteolysis in the regulation of apolipoprotein B secretion by rabbit hepatocytes. *Biochem. Soc. Trans.* **23**: 413S-

89. Boren, J., L. Graham, M. Wettesten, J. Scott, A. White, and S. O. Olofsson. 1992. The assembly and secretion of ApoB 100-containing lipoproteins in Hep G2 cells. ApoB 100 is cotranslationally integrated into lipoproteins. *J. Biol. Chem.* **267**: 9858-9867.

90. Boren, J., S. Rustaeus, and S. O. Olofsson. 1994. Studies on the assembly of apolipoprotein B-100- and B-48-containing very low density lipoproteins in McA-RH7777 cells. *J. Biol. Chem.* **269**: 25879-25888.

91. Spring, D. J., L. W. Chen-Liu, J. E. Chatterton, J. Elovson, and V. N. Schumaker. 1992. Lipoprotein assembly. Apolipoprotein B size determines lipoprotein core circumference. *J. Biol. Chem.* **267**: 14839-14845.

92. Boren, J., A. White, M. Wettesten, J. Scott, L. Graham, and S. O. Olofsson. 1991. The molecular mechanism for the assembly and secretion of ApoB-100-containing lipoproteins. *Prog. Lipid Res.* **30**: 205-218.

93. Rusinol, A. E., E. Y. Chan, and J. E. Vance. 1993. Movement of apolipoprotein B into the lumen of microsomes from hepatocytes is disrupted in membranes enriched in phosphatidylmonomethylethanolamine. *J. Biol. Chem.* **268**: 25168-25175.

94. Swift, L. L. 1995. Assembly of very low density lipoproteins in rat liver: a study of nascent particles recovered from the rough endoplasmic reticulum. *J. Lipid Res.* **36**: 395-406.

95. Alexander, C. A., R. L. Hamilton, and R. J. Havel. 1976. Subcellular localization of B apoprotein of plasma lipoproteins in rat liver. *J. Cell Biol.* **69**: 241-263.

96. Bamberger, M. J. and M. D. Lane. 1988. Assembly of very low density lipoprotein in the hepatocyte. Differential transport of apoproteins through the secretory pathway. *J. Biol. Chem.* **263**: 11868-11878.

97. Cartwright, I. J. and J. A. Higgins. 1992. Quantification of apolipoprotein B-48 and B-100 in rat liver endoplasmic reticulum and Golgi fractions. *Biochem. J.* **285**: 153-159.

98. Cartwright, I. J. and J. A. Higgins. 1995. Intracellular events in the assembly of very-low-density-lipoprotein lipids with apolipoprotein B in isolated rabbit hepatocytes. *Biochem. J.* **310**: 897-907.

99. Higgins, J. A. 1988. Evidence that during very low density lipoprotein assembly in rat hepatocytes most of the triacylglycerol and phospholipid are packaged with apolipoprotein B in the Golgi complex. *FEBS Lett.* **232**: 405-408.

100. Jones, A. L., N. B. Ruderman, and M. G. Herrera. 1967. Electron microscopic and biochemical study of lipoprotein synthesis in the isolated perfused rat liver. *J. Lipid Res.* **8**: 429-446.

101. Bakillah, A., H. Jamil, and M. M. Hussain. 1998. Lysine and arginine residues in the N-terminal 18% of apolipoprotein B are critical for its binding to microsomal triglyceride transfer protein. *Biochemistry.* **37**: 3727-3734.

102. Huang, X. F. and G. S. Shelness. 1997. Identification of cysteine pairs within the amino-terminal 5% of apolipoprotein B essential for hepatic lipoprotein assembly and secretion. *J. Biol. Chem.* **272**: 31872-31876.

103. Bradbury, P., C. J. Mann, S. Kochl, T. A. Anderson, S. A. Chester, J. M. Hancock, P. J. Ritchie, J. Amey, G. B. Harrison, D. G. Levitt, L. J. Banaszak, J. Scott, and C. C. Shoulders. 1999. A common binding site on the microsomal triglyceride transfer protein for apolipoprotein B and protein disulfide isomerase. *J. Biol. Chem.* **274**: 3159-3164.

104. Gretch, D. G., S. L. Sturley, L. Wang, B. A. Lipton, A. Dunning, K. A. Grunwald, J. R. Wetterau, Z. Yao, P. Talmud, and A. D. Attie. 1996. The amino terminus of apolipoprotein B is necessary but not sufficient for microsomal triglyceride transfer protein responsiveness. *J. Biol. Chem.* **271**: 8682-8691.

105. Hussain, M. M., A. Bakillah, N. Nayak, and G. S. Shelness. 1998. Amino acids 430-570 in apolipoprotein B are critical for its binding to microsomal triglyceride transfer protein. *J. Biol. Chem.* **273**: 25612-25615.

106. Tran, K., J. Boren, J. Macri, Y. Wang, R. McLeod, R. K. Avramoglu, K. Adeli, and Z. Yao. 1998. Functional analysis of disulfide linkages clustered within the amino terminus of human apolipoprotein B. *J. Biol. Chem.* **273**: 7244-7251.

107. Stillemark, P., J. Boren, M. Andersson, T. Larsson, S. Rustaeus, K. A. Karlsson, and S. O. Olofsson. 2000. The assembly and secretion of apolipoprotein B-48-containing very low density lipoproteins in McA-RH7777 cells. *J. Biol. Chem.* **275**: 10506-10513.

108. Rustaeus, S., P. Stillemark, K. Lindberg, D. Gordon, and S. O. Olofsson. 1998. The microsomal triglyceride transfer protein catalyzes the post-translational assembly of apolipoprotein B-100 very low density lipoprotein in McA-RH7777 cells. *J. Biol. Chem.* **273**: 5196-5203.

109. Duerden, J. M. and G. F. Gibbons. 1990. Storage, mobilization and secretion of cytosolic triacylglycerol in hepatocyte cultures. The role of insulin. *Biochem. J.* **272**: 583-587.

110. Francone, O. L., A. D. Kalopissis, and G. Griffaton. 1989. Contribution of cytoplasmic storage triacylglycerol to VLDL-triacylglycerol in isolated rat hepatocytes. *Biochim. Biophys. Acta.* **1002**: 28-36.

111. Lehner, R. and D. E. Vance. 1999. Cloning and expression of a cDNA encoding a hepatic microsomal lipase that mobilizes stored triacylglycerol. *Biochem. J.* **343 Pt 1**: 1-10.

112. Lehner, R., Z. Cui, and D. E. Vance. 1999. Subcellular localization, developmental expression and characterization of a liver triacylglycerol hydrolase. *Biochem. J.* **338**: 761-768.

113. Pease, R. J., D. Wiggins, E. D. Saggerson, J. Tree, and G. F. Gibbons. 1999. Metabolic characteristics of a human hepatoma cell line stably transfected with hormone-sensitive lipase. *Biochem. J.* **341**: 453-460.

114. Lankester, D. L., A. M. Brown, and V. A. Zammit. 1998. Use of cytosolic triacylglycerol hydrolysis products and of exogenous fatty acid for the synthesis of triacylglycerol secreted by cultured rat hepatocytes. *J. Lipid Res.* **39**: 1889-1895.

115. Yang, L. Y., A. Kuksis, J. J. Myher, and G. Steiner. 1995. Origin of triacylglycerol moiety of plasma very low density lipoproteins in the rat: structural studies. *J. Lipid Res.* **36**: 125-136.

116. Yang, L. Y., A. Kuksis, J. J. Myher, and G. Steiner. 1996. Contribution of de novo fatty acid synthesis to very low density lipoprotein triacylglycerols: evidence from mass isotopomer distribution analysis of fatty acids synthesized from [2H6]ethanol. *J. Lipid Res.* **37**: 262-274.

117. Gibbons, G. F., R. Khurana, A. Odwell, and M. C. Seelaender. 1994. Lipid balance in HepG2 cells: active synthesis and impaired mobilization. *J. Lipid Res.* **35**: 1801-1808.

118. Thrift, R. N., T. M. Forte, B. E. Cahoon, and V. G. Shore. 1986. Characterization of lipoproteins produced by the human liver cell line, Hep G2, under defined conditions. *J. Lipid Res.* **27**: 236-250.

119. Owen, M. and V. A. Zammit. 1997. Evidence for overt and latent forms of DGAT in rat liver microsomes. Implications for the pathways of triacylglycerol incorporation into VLDL. *Biochem. Soc. Trans.* **25**: 21S-

120. Gibbons, G. F. and D. Wiggins. 1995. Intracellular triacylglycerol lipase: its role in the assembly of hepatic very-low-density lipoprotein (VLDL). *Adv. Enzyme Regul.* **35**: 179-198.

121. Zammit, V. A. 1996. Role of insulin in hepatic fatty acid partitioning: emerging concepts. *Biochem. J.* **314**: 1-14.

122. Wiggins, D. and G. F. Gibbons. 1996. Origin of hepatic very-low-density lipoprotein triacylglycerol: the contribution of cellular phospholipid. *Biochem. J.* **320**: 673-679.

123. Gavino, V. C., J. S. Miller, J. M. Dillman, G. E. Milo, and D. G. Cornwell. 1981. Polyunsaturated fatty acid accumulation in the lipids of cultured fibroblasts and smooth muscle cells. *J. Lipid Res.* **22**: 57-62.

124. Rosenthal, M. D. 1980. Selectivity in incorporation, utilization and retention of oleic and linoleic acids by human skin fibroblasts. *Lipids*. **15**: 838-848.

125. Yao, Z. M. and D. E. Vance. 1988. The active synthesis of phosphatidylcholine is required for very low density lipoprotein secretion from rat hepatocytes. *J. Biol. Chem.* **263**: 2998-3004.

126. Joyce, C., K. Skinner, R. A. Anderson, and L. L. Rudel. 1999. Acyl-coenzyme A:cholesteryl acyltransferase 2. *Curr. Opin. Lipidol.* **10**: 89-95.

127. Fleming, J. F., G. M. Spitsen, T. Y. Hui, L. Olivier, E. Z. Du, M. Raabe, and R. A. Davis. 1999. Chinese hamster ovary cells require the coexpression of microsomal triglyceride transfer protein and cholesterol 7alpha-hydroxylase for the assembly and secretion of apolipoprotein B-containing lipoproteins. *J. Biol. Chem.* **274**: 9509-9514.

128. Miyake, J. H., X. D. Doung, W. Strauss, G. L. Moore, L. W. Castellani, L. K. Curtiss, J. M. Taylor, and R. A. Davis. 2001. Increased production of apolipoprotein B-containing lipoproteins in the absence of hyperlipidemia in transgenic mice expressing cholesterol 7alpha-hydroxylase. *J. Biol. Chem.* **276**: 23304-23311.

129. Wang, Y., K. Tran, and Z. Yao. 1999. The activity of microsomal triglyceride transfer protein is essential for accumulation of triglyceride within microsomes in McA-RH7777 cells. A unified model for the assembly of very low density lipoproteins. *J. Biol. Chem.* **274**: 27793-27800.

130. Wetterau, J. R. and D. B. Zilversmit. 1984. A triglyceride and cholesteryl ester transfer protein associated with liver microsomes. *J. Biol. Chem.* **259**: 10863-10866.

131. Wetterau, J. R. and D. B. Zilversmit. 1986. Localization of intracellular triacylglycerol and cholesteryl ester transfer activity in rat tissues. *Biochim. Biophys. Acta.* **875**: 610-617.

132. Wetterau, J. R., K. A. Combs, S. N. Spinner, and B. J. Joiner. 1990. Protein disulfide isomerase is a component of the microsomal triglyceride transfer protein complex. *J. Biol. Chem.* **265**: 9801-9807.

133. Freedman, R. B., T. R. Hirst, and M. F. Tuite. 1994. Protein disulphide isomerase: building bridges in protein folding. *Trends Biochem. Sci.* **19**: 331-336.

134. Lamberg, A., M. Jauhiainen, J. Metso, C. Ehnholm, C. Shoulders, J. Scott, T. Pihlajaniemi, and K. I. Kivirikko. 1996. The role of protein disulphide isomerase in the microsomal triacylglycerol transfer protein does not reside in its isomerase activity. *Biochem. J.* **315**: 533-536.

135. Ricci, B., D. Sharp, E. O'Rourke, B. Kienzle, L. Blinderman, D. Gordon, C. Smith-Monroy, G. Robinson, R. E. Gregg, D. J. Rader, and . 1995. A 30-amino acid truncation of the microsomal triglyceride transfer protein large subunit disrupts its interaction with protein disulfide-isomerase and causes abetalipoproteinemia. *J. Biol. Chem.* **270**: 14281-14285.

136. Pihlajaniemi, T., T. Helaakoski, K. Tasanen, R. Myllyla, M. L. Huhtala, J. Koivu, and K. I. Kivirikko. 1987. Molecular cloning of the beta-subunit of human prolyl 4-hydroxylase. This subunit and protein disulphide isomerase are products of the same gene. *EMBO J.* **6**: 643-649.

137. Atzel, A. and J. R. Wetterau. 1993. Mechanism of microsomal triglyceride transfer protein catalyzed lipid transport. *Biochemistry.* **32**: 10444-10450.

138. Jamil, H., J. K. Dickson, Jr., C. H. Chu, M. W. Lago, J. K. Rinehart, S. A. Biller, R. E. Gregg, and J. R. Wetterau. 1995. Microsomal triglyceride transfer protein. Specificity of lipid binding and transport. *J. Biol. Chem.* **270**: 6549-6554.

139. Chang, B. H., W. Liao, L. Li, M. Nakamuta, D. Mack, and L. Chan. 1999. Liver-specific inactivation of the abetalipoproteinemia gene completely abrogates very low density lipoprotein/low density lipoprotein production in a viable conditional knockout mouse. *J. Biol. Chem.* **274**: 6051-6055.

140. Liao, W., K. Kobayashi, and L. Chan. 1999. Adenovirus-mediated overexpression of microsomal triglyceride transfer protein (MTP): mechanistic studies on the role of MTP in apolipoprotein B-100 biogenesis, by. *Biochemistry.* **38**: 10215-

141. Gordon, D. A., H. Jamil, D. Sharp, D. Mullaney, Z. Yao, R. E. Gregg, and J. Wetterau. 1994. Secretion of apolipoprotein B-containing lipoproteins from HeLa cells is dependent on expression of the microsomal triglyceride transfer protein and is regulated by lipid availability. *Proc. Natl. Acad. Sci. U. S. A.* **91**: 7628-7632.

142. Leiper, J. M., J. D. Bayliss, R. J. Pease, D. J. Brett, J. Scott, and C. C. Shoulders. 1994. Microsomal triglyceride transfer protein, the abetalipoproteinemia gene product, mediates the secretion of apolipoprotein B-containing lipoproteins from heterologous cells. *J. Biol. Chem.* **269**: 21951-21954.

143. Patel, S. B. and S. M. Grundy. 1996. Interactions between microsomal triglyceride transfer protein and apolipoprotein B within the endoplasmic reticulum in a heterologous expression system. *J. Biol. Chem.* **271**: 18686-18694.

144. Gordon, D. A., H. Jamil, R. E. Gregg, S. O. Olofsson, and J. Boren. 1996. Inhibition of the microsomal triglyceride transfer protein blocks the first step of apolipoprotein B lipoprotein assembly but not the addition of bulk core lipids in the second step. *J. Biol. Chem.* **271**: 33047-33053.

145. Jamil, H., D. A. Gordon, D. C. Eustice, C. M. Brooks, J. K. Dickson, Jr., Y. Chen, B. Ricci, C. H. Chu, T. W. Harrity, C. P. Ciosek, Jr., S. A. Biller, R. E. Gregg, and J. R. Wetterau. 1996. An inhibitor of the microsomal triglyceride transfer protein inhibits apoB secretion from HepG2 cells. *Proc. Natl. Acad. Sci. U. S. A.* **93**: 11991-11995.

146. Pan, M., J. S. Liang Js, E. A. Fisher, and H. N. Ginsberg. 2002. The late addition of core lipids to nascent apolipoprotein B100, resulting in the assembly and secretion of triglyceride-rich lipoproteins, is independent of both microsomal triglyceride transfer protein activity and new triglyceride synthesis. *J. Biol. Chem.* **277**: 4413-4421.

147. Levy, E., S. Stan, E. Delvin, D. Menard, C. Shoulders, C. Garofalo, I. Slight, E. Seidman, G. Mayer, and M. Bendayan. 2002. Localization of microsomal triglyceride transfer protein in the Golgi: Possible role in the assembly of chylomicrons. *J. Biol. Chem.* .:

148. Lang, C. A. and R. A. Davis. 1990. Fish oil fatty acids impair VLDL assembly and/or secretion by cultured rat hepatocytes. *J. Lipid Res.* **31**: 2079-2086.

149. Lewis, G. F., K. D. Uffelman, L. W. Szeto, B. Weller, and G. Steiner. 1995. Interaction between free fatty acids and insulin in the acute control of very low density lipoprotein production in humans. *J. Clin. Invest.* **95**: 158-166.

150. Wang, H., Z. Yao, and E. A. Fisher. 1994. The effects of n-3 fatty acids on the secretion of carboxyl-terminally truncated forms of human apoprotein B. *J. Biol. Chem.* **269**: 18514-18520.

151. Adeli, K., C. Taghibiglou, S. C. Van Iderstine, and G. F. Lewis. 2001. Mechanisms of hepatic very low-density lipoprotein overproduction in insulin resistance. *Trends Cardiovasc. Med.* **11**: 170-176.

152. Bourgeois, C. S., D. Wiggins, R. Hems, and G. F. Gibbons. 1995. VLDL output by hepatocytes from obese Zucker rats is resistant to the inhibitory effect of insulin. *Am. J. Physiol.* **269**: E208-E215.

153. Brown, A. M. and G. F. Gibbons. 2001. Insulin inhibits the maturation phase of VLDL assembly via a phosphoinositide 3-kinase-mediated event. *Arterioscler. Thromb. Vasc. Biol.* **21**: 1656-1661.

154. Maugeais, C., U. J. Tietge, K. Tsukamoto, J. M. Glick, and D. J. Rader. 2000. Hepatic apolipoprotein E expression promotes very low density lipoprotein-apolipoprotein B production in vivo in mice. *J. Lipid Res.* **41**: 1673-1679.

155. Rustaeus, S., K. Lindberg, J. Boren, and S. O. Olofsson. 1995. Brefeldin A reversibly inhibits the assembly of apoB containing lipoproteins in McA-RH7777 cells. *J. Biol. Chem.* **270**: 28879-28886.

156. Klausner, R. D., J. G. Donaldson, and J. Lippincott-Schwartz. 1992. Brefeldin A: insights into the control of membrane traffic and organelle structure. *J. Cell Biol.* **116**: 1071-1080.

157. Hamilton, R. L., L. S. Guo, T. E. Felker, Y. S. Chao, and R. J. Havel. 1986. Nascent high density lipoproteins from liver perfusates of orotic acid-fed rats. *J. Lipid Res.* **27**: 967-978.

158. Von Euler, L. H. and H. G. Windmueller. 1967. Fatty liver in the rat after intravenous infusion of orotic acid. *Proc. Soc. Exp. Biol. Med.* **125**: 1251-1254.

159. Windmueller, H. G. and A. E. Spaeth. 1965. Stimulation of hepatic purine biosynthesis by orotic acid. *J. Biol. Chem.* **240**: 4398-4405.

160. Windmueller, H. G. and R. I. Levy. 1967. Total inhibition of hepatic beta-lipoprotein production in the rat by orotic acid. *J. Biol. Chem.* **242**: 2246-2254.

161. Windmueller, H. G. and L. H. Von Euler. 1971. Prevention of orotic acid-induced fatty liver with allopurinol. *Proc. Soc. Exp. Biol. Med.* **136**: 98-101.

162. Asp, L., C. Claesson, J. Boren, and S. O. Olofsson. 2000. ADP-ribosylation factor 1 and its activation of phospholipase D are important for the assembly of very low density lipoproteins. *J. Biol. Chem.* **275**: 26285-26292.

163. Tran, K., Y. Wang, C. J. DeLong, Z. Cui, and Z. Yao. 2000. The assembly of very low density lipoproteins in rat hepatoma McA-RH7777 cells is inhibited by phospholipase A2 antagonists. *J. Biol. Chem.* **275**: 25023-25030.

164. Zhao, Y., J. B. McCabe, J. Vance, and L. G. Berthiaume. 2000. Palmitoylation of apolipoprotein B is required for proper intracellular sorting and transport of cholesteroyl esters and triglycerides. *Mol. Biol. Cell.* **11**: 721-734.

165. Chen, Z., T. L. Eggerman, and A. P. Patterson. 2001. Phosphorylation is a regulatory mechanism in apolipoprotein B mRNA editing. *Biochem. J.* **357**: 661-672.

166. Sparks, J. D., C. E. Sparks, A. M. Roncone, and J. M. Amatruda. 1988. Secretion of high and low molecular weight phosphorylated apolipoprotein B by hepatocytes from control and diabetic rats. Phosphorylation of APO BH and APO BL. *J. Biol. Chem.* **263**: 5001-5004.

167. Jackson, T. K., A. I. Salhanick, J. Elovson, M. L. Deichman, and J. M. Amatruda. 1990. Insulin regulates apolipoprotein B turnover and phosphorylation in rat hepatocytes. *J. Clin. Invest.* **86**: 1746-1751.

168. Swift, L. L. 1996. Role of the Golgi apparatus in the phosphorylation of apolipoprotein B. *J. Biol. Chem.* **271**: 31491-31495.

169. Wang, S. Y. and D. L. Williams. 1982. Biosynthesis of the vitellogenins. Identification and characterization of nonphosphorylated precursors to avian vitellogenin I and vitellogenin II. *J. Biol. Chem.* **257**: 3837-3846.

170. Bjornsson, O. G., J. D. Sparks, C. E. Sparks, and G. F. Gibbons. 1994. Regulation of VLDL secretion in primary culture of rat hepatocytes: involvement of cAMP and cAMP-dependent protein kinases. *Eur. J. Clin. Invest.* **24**: 137-148.

171. Sato, R., W. Miyamoto, J. Inoue, T. Terada, T. Imanaka, and M. Maeda. 1999. Sterol regulatory element-binding protein negatively regulates microsomal triglyceride transfer protein gene transcription. *J. Biol. Chem.* **274**: 24714-24720.

172. Sparks, J. D. and C. E. Sparks. 1990. Insulin modulation of hepatic synthesis and secretion of apolipoprotein B by rat hepatocytes. *J. Biol. Chem.* **265**: 8854-8862.

173. Patsch, W., A. M. Gotto, Jr., and J. R. Patsch. 1986. Effects of insulin on lipoprotein secretion in rat hepatocyte cultures. The role of the insulin receptor. *J. Biol. Chem.* **261**: 9603-9606.

174. Phung, T. L., A. Roncone, K. L. Jensen, C. E. Sparks, and J. D. Sparks. 1997. Phosphoinositide 3-kinase activity is necessary for insulin-dependent inhibition of apolipoprotein B secretion by rat hepatocytes and localizes to the endoplasmic reticulum. *J. Biol. Chem.* **272**: 30693-30702.

175. Sparks, J. D., T. L. Phung, M. Bolognino, and C. E. Sparks. 1996. Insulin-mediated inhibition of apolipoprotein B secretion requires an intracellular trafficking event and phosphatidylinositol 3-kinase activation: studies with brefeldin A and wortmannin in primary cultures of rat hepatocytes. *Biochem. J.* **313**: 567-574.

176. Herscovitz, H., M. Hadzopoulou-Cladaras, M. T. Walsh, C. Cladaras, V. I. Zannis, and D. M. Small. 1991. Expression, secretion, and lipid-binding characterization of the N-terminal 17% of apolipoprotein B. *Proc. Natl. Acad. Sci. U. S. A.* **88**: 7313-7317.

177. Shelness, G. S. and J. T. Thornburg. 1996. Role of intramolecular disulfide bond formation in the assembly and secretion of apolipoprotein B-100-containing lipoproteins. *J. Lipid Res.* **37**: 408-419.

178. Burch, W. L. and H. Herscovitz. 2000. Disulfide bonds are required for folding and secretion of apolipoprotein B regardless of its lipidation state. *J. Biol. Chem.* **275**: 16267-16274.

179. Chen, Y., F. Le Caherec, and S. L. Chuck. 1998. Calnexin and other factors that alter translocation affect the rapid binding of ubiquitin to apoB in the Sec61 complex. *J. Biol. Chem.* **273**: 11887-11894.

180. Fisher, E. A., M. Zhou, D. M. Mitchell, X. Wu, S. Omura, H. Wang, A. L. Goldberg, and H. N. Ginsberg. 1997. The degradation of apolipoprotein B100 is mediated by the ubiquitin-proteasome pathway and involves heat shock protein 70. *J. Biol. Chem.* **272**: 20427-20434.

181. Linnik, K. M. and H. Herscovitz. 1998. Multiple molecular chaperones interact with apolipoprotein B during its maturation. The network of endoplasmic reticulum-resident chaperones (ERp72, GRP94, calreticulin, and BiP) interacts with apolipoprotein b regardless of its lipidation state. *J. Biol. Chem.* **273**: 21368-21373.

182. Tatu, U. and A. Helenius. 1999. Interaction of newly synthesized apolipoprotein B with calnexin and calreticulin requires glucose trimming in the endoplasmic reticulum. *Biosci. Rep.* **19**: 189-196.

183. Fewell, S. W., K. J. Travers, J. S. Weissman, and J. L. Brodsky. 2001. The action of molecular chaperones in the early secretory pathway. *Annu. Rev. Genet.* **35** : 149-191.

184. Hammond, C. and A. Helenius. 1995. Quality control in the secretory pathway. *Curr. Opin. Cell Biol.* **7**: 523-529.

185. Hammond, C., I. Braakman, and A. Helenius. 1994. Role of N-linked oligosaccharide recognition, glucose trimming, and calnexin in glycoprotein folding and quality control. *Proc. Natl. Acad. Sci. U. S. A.* **91**: 913-917.

186. Ou, W. J., P. H. Cameron, D. Y. Thomas, and J. J. Bergeron. 1993. Association of folding intermediates of glycoproteins with calnexin during protein maturation. *Nature.* **364**: 771-776.

187. Molinari, M. and A. Helenius. 2000. Chaperone selection during glycoprotein translocation into the endoplasmic reticulum. *Science.* **288**: 331-333.

188. Oliver, J. D., F. J. van der Wal, N. J. Bulleid, and S. High. 1997. Interaction of the thiol-dependent reductase ERp57 with nascent glycoproteins. *Science.* **275**: 86-88.

189. Schrag, J. D., J. J. Bergeron, Y. Li, S. Borisova, M. Hahn, D. Y. Thomas, and M. Cygler. 2001. The Structure of calnexin, an ER chaperone involved in quality control of protein folding. *Mol. Cell.* **8**: 633-644.

190. Helenius, A. and M. Aebi. 2001. Intracellular functions of N-linked glycans. *Science.* **291**: 2364-2369.

191. Trombetta, E. S., J. F. Simons, and A. Helenius. 1996. Endoplasmic reticulum glucosidase II is composed of a catalytic subunit, conserved from yeast to mammals, and a tightly bound noncatalytic HDEL-containing subunit. *J. Biol. Chem.* **271**: 27509-27516.

192. Brodsky, J. L. and A. A. McCracken. 1999. ER protein quality control and proteasome-mediated protein degradation. *Semin. Cell Dev. Biol.* **10**: 507-513.

193. Vashist, S., W. Kim, W. J. Belden, E. D. Spear, C. Barlowe, and D. T. Ng. 2001. Distinct retrieval and retention mechanisms are required for the quality control of endoplasmic reticulum protein folding. *J. Cell Biol.* **155**: 355-368.

194. Chapman, R., C. Sidrauski, and P. Walter. 1998. Intracellular signaling from the endoplasmic reticulum to the nucleus. *Annu. Rev. Cell Dev. Biol.* **14**: 459-485.

195. Ma, Y. and L. M. Hendershot. 2001. The unfolding tale of the unfolded protein response. *Cell.* **107**: 827-830.

196. Bertolotti, A., Y. Zhang, L. M. Hendershot, H. P. Harding, and D. Ron. 2000. Dynamic interaction of BiP and ER stress transducers in the unfolded-protein response. *Nat. Cell Biol.* **2**: 326-332.

197. Okamura, K., Y. Kimata, H. Higashio, A. Tsuru, and K. Kohno. 2000. Dissociation of Kar2p/BiP from an ER sensory molecule, Ire1p, triggers the unfolded protein response in yeast. *Biochem. Biophys. Res. Commun.* **279**: 445-450.

198. Gonzalez, T. N., C. Sidrauski, S. Dorfler, and P. Walter. 1999. Mechanism of non-spliceosomal mRNA splicing in the unfolded protein response pathway. *EMBO J.* **18**: 3119-3132.

199. Tirasophon, W., A. A. Welihinda, and R. J. Kaufman. 1998. A stress response pathway from the endoplasmic reticulum to the nucleus requires a novel bifunctional protein kinase/endoribonuclease (Ire1p) in mammalian cells. *Genes Dev.* **12**: 1812-1824.

200. Wang, X. Z., H. P. Harding, Y. Zhang, E. M. Jolicoeur, M. Kuroda, and D. Ron. 1998. Cloning of mammalian Ire1 reveals diversity in the ER stress responses. *EMBO J.* **17**: 5708-5717.

201. Harding, H. P., Y. Zhang, and D. Ron. 1999. Protein translation and folding are coupled by an endoplasmic-reticulum-resident kinase. *Nature.* **397**: 271-274.

202. Kim, P. S. and P. Arvan. 1998. Endocrinopathies in the family of endoplasmic reticulum (ER) storage diseases: disorders of protein trafficking and the role of ER molecular chaperones. *Endocr. Rev.* **19**: 173-202.

203. Werstuck, G. H., S. R. Lentz, S. Dayal, G. S. Hossain, S. K. Sood, Y. Y. Shi, J. Zhou, N. Maeda, S. K. Krisans, M. R. Malinow, and R. C. Austin. 2001. Homocysteine-induced endoplasmic reticulum stress causes dysregulation of the cholesterol and triglyceride biosynthetic pathways. *J. Clin. Invest.* **107**: 1263-1273.

204. Silberstein, S. and R. Gilmore. 1996. Biochemistry, molecular biology, and genetics of the oligosaccharyltransferase. *FASEB J.* **10**: 849-858.

205. Opdenakker, G., P. M. Rudd, C. P. Ponting, and R. A. Dwek. 1993. Concepts and principles of glycobiology. *FASEB J.* **7**: 1330-1337.

206. Sasak, W. V., J. S. Lown, and K. A. Colburn. 1991. Human small-intestinal apolipoprotein B-48 oligosaccharide chains. *Biochem. J.* **274**: 159-165.

207. Taniguchi, T., Y. Ishikawa, M. Tsunemitsu, and H. Fukuzaki. 1989. The structures of the asparagine-linked sugar chains of human apolipoprotein B-100. *Arch. Biochem. Biophys.* **273**: 197-205.

208. Attie, A. D., D. B. Weinstein, H. H. Freeze, R. C. Pittman, and D. Steinberg. 1979. Unaltered catabolism of desialylated low-density lipoprotein in the pig and in cultured rat hepatocytes. *Biochem. J.* **180**: 647-654.

209. Camejo, G., S. Waich, L. Mateu, H. Acquatella, F. Lalaguna, G. Quintero, and M. L. Berrizbeitia. 1976. Differences in the structure of plasma low-density lipoproteins and their relationship to the extent of interaction with arterial wall-components. *Ann. N. Y. Acad. Sci.* **275**: 153-168.

210. Filipovic, I., G. Schwarzmann, W. Mraz, H. Wiegandt, and E. Buddecke. 1979. Sialic-acid content of low-density lipoproteins controls their binding and uptake by cultured cells. *Eur. J. Biochem.* **93**: 51-55.

211. Shireman, R. B. and W. R. Fisher. 1979. The absence of a role for the carbohydrate moiety in the binding of apolipoprotein B to the low density lipoprotein receptor. *Biochim. Biophys. Acta.* **572**: 537-540.

212. Ihara, Y., M. Yoshimura, E. Miyoshi, A. Nishikawa, A. S. Sultan, S. Toyosawa, A. Ohnishi, M. Suzuki, K. Yamamura, N. Ijuhin, and N. Taniguchi. 1998. Ectopic expression of N-acetylglucosaminyltransferase III in transgenic hepatocytes disrupts apolipoprotein B secretion and induces aberrant cellular morphology with lipid storage. *Proc. Natl. Acad. Sci. U. S. A.* **95**: 2526-2530.

213. Bell-Quint, J., T. Forte, and P. Graham. 1981. Glycosylation of apolipoproteins by cultured rat hepatocytes. Effect of tunicamycin on lipoprotein secretion. *Biochem. J.* **200**: 409-414.

214. Struck, D. K., P. B. Siuta, M. D. Lane, and W. J. Lennarz. 1978. Effect of tunicamycin on the secretion of serum proteins by primary cultures of rat and chick hepatocytes. Studies on transferrin, very low density lipoprotein, and serum albumin. *J. Biol. Chem.* **253**: 5332-5337.

215. Bonen, D. K., F. Nassir, A. M. Hausman, and N. O. Davidson. 1998. Inhibition of N-linked glycosylation results in retention of intracellular apo[a] in hepatoma cells, although nonglycosylated and immature forms of apolipoprotein[a] are competent to associate with apolipoprotein B-100 in vitro. *J. Lipid Res.* **39**: 1629-1640.

216. Liao, W. and L. Chan. 2001. Tunicamycin induces ubiquitination and degradation of apolipoprotein B in HepG2 cells. *Biochem. J.* **353**: 493-501.

217. Macri, J. and K. Adeli. 1997. Conformational changes in apolipoprotein B modulate intracellular assembly and degradation of ApoB-containing lipoprotein particles in HepG2 cells. *Arterioscler. Thromb. Vasc. Biol.* **17**: 2982-2994.

218. Resh, M. D. 1996. Regulation of cellular signaling by fatty acid acylation and prenylation of signal transduction proteins. *Cell Signal.* **8**: 403-412.

219. Resh, M. D. 1999. Fatty acylation of proteins: new insights into membrane targeting of myristoylated and palmitoylated proteins. *Biochim. Biophys. Acta.* **1451**: 1-16.

220. Berthiaume, L. and M. D. Resh. 1995. Biochemical characterization of a palmitoyl acyltransferase activity that palmitoylates myristoylated proteins. *J. Biol. Chem.* **270**: 22399-22405.

221. Duncan, J. A. and A. G. Gilman. 1998. A cytoplasmic acyl-protein thioesterase that removes palmitate from G protein alpha subunits and p21(RAS). *J. Biol. Chem.* **273**: 15830-15837.

222. Berthiaume, L., I. Deichaite, S. Peseckis, and M. D. Resh. 1994. Regulation of enzymatic activity by active site fatty acylation. A new role for long chain fatty acid acylation of proteins. *J. Biol. Chem.* **269**: 6498-6505.

223. Dunphy, J. T. and M. E. Linder. 1998. Signaling functions of protein palmitoylation. *Biochim. Biophys. Acta.* **1436**: 245-261.

224. El Husseini, A., E. Schnell, S. Dakoji, N. Sweeney, Q. Zhou, O. Prange, C. Gauthier-Campbell, A. Aguilera-Moreno, R. A. Nicoll, and D. S. Bredt. 2002. Synaptic Strength Regulated by Palmitate Cycling on PSD-95. *Cell.* **108**: 849-863.

225. Rustaeus, S., K. Lindberg, P. Stillemark, C. Claesson, L. Asp, T. Larsson, J. Boren, and S. O. Olofsson. 1999. Assembly of very low density lipoprotein: a two-step process of apolipoprotein B core lipidation. *J. Nutr.* **129**: 463S-466S.

226. Raag, R., K. Appelt, N. H. Xuong, and L. Banaszak. 1988. Structure of the lamprey yolk lipid-protein complex lipovitellin-phosvitin at 2.8 A resolution. *J. Mol. Biol.* **200**: 553-569.

227. Wang, S., R. S. McLeod, D. A. Gordon, and Z. Yao. 1996. The microsomal triglyceride transfer protein facilitates assembly and secretion of apolipoprotein B-containing lipoproteins and decreases cotranslational degradation of apolipoprotein B in transfected COS-7 cells. *J. Biol. Chem.* **271**: 14124-14133.

228. Nishimaki-Mogami, T., K. Suzuki, and A. Takahashi. 1996. The role of phosphatidylethanolamine methylation in the secretion of very low density lipoproteins by cultured rat hepatocytes: rapid inhibition of phosphatidylethanolamine methylation by bezafibrate increases the density of apolipoprotein B48-containing lipoproteins. *Biochim. Biophys. Acta.* **1304**: 21-31.

229. Wang, C. N., R. S. McLeod, Z. Yao, and D. N. Brindley. 1995. Effects of dexamethasone on the synthesis, degradation, and secretion of apolipoprotein B in cultured rat hepatocytes. *Arterioscler. Thromb. Vasc. Biol.* **15**: 1481-1491.

230. Sjoberg, A., J. Oscarsson, J. Boren, S. Eden, and S. O. Olofsson. 1996. Mode of growth hormone administration influences triacylglycerol synthesis and assembly of apolipoprotein B-containing lipoproteins in cultured rat hepatocytes. *J. Lipid Res.* **37**: 275-289.

231. Hussain, M. M., Y. Zhao, R. K. Kancha, B. D. Blackhart, and Z. Yao. 1995. Characterization of recombinant human apoB-48-containing lipoproteins in rat hepatoma McA-RH7777 cells transfected with apoB-48 cDNA. Overexpression of apoB-48 decreases synthesis of endogenous apoB-100. *Arterioscler. Thromb. Vasc. Biol.* **15**: 485-494.

232. Blackhart, B. D., Z. M. Yao, and B. J. McCarthy. 1990. An expression system for human apolipoprotein B100 in a rat hepatoma cell line. *J. Biol. Chem.* **265**: 8358-8360.

233. Lowry, O. H., D. W. Schulz, and J. V. Passonneau. 1967. The kinetics of glycogen phosphorylases from brain and muscle. *J. Biol. Chem.* **242**: 271-280.

234. Hammond, C. and A. Helenius. 1994. Quality control in the secretory pathway: retention of a misfolded viral membrane glycoprotein involves cycling between the ER, intermediate compartment, and Golgi apparatus. *J. Cell Biol.* **126**: 41-52.

235. Nohturfft, A., R. A. DeBose-Boyd, S. Scheek, J. L. Goldstein, and M. S. Brown. 1999. Sterols regulate cycling of SREBP cleavage-activating protein (SCAP) between endoplasmic reticulum and Golgi. *Proc. Natl. Acad. Sci. U. S. A.* **96**: 11235-11240.

236. Neri, B. P. and C. S. Frings. 1973. Improved method for determination of triglycerides in serum. *Clin. Chem.* **19**: 1201-1202.

237. Elbein, A. D. 1983. Inhibitors of glycoprotein synthesis. *Methods Enzymol.* **98**: 135-154.

238. Yao, Z., K. Tran, and R. S. McLeod. 1997. Intracellular degradation of newly synthesized apolipoprotein B. *J. Lipid Res.* **38**: 1937-1953.

239. Hoe, M. H. and R. C. Hunt. 1992. Loss of one asparagine-linked oligosaccharide from human transferrin receptors results in specific cleavage and association with the endoplasmic reticulum. *J. Biol. Chem.* **267**: 4916-4923.

240. Yao, Z. and R. S. McLeod. 1994. Synthesis and secretion of hepatic apolipoprotein B-containing lipoproteins. *Biochim. Biophys. Acta.* **1212**: 152-166.

241. Nicodeme, E., F. Benoist, R. McLeod, Z. Yao, J. Scott, C. C. Shoulders, and T. Grand-Perret. 1999. Identification of domains in apolipoprotein B100 that confer a high requirement for the microsomal triglyceride transfer protein. *J. Biol. Chem.* **274**: 1986-1993.

242. Linton, M. F., R. V. Farese, Jr., and S. G. Young. 1993. Familial hypobetalipoproteinemia. *J. Lipid Res.* **34**: 521-541.

243. Bakillah, A., N. Nayak, U. Saxena, R. M. Medford, and M. M. Hussain. 2000. Decreased secretion of ApoB follows inhibition of ApoB-MTP binding by a novel antagonist. *Biochemistry.* **39**: 4892-4899.

244. Webb, Y., L. Hermida-Matsumoto, and M. D. Resh. 2000. Inhibition of protein palmitoylation, raft localization, and T cell signaling by 2-bromopalmitate and polyunsaturated fatty acids. *J. Biol. Chem.* **275**: 261-270.

245. Springer, T. A. 1998. An extracellular beta-propeller module predicted in lipoprotein and scavenger receptors, tyrosine kinases, epidermal growth factor precursor, and extracellular matrix components. *J. Mol. Biol.* **283**: 837-862.

246. Herz, J., R. C. Kowal, J. L. Goldstein, and M. S. Brown. 1990. Proteolytic processing of the 600 kd low density lipoprotein receptor-related protein (LRP) occurs in a trans-Golgi compartment. *EMBO J.* **9**: 1769-1776.

247. Warshawsky, I., G. Bu, and A. L. Schwartz. 1993. Identification of domains on the 39-kDa protein that inhibit the binding of ligands to the low density lipoprotein receptor-related protein. *J. Biol. Chem.* **268**: 22046-22054.

248. Nissim, A., H. R. Hoogenboom, I. M. Tomlinson, G. Flynn, C. Midgley, D. Lane, and G. Winter. 1994. Antibody fragments from a 'single pot' phage display library as immunochemical reagents. *EMBO J.* **13**: 692-698.

Curriculum Vitae

Jelena Vukmirica

Date of Birth: November 14, 1974

Work address: Lipoprotein & Atherosclerosis Group H447
University of Ottawa Heart Institute
40 Ruskin Street
Ottawa, ON
K1Y 4W7
Phone: (613) 798-5555 ext. 18712
Fax: (613) 761-5281
e-mail: jvukmirica@ottawaheart.ca

Education:

1992-1996	B.Sc. (Honours), Biochemistry, University of Ottawa, Ottawa, Canada
1996-1998	M.Sc. Candidate, Biochemistry, University of Ottawa, Ottawa, Canada
1998-	Ph.D. Candidate, Biochemistry, University of Ottawa, Ottawa, Canada

Distinctions and Awards:

1992-1993	University of Ottawa Admission Scholarship
1992-1993	Canadian Scholarship in Sciences & Engineering
1994	University of Ottawa Dean's Honor List
1996	Graduation *magna cum laude* (University of Ottawa)
1996	Best Basic Science Presentation (Ottawa Institute Research Day)
1997–1998	Ontario Graduate Scholarship
1997-1998	University of Ottawa Excellence Scholarship
1999	Honorary Mention (Ottawa Heart Institute Research Day)
1999	Best Graduate Student Presentation (Annual Research Day)
1999-2002	Medical Research Council Doctoral Award
1999-2002	University of Ottawa Excellence Scholarship

Professional Societies:

1998-	Member, American Society for Cell Biology
1999-	Member, Canadian Society for Biochemistry, Molecular and Cellular Biology

Refereed Journal Publications:

1. Ko, K.W.S., McLeod, R.S., Kohen Avramoglu, R., Nimpf, J., FitzGerald, D.J., **Vukmirica, J.**, and Yao, Z. (1998) Mutation at the processing site of chicken low density lipoprotein receptor-related protein impairs efficient endoplasmic reticulum exit, but proteolytic cleavage is not essential for its endocytic functions. *J. Biol. Chem.* **273,** 27779-27785.

2. Raffai, R., **Vukmirica, J.**, Weisgraber, K., Rassart, E., Innerarity, T., and Milne, R. (1999) Bacterial expression and purification of the Fab fragment of a monoclonal antibody specific for the low-density lipoprotein receptor-binding site of human apolipoprotein E. *Protein Expression and Purification* **16,** 84-90.

3. Ko, K. W. S., Avramoglu, R. K., McLeod, R. S., **Vukmirica, J.**, and Yao, Z. (2000) The insulin-stimulated cell surface presentation of low density lipoprotein receptor-related protein in 3T3-L1 adipocytes is sensitive to phosphatidylinositide 3-kinase inhibition. *Biochemistry* **40,** 752-759.

4. **Vukmirica, J.**, Nishimaki-Mogami, T., Tran, K., Shan, J., McLeod, R. S., Yuan, J., and Yao, Z. The N-linked oligosaccharides at the amino terminus of human apoB are important for the assembly and secretion of VLDL. *J. Lipid Res.* **43,** 1496-1507.

5. **Vukmirica, J.**, Yuan, J., Tran, K., Shan, J., Liang, X., and Yao, Z. Palmitoylation is not required for human apoB48-VLDL assembly and secretion. (in preparation)

Non-refereed Contributions:

1. **Vukmirica, J.**, Raffai, R., and Yao, Z. Generation of monoclonal antibody fragments using the technology of phage display. (Oral Presentation at Heart Institute Research Day Annual Competition: Best Basic Science Presentation, 1997)

2. **Vukmirica, J.**, and Yao, Z. Role of N-linked glycosylation of apolipoprotein B in VLDL assembly. (Oral Presentation at Heart Institute Research Day Annual Competition, 1998)

3. **Vukmirica, J.**, Nishimaki-Mogami, T., McLeod, R.S., and Yao, Z. N-linked glycosylation is important for post-translational stability and efficient secretion of apoB. (Poster Presentation at American Society for Cell Biology 38th Annual Meeting, San Francisco, 1998)

4. Ko, K.W.S., McLeod, R.S., Kohen Avramoglu, R., Nimpf, J., FitzGerald, D.J., **Vukmirica, J.**, and Yao, Z. Mutation at the furin cleavage site of LRP impairs exit from ER but does not affect endocytosis. (Poster Presentation at American Society for Cell Biology 38th Annual Meeting, San Francisco, 1998)

5. **Vukmirica, J.**, Nishimaki-Mogami, T., McLeod, R.S., and Yao, Z. N-linked glycosylation is important for post-translational stability and efficient secretion of apoB. (Oral Presentation at Heart Institute Research Day Annual Competition: Honourable Mention, 1999)

6. **Vukmirica, J.**, Nishimaki-Mogami, T., McLeod, R.S., and Yao, Z. N-linked glycosylation is important for post-translational stability and efficient secretion of apoB. (Poster Presentation at University of Ottawa Department of Pathology and Laboratory Medicine Annual Research Day: Best Graduate Student Presentation, 1999)

7. **Vukmirica, J.**, Nishimaki-Mogami, T., McLeod, R.S., and Yao, Z. Functional analysis of the role of N-linked glycosylation of apoB in lipoprotein assembly and secretion. (Oral Presentation at Canadian Lipoprotein Conference Annual Meeting, Mont-Tremblant, 1999)

8. **Vukmirica, J.**, Nishimaki-Mogami, T., McLeod, R.S., and Yao, Z. Functional analysis of the role of N-linked glycosylation of apoB in lipoprotein assembly and secretion. (Oral Presentation at American Heart Association 72nd Scientific Sessions, Atlanta, 1999)

9. Kohen Avramoglu, R., Ko, W.S., Brown, R.J., **Vukmirica, J.**, and Yao, Z. The YWTD motifs within LDL receptor-related protein (LRP) are important for efficient intracellular trafficking. (Oral Presentation at American Society for Biochemistry and Molecular Biology Meeting, Boston, Massachusets, 2000)

10. **Vukmirica, J.**, Nishimaki-Mogami, T., McLeod, R.S., and Yao, Z. Functional analysis of the role of N-linked glycosylation of apoB in lipoprotein assembly and secretion. (Oral Presentation at Canadian Lipoprotein Conference Annual Meeting, Vancouver, 2000)

11. Tran, K., **Vukmirica, J.**, and Yao, Z. New insight of the assembly of very low density lipoproteins in McA-RH7777 cells. (Poster Presentation at American Society for Cell Biology 40th Annual Meeting, San Francisco, 2000)

12. **Vukmirica, J.**, Tran, K., and Yao, Z. The role of N-linked oligosaccharides of human apolipoprotein B in the assembly and secretion of apolipoprotein B-containing very low density lipoproteins. (Poster Presentation at Canadian Lipoprotein Conference Annual Meeting, Halifax, 2001)

13. **Vukmirica, J.**, Yuan J., and Yao, Z. New insights into the role of post-translational modification of human apoB in the assembly and secretion of VLDL. (Oral Presentation at American Heart Association 74th Scientific Sessions, Anaheim, 2001)

A Statement of Contribution of Collaborators

For all the experimental procedures presented in this thesis, I have taken charge in the experimental design, conduct of the experiments, interpretation of the data, and drawing of the figures.

I acknowledge the participation of the following collaborators in conducting the experiments:

Collaborator	**Experimental results shown in**
Roger McLeod	Fig. 3.1.4.
Khai Tran	Figs. 3.1.8., 3.1.10., and 3.2.4*A*
Jing Shan	Figs. 3.3.5. and 4.1.6.
Jane Yuan	Figs. 2.2. and 4.1.2*B*
Xiquan Liang	Fig. 4.1.2*C*